UNIVERSITY OF BRASÍLIA

INSTITUTE OF PHYSICS

RAFAEL FERREIRA DE MENEZES

ADSORPTION OF CO, NO_2 , SO_2, AND NH_3 ON GRAPHENE QUANTUM DOTS: A SEARCH FOR POLLUTANT GAS SENSORS

BRASÍLIA

OCTOBER 5TH 2021

Rafael Ferreira de Menezes

Adsorption of CO, NO_2 , SO_2, and NH_3 on Graphene Quantum Dots: a Search for Pollutant Gas Sensors

Final undergraduate paper presented to the Institute of Physics of the University of Brasília as part of the requirements for obtaining a Bachelor's Degree in Physics.

Supervisor: Ricardo Gargano

University of Brasília – UnB

Institute of Physics

Brasília

october 5th 2021

Rafael Ferreira de Menezes

Adsorption of CO, NO_2 , SO_2, and NH_3 on Graphene Quantum Dots: a Search for Pollutant Gas Sensors/ Rafael Ferreira de Menezes. – Brasília, october 5th 2021-

126 p. : il. (algumas color.) ; 30 cm.

Supervisor: Ricardo Gargano

Final undergraduate paper – University of Brasília – UnB
Institute of Physics, october 5th 2021.

1. Graphene. 2. Gas Adsorption. 3. Pollutant Gas Sensors. 4. Potential Energy Curves. 5. Spectroscopic Properties I. Ricardo Gargano. II. University of Brasília. III. Institute of Physics. IV. Adsorption of CO, NO_2 , SO_2, and NH_3 on Graphene Quantum Dots: a Search for Pollutant Gas Sensors

CDU 02:141:005.7

Rafael Ferreira de Menezes

Adsorption of CO, NO_2 , SO_2, and NH_3 on Graphene Quantum Dots: a Search for Pollutant Gas Sensors

Final undergraduate paper presented to the Institute of Physics of the University of Brasília as part of the requirements for obtaining a Bachelor's Degree in Physics.

Approved paper. Brasília, october 5th 2021:

Ricardo Gargano
Advisor

Wiliam Ferreira da Cunha
Professor

Cecilia Coletti
Professor

Brasília
october 5th 2021

I dedicate this work to the previous generations, who laid the foundations that made this work possible. I also dedicate it to the next generations, who will continue this infinite investigation of reality.

Acknowledgements

This work was only possible because of the influence of many great people in my life. First, I would like to thank my family, especially my grandmother Luiza, my mother Luciana, and my aunt Luciene. I had the honor of being raised by those three amazing people who did everything in their power to give me the opportunities they never had. Vovó, mamãe e titia, you were and always will be my heroines and I hope to make you proud.

I would also like to thank my teachers and professors, all of them, from elementary school teachers to university professors. The knowledge I have today was shared with me by incredible people that dedicate their lives to sharing their knowledge. Growing up, my teachers were always a source of inspiration for me, and I carry all their memories fondly in my heart.

One professor in especial needs to be mentioned, Professor Ricardo Gargano, a great inspiration and dear friend. Thank you for all the support and advice you gave me in the last few years. You helped me grow from a physics student to a scientist, and your passion for what you do is remarkable and leaves a positive impact everywhere you go and in every class you teach. I hope to keep collaborating with you and publishing articles together for a very long time.

I was very lucky to have amazing friends in my life, with whom I could always count on. Ricardo Venturini and Victor Vendramini, thank you for being part of my journey and letting me being part of yours. You guys helped me overcome many obstacles, and taught me the importance of maintaining a positive view of things. Rica and Vendra, thank you!

These acknowledgments would never be complete without one person. This is the person on whose shoulders I cry when I am sad, the person with whom I most like to share a laugh, the person who is always there for me, the person that changed my life forever, the love of my life. Beatrice Irene Neal de Souza, there are not enough words in any language to express how grateful I am to have met you. Thank you and your family for accepting and welcoming me. It has been 7 years and many more to come. Sharing my life with you is the best thing that could ever happen to me. I love you!

"Somewhere, something incredible
is waiting to be known."
(Carl Sagan)

Abstract

The development of more sensitive and accurate sensors is essential to monitor the levels of pollutant gases that are causing high damage to the biosphere. One of the most promising materials for such application is graphene, which, due to its extensive collection of properties, has shown itself capable of adsorbing gas molecules. Thus, the present work aims at investigating the adsorption of carbon monoxide (CO), nitrogen dioxide (NO_2), sulfur dioxide (SO_2), and ammonia (NH_3) in Graphene Quantum Dots (GQD) through electronic structure and molecular dynamics calculations. The data suggest that doping GQDs with boron, nitrogen, or aluminum can greatly improve their adsorbing capabilities. For both CO and NH_3, functionalizations with Al are the most effective, while the adsorption of SO_2 was not very affected by any of the doping designs. Notably, quantum dots doped with either B or Al are extremely promising with respect to application in NO_2 gas sensors. Thereby, the results indicate that accurate, and resilient gas sensors based on doped GQDs may be a good substitute for the current sensors in the market.

Key-words: Graphene. Gas Adsorption. Pollutant Gas Sensors. Potential Energy Curves. Spectroscopic Properties.

List of Figures

List of Tables

List of abbreviations and acronyms

GQD	Graphene Quantum Dot
PEC	Potential Energy Curve
PES	Potential Energy Surface
SAPT	Symmetry-Adapted Perturbation Theory
NBO	Natural Bond Orbital
BOA	Born-Oppenheimer Approximation
DFT	Density Functional Theory
HF	Hartree-Fock
SCF	Self Consistent Field
DVR	Discrete Variable Representation
WBK	Wentzel-Brillouin-Kramers Method
RMSD	Root-Mean-Square Deviation

Contents

Introduction

Currently, there is a great demand for more accurate and selective gas sensors due to the numerous applications in environmental monitoring, medicine, industry, and even in space missions (HUANG et al., 2008). The detection of polluting gases such as carbon monoxide (CO), nitrogen dioxide (NO_2), sulfur dioxide (SO_2), and ammonia (NH_3) is extremely important due to the harmful effects these molecules have on ecosystems when present in high quantities due to anthropogenic activities (KRUPA, 2003; PEEL et al., 2005; BIGGERI; BELLINI; TERRACINI, 2004).

Graphene, due to its properties, sparked the interest of the scientific community for studies of nanosensors based on this extraordinary material. Experimental investigations have pointed out that such systems can indeed be used as excellent gas sensors (FOWLER et al., 2009). An exciting possibility is the use of graphene quantum dots (GQD) to adsorb small molecules. The generic term "quantum dot" refers to semiconductor particles with sizes up to a few nanometers. GQDs are a particular type of quantum dot obtained from nanometric fragments of graphene sheets.

In this work, the adsorption of CO, NO_2, SO_2, and NH_3 molecules on Graphene Quantum Dots (GQDs) will be investigated through a first-principles study. The systems formed by each of these molecules will be evaluated with pure GQD, and also with GQDs functionalized by three different dopants: boron (B), nitrogen (N), and aluminum (Al). Boron and nitrogen are the most common dopants due to their proximity to carbon. Aluminum belongs to the same family as Boron and, therefore, has similar properties, with the difference that it is a more massive atom than boron, a factor that can be fundamental to increase the adsorption energy of the molecules of interest. Doping with B and Al atoms (with an electronic configuration ns^2np^1) generates on the nanostructure a vacancy or defect of electron, while the doping with N ($2s^22p^3$) provides the excess of 1 electron.

To assess the effectiveness of these systems, the following strategy will be used:

- Investigation of the electronic structure of each system evaluated through potential energy curves (PEC) to determine if there is in fact adsorption;
- Characterization of the interaction between the GQD and the adsorbate using Symmetry Adapted Perturbation Theory (SAPT) (JEZIORSKI; MOSZYNSKI; SZALEWICZ, 1994) and Natural Bond Orbital analysis (NBO) (WEINHOLD, 2012);
- Study of spectroscopic constants to enable the understanding of the dynamics of the adsorption process;

- Determination of the lifetime of the adsorbent-adsorbate complex to gauge the stability of the system.

The literature is rich in works that seek to understand the process of adsorption on graphene, however, a study that evaluates all aspects simultaneously, especially the characterization of the interaction between the GQD and the adsorbate is lacking. In addition, many papers study only one complex (WANNO; TABTIMSAI, 2014; WEHLING et al., 2008) and implement the usage of different software, which makes it difficult to compare the data. Even when more than one system is investigated, functionalization designs are usually not considered, and only interactions with pristine graphene sheets are studied (LIN; NI; FANG, 2013). As a result, the main contribution of the present work is to perform a broader and more complete investigation of several systems and functionalizations from the perspective of the same calculation level and basis, enabling a direct comparison among the systems.

Part I

Graphene Quantum Dots

1 Graphene

Carbon is the raw material of life and the basis of all organic chemistry. Due to the flexibility of their bonds, carbon-based systems have a wide range of structures with an immense variety of properties. These properties are mainly a result of the dimensionality of these structures.

In 2004, Konstantin Novoselov, Andre Geim *et al.* isolated a two-dimensional stable graphite crystal named graphene for the first time (NOVOSELOV et al., 2004). In 2010, both authors received the Nobel Prize in Physics for their studies of this material.

Graphene consists of carbons arranged in a hexagonal structure (Figure 1) that collects a set of properties of extreme interest. Due to its two-dimensional structure, it is the thinnest material we know, being only one atom thick, it is also the strongest material with a tensile strength of 42 N/m, the most rigid material with Young's modulus equal to 1 TPa, and the most elastic crystal known (GEIM, 2009; GEIM; NOVOSELOV, 2010).

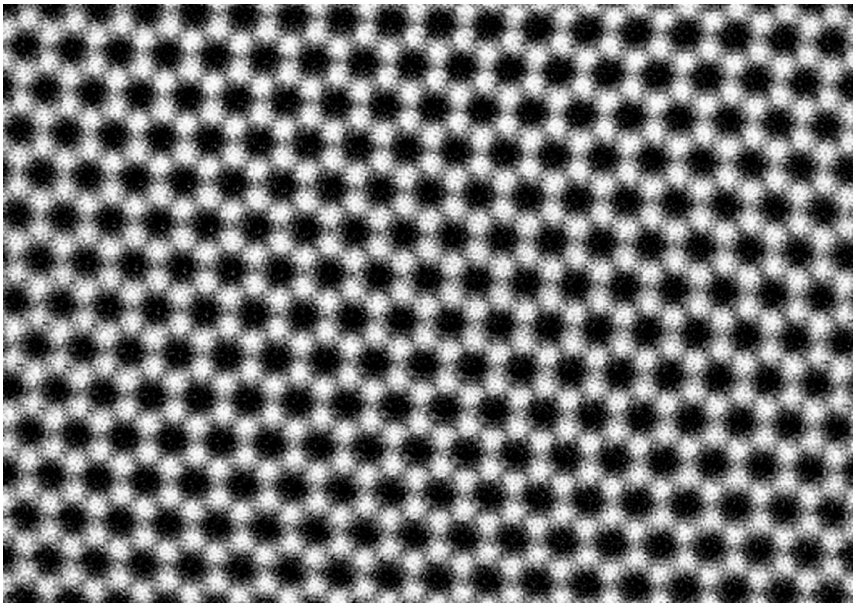

Figure 1 – The hexagonal structure of graphene captured by a transmission electron microscope.

2 Graphene as a gas sensor

The viability of a gas sensor is associated with the ability to adsorb the molecules of interest. Since graphene is the material with the highest surface-to-mass ratio, it maximizes the interaction with the adsorbate, making it extremely promising for application in sensors. Nevertheless, a major limitation for its use as a gas sensor is the fact that pure graphene is chemically inert due to the sp^2 type bond that occurs between carbon atoms, which implies low adsorption energies. However, recent studies indicate that the electronic properties of graphene can be adapted through functionalization with heteroatoms to increase its sensitivity and, thus, develop more accurate and selective sensors. (LIU; LIU; ZHU, 2011; DAI; YUAN; GIANNOZZI, 2009; ZHANG et al., 2009).

Most commercial gas sensors are based on semiconductor metal oxides or polymeric materials. These sensors generally have at least one of the following limitations: high production cost, low selectivity, short lifespan, limited reuse, and high energy consumption. Hence, nanomaterial-based gas sensors have gained significant momentum aiming to overcome these limitations.

By reducing the size of graphene to the nanoscale, we obtain the so-called graphene quantum dots (GQD). GQDs have unique electronic properties that have been attracting great scientific interest (TIAN et al., 2018; RAEYANI; SHOJAEI; AHMADI-KANDJANI, 2020), which has further fueled enthusiasm for graphene applications as a gas sensor.

Part II

Methodologies

3 The Electronic Problem

The fundamental objective of a molecular problem in quantum mechanics is to solve the time-dependent or time-independent Schrödinger equation. A system formed by M nuclei, whose positions are described by the set of coordinates $\mathbf{R} \equiv \{\mathbf{R}_1, \mathbf{R}_2, \ldots, \mathbf{R}_M\}$, and N electrons, whose positions are described by the coordinate set $\mathbf{r} \equiv \{\mathbf{r}_1, \mathbf{r}_2, \ldots, \mathbf{r}_N\}$, is represented in figure 2:

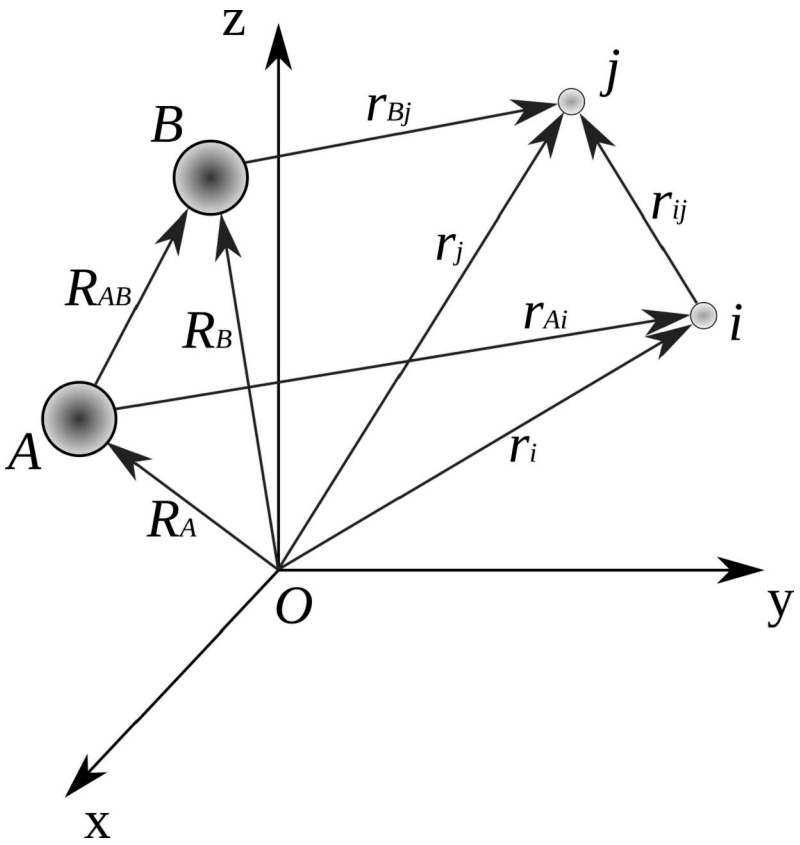

Figure 2 – Representation of a molecular system in Cartesian coordinates.

Seeking to describe the electronic structure and dynamics of molecular systems, it is necessary to solve the non-relativistic time-independent Schrödinger equation given by:

$$\hat{H}\Psi(\mathbf{r}, \mathbf{R}) = E\Psi(\mathbf{r}, \mathbf{R}) \tag{3.1}$$

where $\Psi(\mathbf{r}, \mathbf{R})$ is the wavefunction of the molecular system, E is the energy, and $\hat{H}$ is the Hamiltonian operator, which is described by:

$$\hat{H} = \hat{T}_e + \hat{T}_n + \hat{V}_{en} + \hat{V}_{ee} + \hat{V}_{nn} \tag{3.2}$$

where:

$\hat{T}_e \equiv$ kinetic energy operator of electrons;
$\hat{T}_n \equiv$ kinetic energy operator of the nuclei;
$\hat{V}_{en} \equiv$ potential energy operator due to the Coulomb electron-nucleus attraction;
$\hat{V}_{ee} \equiv$ potential energy operator due to Coulomb electron-electron repulsion;
$\hat{V}_{nn} \equiv$ potential energy operator due to nucleus-nucleus Coulomb repulsion.

The kinetic terms are obtained, within the configuration space, from the canonical definition of the kinetic energy operator $\hat{T} \equiv \hat{p}^2/2m$, where $\hat{p} \equiv -i\,\hbar\nabla$ (SZABO; OSTLUND, 2012), while the Coulomb potential terms are taken from the usual expression $U = kq_1q_2/r_{12}$, where $k = 1/4\pi\varepsilon_0$ (JACKSON, 1999). Thus, we have that the Hamiltonian operator is given by:

$$\hat{H} = -\frac{\hbar^2}{2m_e}\sum_{i=1}^{N}\nabla_i^2 - \frac{\hbar^2}{2}\sum_{A=1}^{M}\frac{\nabla_A^2}{M_A} - \sum_{A=1}^{M}\sum_{i=1}^{N}k\frac{Z_Ae^2}{r_{Ai}} + \sum_{i=1}^{N-1}\sum_{j>i}^{N}k\frac{e^2}{r_{ij}} + \sum_{A=1}^{M-1}\sum_{B>A}^{M}k\frac{(Z_Ae)(Z_Be)}{R_{AB}} \tag{3.3}$$

where M_A is the mass of the atomic nucleus A, Z_A is the atomic number of the nucleus A, e is the elementary charge, and m_e is the electron rest mass.

Within Atomic and Molecular Physics, it is usual to work with atomic units (a.u.): $\hbar = c = m_e = e = k = 1$. In this system, the energy unit is Hartree (Ha). Therefore, the mathematical treatment of this work will take place primarily in this system of units. Thus, converting the Hamiltonian operator (3.3) to atomic units and replacing it in the equation (3.1), the time independent Schrödinger equation that describes a molecular system is obtained:

$$\left[-\frac{1}{2}\sum_{i=1}^{N}\nabla_i^2 - \frac{1}{2}\sum_{A=1}^{M}\frac{\nabla_A^2}{M_A} - \sum_{A=1}^{M}\sum_{i=1}^{N}\frac{Z_A}{r_{Ai}} + \sum_{i=1}^{N-1}\sum_{j>i}^{N}\frac{1}{r_{ij}} + \sum_{A=1}^{M-1}\sum_{B>A}^{M}\frac{Z_AZ_B}{R_{AB}}\right]\Psi = E\Psi \tag{3.4}$$

The equation (3.4) is extremely complex, therefore, solving it analytically or numerically, is a difficult task due to the coupling between electrons and nuclei. For systems with $N > 2$ this equation does not even have an analytical solution. Thus, it is necessary to use some approximations. The decisive approximation to be used is the Born-Oppenheimer Approximation (BOA) (BORN; OPPENHEIMER, 2000).

3.1 Born-Oppenheimer Approximation (BOA)

Firstly, it is necessary to consider the adiabatic expansion (KOŁSOS, 1970), which assumes that if a given perturbation in a system is slow enough, the system can adjust to the new configuration so that its eigenstate is conserved. Consequently, separation of

variables can be performed so that the wavefunction of the molecular system is separated into a wavefunction that describes its nuclear properties Ψ_N, and another wavefunction that describes its electronic properties Ψ_e.

$$\Psi(\mathbf{r},\mathbf{R}) = \Psi_e(\mathbf{r};\mathbf{R})\Psi_N(\mathbf{R}) \tag{3.5}$$

where $\Psi_e(\mathbf{r};\mathbf{R})$ depends explicitly on the electronic coordinates and parametrically on the nuclear coordinates, in other words, for different nuclear configurations, Ψ_e is a distinct function of the electronic coordinates. On the other hand, $\Psi_N(\mathbf{R})$ depends only on the nuclei coordinates. Thus, plugging the equation (3.5) into (3.4), one gets:

$$\begin{aligned} &-\frac{1}{2}\sum_{i=1}^{N}\nabla_i^2(\Psi_e\Psi_N) - \frac{1}{2}\sum_{A=1}^{M}\frac{\nabla_A^2}{M_A}(\Psi_e\Psi_N) - \sum_{A=1}^{M}\sum_{i=1}^{N}\frac{Z_A}{r_{Ai}}\Psi_e\Psi_N + \\ &+\sum_{i=1}^{N-1}\sum_{j>i}^{N}\frac{1}{r_{ij}}\Psi_e\Psi_N + \sum_{A=1}^{M-1}\sum_{B>A}^{M}\frac{Z_AZ_B}{R_{AB}}\Psi_e\Psi_N = E\Psi_e\Psi_N \end{aligned} \tag{3.6}$$

Recognizing that the Laplacian is the divergent of the gradient, the Laplacian present in the second term of the above equation can be rewritten as follows:

$$\begin{aligned} \nabla_A^2(\Psi_e\Psi_N) &= \nabla_A.\nabla_A(\Psi_e\Psi_N) \\ &= \nabla_A\left(\Psi_N\nabla_A\Psi_e + \Psi_e\nabla_A\Psi_N\right) \\ &= \Psi_N\nabla_A.\nabla_A\Psi_e + \nabla_A\Psi_N.\nabla_A\Psi_e + \nabla_A\Psi_e.\nabla_A\Psi_N + \Psi_e\nabla_A.\nabla_A\Psi_N \\ &= \Psi_N\nabla_A^2\Psi_e + 2\nabla_A\Psi_e.\nabla_A\Psi_N + \Psi_e\nabla_A^2\Psi_N \end{aligned} \tag{3.7}$$

Thus, the second term of the equation (3.6) becomes:

$$-\frac{1}{2}\sum_{A=1}^{M}\frac{\nabla_A^2}{M_A}(\Psi_e\Psi_N) = -\frac{1}{2}\sum_{A=1}^{M}\frac{\Psi_N\nabla_A^2\Psi_e + 2\nabla_A\Psi_e.\nabla_A\Psi_N + \Psi_e\nabla_A^2\Psi_N}{M_A} \tag{3.8}$$

Since nuclei are considerably more massive than electrons, they move more slowly and therefore the problem can be approximated to a system where electrons move in a field of fixed nuclei. Hence, the terms $\nabla_A^2\Psi_e$ and $\nabla_A\Psi_e$ present in (3.8) are negligible. This approximation is the famous Born-Oppenheimer approximation:

$$-\frac{1}{2}\sum_{A=1}^{M}\frac{\nabla_A^2}{M_A}[\Psi_e(\mathbf{r};\mathbf{R})\Psi_N(\mathbf{R})] \approx -\frac{1}{2}\Psi_e(\mathbf{r};\mathbf{R})\sum_{A=1}^{M}\frac{\nabla_A^2}{M_A}\Psi_N(\mathbf{R}) \tag{3.9}$$

From the application of the BOA, the time-independent Schrödinger equation can be decoupled into an electronic part and a nuclear part by plugging the equation (3.9) in the equation (3.6):

$$\begin{aligned} &-\frac{1}{2}\sum_{i=1}^{N}\nabla_i^2[\Psi_e\Psi_N] - \frac{1}{2}\Psi_e\sum_{A=1}^{M}\frac{\nabla_A^2}{M_A}\Psi_N - \sum_{A=1}^{M}\sum_{i=1}^{N}\frac{Z_A}{r_{Ai}}\Psi_e\Psi_N + \\ &+\sum_{i=1}^{N-1}\sum_{j>i}^{N}\frac{1}{r_{ij}}\Psi_e\Psi_N + \sum_{A=1}^{M-1}\sum_{B>A}^{M}\frac{Z_AZ_B}{R_{AB}}\Psi_e\Psi_N = E\Psi_e\Psi_N \end{aligned} \tag{3.10}$$

Dividing the equation (3.10) by $\Psi_e(\mathbf{r};\mathbf{R})\Psi_N(\mathbf{R})$ and then separating the terms with $\Psi_e(\mathbf{r};\mathbf{R})$ and $\Psi_N(\mathbf{R})$, that is, separating the electronic part from the nuclear part, one obtains:

$$-\frac{1}{2\Psi_e}\sum_{i=1}^{N}\nabla_i^2\Psi_e-\sum_{A=1}^{M}\sum_{i=1}^{N}\frac{Z_A}{r_{Ai}}+\sum_{i=1}^{N-1}\sum_{j>i}^{N}\frac{1}{r_{ij}}=\frac{1}{2\Psi_N}\sum_{A=1}^{M}\frac{\nabla_A^2}{M_A}\Psi_N-\sum_{A=1}^{M-1}\sum_{B>A}^{M}\frac{Z_AZ_B}{R_{AB}}+E \tag{3.11}$$

The equality above is correct provided that both sides are equal to a separation constant $\varepsilon(\mathbf{R})$:

$$-\frac{1}{2\Psi_e}\sum_{i=1}^{N}\nabla_i^2\Psi_e-\sum_{A=1}^{M}\sum_{i=1}^{N}\frac{Z_A}{r_{Ai}}+\sum_{i=1}^{N-1}\sum_{j>i}^{N}\frac{1}{r_{ij}}=\varepsilon(\mathbf{R}) \tag{3.12}$$

$$\frac{1}{2\Psi_N}\sum_{A=1}^{M}\frac{\nabla_A^2}{M_A}\Psi_N-\sum_{A=1}^{M-1}\sum_{B>A}^{M}\frac{Z_AZ_B}{R_{AB}}+E=\varepsilon(\mathbf{R}) \tag{3.13}$$

To obtain the electronic Schrödinger equation, the equation (3.12) must be multiplied by $\Psi_e(\mathbf{r};\mathbf{R})$:

$$\left(-\frac{1}{2}\sum_{i=1}^{N}\nabla_i^2-\sum_{A=1}^{M}\sum_{i=1}^{N}\frac{Z_A}{r_{Ai}}+\sum_{i=1}^{N-1}\sum_{j>i}^{N}\frac{1}{r_{ij}}\right)\Psi_e(\mathbf{r};\mathbf{R})=\varepsilon(\mathbf{R})\Psi_e(\mathbf{r};\mathbf{R}) \tag{3.14}$$

Thus, the electronic Hamiltonian operator is given by:

$$\hat{H}_e=-\frac{1}{2}\sum_{i=1}^{N}\nabla_i^2-\sum_{A=1}^{M}\sum_{i=1}^{N}\frac{Z_A}{r_{Ai}}+\sum_{i=1}^{N-1}\sum_{j>i}^{N}\frac{1}{r_{ij}} \tag{3.15}$$

Similarly, multiplying the equation (3.13) by $\Psi_N(\mathbf{R})$ and rearranging its terms, the nuclear Schrödinger equation is obtained:

$$\left(-\frac{1}{2}\sum_{A=1}^{M}\frac{\nabla_A^2}{M_A}+\sum_{A=1}^{M-1}\sum_{B>A}^{M}\frac{Z_AZ_B}{R_{AB}}+\varepsilon(\mathbf{R})\right)\Psi_N(\mathbf{R})=E\Psi_N(\mathbf{R}) \tag{3.16}$$

The term $\varepsilon(\mathbf{R})$ can be interpreted as the electronic potential energy that acts on the nuclei for a given nuclear configuration $\mathbf{R}$. Thus, it is possible to define a total potential to which the nuclei are subjugated by adding $\varepsilon(\mathbf{R})$ and the potential due to the nucleus-nucleus Coulomb repulsion:

$$V(\mathbf{R})\equiv\sum_{A=1}^{M-1}\sum_{B>A}^{M}\frac{Z_AZ_B}{R_{AB}}+\varepsilon(\mathbf{R}) \tag{3.17}$$

Hence, the Hamiltonian operator is given by:

$$\hat{H}_N=-\frac{1}{2}\sum_{A=1}^{M}\frac{\nabla_A^2}{M_A}+V(\mathbf{R}) \tag{3.18}$$

Thereby, the molecular problem is properly characterized. Solving the electronic Schrödinger equation (3.14) for different nuclear configurations leads to the potential energy curve (PEC), for a system consisting of two bodies, or potential energy surface (PES), for molecular systems composed of more than two bodies. Hence, the nuclear Schrodinger equation (3.16) can then be solved.

4 Variational Method

The variational principle is a method to approximate the energies of a system for which the Hamiltonian is known. It is based on the simple observation that for any normalized wave function, the expected energy value is greater than the ground state energy E_0. Without much detail, this occurs because a normalized wavefunction, other than the ground-state wavefunction, will be a linear combination of other wavefunctions, which shifts the expected value of energy upwards. Thus, the method consists of choosing a trial function with adjustable parameters, finding the expected energy value, and then minimizing this result in relation to the adjustment parameters.

In the study of molecular systems, it is common to use a trial function given by the linear combination of n linearly independent functions:

$$|\psi_{\text{trial}}\rangle = \sum_{j=1}^{n} c_j |\phi_j\rangle \,; \;\; \langle\psi_{\text{trial}}| = \sum_{j=1}^{n} c_j^* \langle\phi_j| \tag{4.1}$$

Thus, the variational energy is obtained by the expected value of the system's Hamiltonian:

$$E_{\text{trial}} = \frac{\langle\psi_{\text{trial}}| \hat{H} |\psi_{\text{trial}}\rangle}{\langle\psi_{\text{trial}}|\psi_{\text{trial}}\rangle} = \frac{\sum\limits_{i=1}^{n}\sum\limits_{j=1}^{n} c_i^* c_j \langle\phi_i| \hat{H} |\phi_j\rangle}{\sum\limits_{i=1}^{n}\sum\limits_{j=1}^{n} c_i^* c_j \langle\phi_i|\phi_j\rangle} \tag{4.2}$$

Considering the matrix representation, the term $\langle\phi_i| \hat{H} |\phi_j\rangle$ corresponds to the element H_{ij} of the Hamiltonian matrix while $\langle\phi_i|\phi_j\rangle$ corresponds to the element S_{ij} of the overlap matrix. Thus:

$$E_{\text{trial}} = \frac{\sum\limits_{i=1}^{n}\sum\limits_{j=1}^{n} c_i^* c_j H_{ij}}{\sum\limits_{i=1}^{n}\sum\limits_{j=1}^{n} c_i^* c_j S_{ij}} \tag{4.3}$$

Rearranging the equation (4.3):

$$\sum_{i=1}^{n}\sum_{j=1}^{n} c_i^* c_j H_{ij} = E_{\text{trial}} \sum_{i=1}^{n}\sum_{j=1}^{n} c_i^* c_j S_{ij} \tag{4.4}$$

The coefficients c_i are adjustable parameters that must be optimized to provide a trial function that approximates to the true function. Therefore, the variational energy is minimized with respect to the linear coefficients c_i:

$$\frac{\partial E_{\text{trial}}}{\partial c_i} = 0 \tag{4.5}$$

Differentiating both sides of the equation (4.4) with respect to the kth coefficient, one obtains:

$$\sum_{i=1}^{n}\sum_{j=1}^{n}\left[\frac{\partial c_i^*}{\partial c_k}c_j + \frac{\partial c_j}{\partial c_k}c_i^*\right]H_{ij} = \frac{\partial E_{\text{trial}}}{\partial c_k}\sum_{i=1}^{n}\sum_{j=1}^{n}c_i^* c_j S_{ij} + E_{\text{trial}}\sum_{i=1}^{n}\sum_{j=1}^{n}\left[\frac{\partial c_i^*}{\partial c_k}c_j + \frac{\partial c_j}{\partial c_k}c_i^*\right]S_{ij} \tag{4.6}$$

At the minimum variational energy, when $\frac{\partial E_{\text{trial}}}{\partial c_k} = 0$, the equation above can be simplified to:

$$\sum_{i=1}^{n}\sum_{j=1}^{n}\left[\frac{\partial c_i^*}{\partial c_k}c_j + \frac{\partial c_j}{\partial c_k}c_i^*\right]H_{ij} = E_{\text{trial}}\sum_{i=1}^{n}\sum_{j=1}^{n}\left[\frac{\partial c_i^*}{\partial c_k}c_j + \frac{\partial c_j}{\partial c_k}c_i^*\right]S_{ij} \tag{4.7}$$

Since the coefficients are independent, one can show that $\frac{\partial c_i^*}{\partial a_k} = \delta_{ik}$. Moreover, the Hamiltonian operator is Hermitian , and the definition of S_{ij} implies that $S_{ij} = S_{ji}$. Therefore, the equation (4.7) reduces to:

$$\sum_{j=1}^{n}H_{kj}c_j = E_{\text{trial}}\sum_{j=1}^{n}S_{kj}c_j \tag{4.8}$$

The equation (4.8) is a secular equation.

Provided that the basis functions are orthonormal, that is, $S_{kj} = \delta_{kj}$, the equation (4.8) can be simplified to the well-known eigenvalue problem:

$$\sum_{j=1}^{n}H_{kj}c_j = E_{\text{trial}}c_k \tag{4.9}$$

Rewriting in matrix notation:

$$\mathbf{HC} = E_{\text{trial}}\mathbf{C} \tag{4.10}$$

where $\mathbf{C}$ is the coefficients matrix.

Thus, the equation above can be solved in such a way as to generate n orthonormal eigenvectors $\mathbf{C}^\alpha$ associated with their eigenvalues E_α, which for convenience are indexed so that $E_0 \leq E_1 \leq \cdots \leq E_{n-1}$. Then, the eigenvector $\mathbf{C}^0$ gives an approximation to the ground state, $\mathbf{C}^1$ gives an approximation to the first excited state, and so on.

5 Electronic Schrödinger Equation

The electronic Schrödinger equation, expressed in the equation (3.14), describes the movement of electrons given a nuclear configuration. Hence, $\varepsilon(\mathbf{R})$ corresponds to the electronic energy of the system. Thus, the solutions of (3.14) for different nuclear configurations allow obtaining a PEC or a PES, which can then be adjusted by analytical expressions.

Finding approximate solutions for the electronic Schrödinger equation has been one of the biggest concerns of quantum physicists and chemists since the birth of Quantum Mechanics. At the heart of all this problem is the Hartree-Fock approximation, which served as a foundation for the development of more accurate approximations. Thus, the understanding of this approximation is fundamental to understand current methods, such as the density functional theory (DFT), which will be used in this work to determine the electronic properties of the systems comprised by the graphene quantum dot and the adsorbates: CO, NO_2, SO_2, and NH_3.

5.1 Hartree-Fock Approximation

One of the first models that achieved relative success in solving the electronic Schrödinger equation and representing the electronic structure of a microscopic system was the Hartree-Fock (HF) model, proposed by physicists Douglas Rayner Hartree (HARTREE, 1957) and Vladimir Aleksandrovich Fock (FOCK, 2004). This model was so effective at the time that it became a reference in the study of the representation of atomic and molecular systems, constituting the first approximation for later and more accurate models.

The electronic Hamiltonian (3.15) depends only on the spatial coordinates of the electrons. However, to fully describe an electron it is necessary to specify its spin. Therefore, the spin functions $\alpha(\omega)$ and $\beta(\omega)$ are introduced, which correspond to spin $+\frac{1}{2}$ and spin $-\frac{1}{2}$ respectively. These spin functions are orthonormal so that:

$$\int \alpha^*(\omega)\alpha(\omega)d\omega = \int \beta^*(\omega)\beta(\omega)d\omega = 1 \tag{5.1}$$

$$\int \alpha^*(\omega)\beta(\omega)d\omega = \int \beta^*(\omega)\alpha(\omega)d\omega = 0 \tag{5.2}$$

Thus, in addition to the three spatial coordinates $\mathbf{r}$, a spin coordinate ω is needed to describe the electron. The set of spatial coordinates with the spin coordinate is denoted

by $\mathbf{x}$:

$$\mathbf{x} \equiv \{\mathbf{r}, \omega\} \tag{5.3}$$

Hence, the wavefunction of an N-electron system can be written as $\Psi_e(\mathbf{x}_1, \ldots, \mathbf{x}_N)$. Nonetheless, to satisfactorily describe an electronic system, the wave function Ψ_e, in addition to satisfying the Schrödinger electronics (3.14), must obey Pauli's Exclusion Principle: "Two or more identical fermions cannot occupy the same quantum state simultaneously"(SZABO; OSTLUND, 2012). This principle implies that the wavefunction of many electrons must be antisymmetric with respect to an exchange of coordinates $\mathbf{x}$ of any two electrons in the system:

$$\Psi_e(\mathbf{x}_1, \ldots, \mathbf{x}_i, \ldots, \mathbf{x}_j, \ldots, \mathbf{x}_N) = -\Psi_e(\mathbf{x}_1, \ldots, \mathbf{x}_j, \ldots, \mathbf{x}_i, \ldots, \mathbf{x}_N) \tag{5.4}$$

An orbital is defined as the wave function for an electron. A spatial orbital $\psi_i(\mathbf{r})$ is the wavefunction that describes the spatial distribution of an electron such that $|\psi_i(\mathbf{r})|^2 d\mathbf{r}$ is the probability of finding the electron in an infinitesimal volume element $d\mathbf{r}$ around $\mathbf{r}$. It is usually assumed that space orbitals form an orthonormal set:

$$\int \psi_i^*(\mathbf{r})\psi_j(\mathbf{r})d\mathbf{r} = \delta_{ij} \tag{5.5}$$

On the other hand, the wavefunction of an electron that describes both its spatial distribution and its spin is called spin-orbital $\chi(\mathbf{x})$. Thus, from a spatial orbital, one can form two distinct spin-orbitals, one corresponding to spin $\frac{1}{2}$ and the other to spin $-\frac{1}{2}$:

$$\chi(\mathbf{x}) = \begin{cases} \psi(\mathbf{r})\alpha(\omega) \\ \quad \text{Ou} \\ \psi(\mathbf{r})\beta(\omega) \end{cases} \tag{5.6}$$

Given a set of K spatial-orbitals $\{\psi_1, \psi_2, \ldots, \psi_K\}$, it is possible to generate a set of $2K$ spin-orbitals $\{\chi_1, \chi_2, \ldots, \chi_{2K}\}$ where:

$$\begin{aligned} \psi_i(\mathbf{r})\alpha(\omega) &= \chi_{2i-1}(\mathbf{x}) \\ \psi_i(\mathbf{r})\beta(\omega) &= \chi_{2i}(\mathbf{x}) \end{aligned} \tag{5.7}$$

A first attempt at formulating a many-electron wavefunction came in the form of the Hartree product, which is a wavefunction obtained from the product of the spin-orbitals of each electron in the system:

$$\Psi^{HP}(\chi_1, \chi_2, \ldots, \chi_N) = \chi_1(\mathbf{x}_1) \times \chi_2(\mathbf{x}_2) \times \cdots \times \chi_N(\mathbf{x}_N) \tag{5.8}$$

Hartree's product does not satisfy the antisymmetry principle. However, it is possible to obtain an antisymmetric wave function by applying the antisymmetric operator.

This process is equivalent to calculating the Slater determinant (SLATER, 1929):

$$\Psi(\mathbf{x}_1, \mathbf{x}_2, \ldots, \mathbf{x}_N) = \frac{1}{\sqrt{N!}} \begin{vmatrix} \chi_1(\mathbf{x}_1) & \chi_2(\mathbf{x}_1) & \cdots & \chi_N(\mathbf{x}_1) \\ \chi_1(\mathbf{x}_2) & \chi_2(\mathbf{x}_2) & \cdots & \chi_N(\mathbf{x}_2) \\ \vdots & \vdots & \ddots & \vdots \\ \chi_1(\mathbf{x}_N) & \chi_2(\mathbf{x}_N) & \cdots & \chi_N(\mathbf{x}_N) \end{vmatrix} \tag{5.9}$$

where $1/\sqrt{N!}$ is the normalization factor.

It is convenient to write the Slater determinant using a simpler notation that already includes the normalization term:

$$\Psi(\mathbf{x}_1, \mathbf{x}_2, \ldots, \mathbf{x}_N) = |\chi_1 \chi_2 \cdots \chi_N\rangle \tag{5.10}$$

Thus, the Slater determinant provides the simplest antisymmetric wavefunction that can describe the ground state of an N-electron system.

$$|\Psi_0\rangle = |\chi_1 \chi_2 \cdots \chi_N\rangle \tag{5.11}$$

Regarding the variational principle, the Slater determinant that best describes the ground state is the one for which energy is minimal:

$$E_0 = \langle \Psi_0 | \, \hat{H}_e \, | \Psi_0 \rangle \tag{5.12}$$

where $\hat{H}_e$ is the electronic Hamiltonian (3.15).

The variational flexibility of (5.11) lies in the choice of spin-orbitals. Thereby, by minimizing E_0 with respect to the choice of these orbitals, the Hartree-Fock equation (SZABO; OSTLUND, 2012) is found:

$$\hat{f}_i \chi_a(\mathbf{x}_i) = \varepsilon \chi_a(\mathbf{x}_i) \tag{5.13}$$

where $\hat{f}_i$ is an effective one-electron operator, called the Fock operator:

$$\hat{f}_i = \hat{h}_i + V_i^{HF} \tag{5.14}$$

$\hat{h}(\mathbf{r}_i)$ is the core-Hamiltonian of one particle:

$$\hat{h}_i = -\frac{1}{2}\nabla_i^2 - \sum_{A=1}^{M} \frac{Z_A}{r_{iA}} \tag{5.15}$$

The Hartree-Fock potential, V^{HF}, is the average potential experienced by the ith electron due to the presence of other electrons:

$$V_i^{HF} = \sum_{b \neq a}^{N} [\hat{J}_b(\mathbf{x}_i) - \hat{K}_b(\mathbf{x}_i)] \tag{5.16}$$

where $\hat{J}$ and $\hat{K}$ are the Coulomb operator and exchange operator respectively, given by:

$$\hat{J}_b(\mathbf{x}_i)\chi_a(\mathbf{x}_i) = \left[\int \chi_b^*(\mathbf{x}_j)\frac{1}{r_{ij}}\chi_b(\mathbf{x}_j)d\mathbf{x}_j\right]\chi_a(\mathbf{x}_i) \tag{5.17}$$

$$\hat{K}_b(\mathbf{x}_i)\chi_a(\mathbf{x}_i) = \left[\int \chi_b^*(\mathbf{x}_j)\frac{1}{r_{ij}}\chi_a(\mathbf{x}_j)d\mathbf{x}_j\right]\chi_b(\mathbf{x}_i) \tag{5.18}$$

Since the potential perceived by the ith electron depends on the spin-orbitals of the other electrons, the Hartree-Fock equation (5.13) is nonlinear and, therefore, will be solved iteratively. The procedure to solve the Hartree-Fock equation is called the self-consistent field method (SCF).

The basic idea behind the SCF method is that one can calculate the average field V^{HF}, perceived by each electron, from an initial guess of the orbital spins, and thus solve (5.13) to obtain a new set of orbitals. Using these new orbitals a new field is obtained so that this procedure is repeated until the change in V^{HF} is minimal.

From the solution of the Hartree-Fock equation, an orthonormal set $\{\chi_k\}$ of spin-orbitals with energies $\{\varepsilon_k\}$ is obtained. The N spin-orbitals with lower energies are called occupied orbitals. Thus, the Slater determinant formed from these occupied orbitals constitutes the Hartree-Fock wave function for the ground state, so that it represents the best variational approximation for the ground state of the system.

Unoccupied spin-orbitals are called virtual orbitals. In the mathematical treatment done in this work, these orbitals will be indexed with the indices $(r, s, t, \dots)$ while the occupied orbitals are indexed by $(a, b, c, \dots)$.

Theoretically, there are infinite solutions to the Hartree-Fock equation and, consequently, infinite virtual orbitals. However, in practice, the equation (5.13) is solved by introducing a finite set of spatial functions $\{\phi_1(\mathbf{r}), \phi_2(\mathbf{r}), \dots, \phi_{2K}(\mathbf{r})\}$. The larger the set, the greater the variational flexibility and, consequently, the smaller the expected value $E_0 = \langle\Psi_0|\,\hat{H}_e\,|\Psi_0\rangle$.

Therefore, the spatial parts of spin-orbitals with spin $+\frac{1}{2}$ can be written in terms of these set of functions. Similarly, the spatial parts of spin-orbitals with spin $-\frac{1}{2}$ spin can also be written in terms of this set.

Thus, the spatial orbitals in (5.13) are approximated by a linear combination of known spatial functions:

$$\psi_a(\mathbf{r}_i) = \sum_{\nu=1}^{K} c_{\nu a}\phi_\nu(\mathbf{r}_i) \tag{5.19}$$

Substituting this expansion in the Hartree-Fock equation and following the variational method procedure produces the following secular equation:

$$\sum_{\nu=1}^{K} F_{\mu\nu}c_{\nu a} = \varepsilon\sum_{\nu=1}^{K} S_{\mu\nu}c_{\nu a} \tag{5.20}$$

Rewriting in matrix notation:

$$\mathbf{FC} = \varepsilon\mathbf{SC} \tag{5.21}$$

where $\mathbf{F}$ is the matrix representation of the Fock operator, $\mathbf{C}$ is the matrix of coefficients and $\mathbf{S}$ is the overlap matrix. This equation is called the Hartree-Fock-Roothaan (ROOTHAAN, 1951) equation. The matrix elements of the Fock matrix are given by:

$$F_{\mu\nu} = H_{\mu\nu} + G_{\mu\nu} \tag{5.22}$$

where H_{ij} is the one-electron integral:

$$H_{ij} = \int \phi_\mu(\mathbf{r}_i)\hat{h}\phi_\nu(\mathbf{r}_j)d\mathbf{r} \tag{5.23}$$

and $G_{\mu\nu}$ is the two-electron integral:

$$\begin{aligned} G_{\mu\nu} = \sum_{\lambda\sigma} P_{\lambda\sigma} \Bigg[\int\int \phi_\mu^*(\mathbf{r}_i)\phi_\nu(\mathbf{r}_i)\frac{1}{r_{ij}}\phi_\lambda^*(\mathbf{r}_j)\phi_\sigma(\mathbf{r}_j)d\mathbf{r}_i d\mathbf{r}_j \\ -\frac{1}{2}\int\int \phi_\mu^*(\mathbf{r}_i)\phi_\sigma(\mathbf{r}_i)\frac{1}{r_{ij}}\phi_\lambda^*(\mathbf{r}_j)\phi_\nu(\mathbf{r}_j)d\mathbf{r}_i d\mathbf{r}_j \Bigg] \end{aligned} \tag{5.24}$$

where $P_{\lambda\sigma}$ is a density matrix element, defined as:

$$P_{\lambda\sigma} = 2\sum_{a=1}^{N/2} c_{\lambda a}^* c_{\sigma a} \tag{5.25}$$

The matrix $\mathbf{P}$ completely specifies the electronic density:

$$\rho(\mathbf{r}) = 2\sum_{a=1}^{N/2} \psi_a^*(\mathbf{r})\psi_a(\mathbf{r}) = \sum_{\lambda\sigma} P_{\lambda\sigma}\phi_\lambda^*(\mathbf{r})\phi_\sigma(\mathbf{r}) \tag{5.26}$$

Summarily, the SCF method in the context of the Hartree-Fock approximation (Figure 3) consists of the following steps:

1. Specify coordinates and nuclear charges, and a base set $\phi_\nu(\mathbf{r}_i)$;
2. Determine the coefficients of the expansion (5.19);
3. Calculate the matrix elements of $\mathbf{F}$ and $\mathbf{S}$;
4. Diagonalize the Fock matrix;
5. Solve the Roothaan equation (5.21) in order to determine a new set of coefficients;
6. Repeat steps 2 to 5 until the convergence criteria is met.

In possession of the final results, one can proceed to calculations of electronic properties. It is also possible to adjust the obtained PEC or PES to an analytical form that will be placed in the nuclear Schrödinger equation and then investigate the dynamic properties

of the system, such as rotation and vibration.

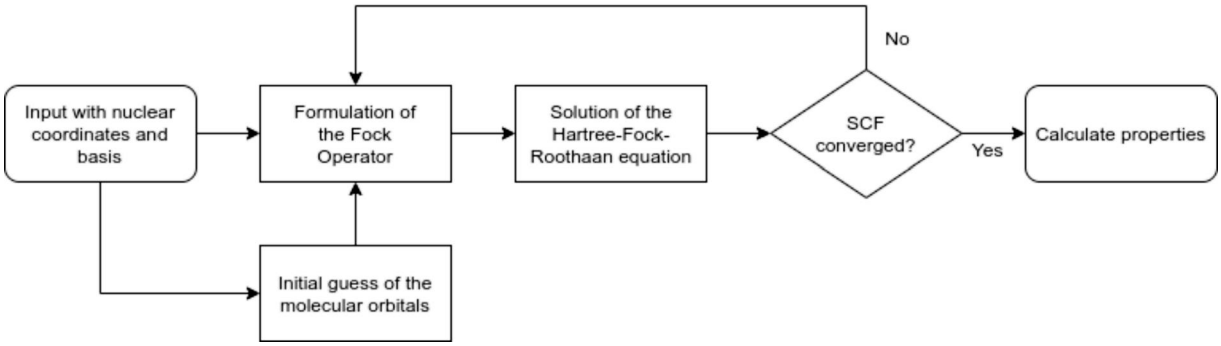

Figure 3 – Flowchart of the self-consistent field method in the context of the Hartree-Fock approximation.

Describing the ground state of a many-electron system considering only one Slater determinant yields a difference between the exact (non-relativistic) energy and the energy found by the Hartree-Fock approximation. This difference is called electronic correlation energy:

$$E_{corr} = E_{exact} - E_{HF} \tag{5.27}$$

The cause of this difference is the fact that in the Hartree-Fock approximation the ith electron responds to the average location of the other electrons, a fact that ignores the instantaneous tendency of the electrons to avoid each other to minimize repulsion, in other words, it ignores the electronic correlation. The Hartree-Fock approximation laid the foundations for many methods that include electronic correlation effects. Among these post-HF methods, the following stand out: Møller-plessest (MØLLER; PLESSET, 1934), Configuration Interaction (FANO, 1961), and Coulple Cluster (III; BARTLETT, 1982).

An alternative way to solve the many-electron problem is to use the electron density $\rho(\mathbf{r})$ instead of N wave eigenfunctions $\psi(\mathbf{r})$, so that electronic correlation is not ignored. This methodology is called Density Functional Theory (DFT) and will be discussed in more detail in the next section.

5.2 Density Functional Theory

In 1927, Llewellyn Thomas and Enrico Fermi were the first to use the electron density $\rho(\mathbf{r})$ as a fundamental variable in the description of a many-electron system through an approximation that became known as the Thomas-Fermi approximation. However, it was only in 1968 that W. Kohn and L. J. Sham presented an exact solution to the problem

of many electrons using electron density, such an accomplishment granted them the Nobel Prize in Chemistry in 1998.

Density Functional theory provides an approach to solving the many-electron problem, in which the energy of the system is described as an electron density functional. This theory has become extremely popular mainly because it requires less computational power when compared to post-HF methods.

The main idea behind the Kohn-Sham formalism was to consider that the ground-state electron density of a many-electron system can be expressed as the ground-state density of a non-interacting electron system.

The DFT was built from two theorems established by Hohenberg and Kohn (KOHN; SHAM, 1965):

Theorem 1: *The external potential $V_{ext}(\mathbf{r})$, and hence the total energy, is a unique functional of the electron density.*

Theorem 2: *One can define a universal functional $F[\rho(\mathbf{r})]$ in terms of density, such that the ground state energy corresponds to the global minimum of this functional.*

Therefore, the first theorem implies that the ground-state electron density must contain the same information as the wavefunction associated with the same system. The second theorem states that the ground-state energy can be obtained by the variational method, that is, $E_{KS}[\rho_0] \geq E_0$, where ρ_0 is the density that minimizes the energy functional.

Within the proposed Kohn and Sham model, comprised of non-interacting particles, the energy functional is given by:

$$E_{KS}[\rho] = T_0[\rho] + \int V_{ext}(\mathbf{r})\rho(\mathbf{r})d\mathbf{r} + E_H[\rho] + E_{XC}[\rho] \tag{5.28}$$

where $T_0[\rho]$ is the average kinetic energy of a non-interacting electron system, whose density is equal to that of an interacting system, $E_H[\rho] \equiv \frac{1}{2}\int\int \frac{\rho(\mathbf{r})\rho(\mathbf{r}')}{|\mathbf{r}-\mathbf{r}'|}d\mathbf{r}d\mathbf{r}'$ is Hartree's energy and E_{XC} is the exchange-correlation energy. Thus, the universal functional is given by:

$$F[\rho(\mathbf{r})] = E_{KS}[\rho] - \lambda\left(\int \rho(\mathbf{r})d\mathbf{r} - N\right) \tag{5.29}$$

where λ is a Lagrange multiplier. Hence, to minimize this functional, one must calculate:

$$\frac{\delta F[\rho]}{\delta \rho} = 0 \tag{5.30}$$

Thus, applying the definition of electron density $\rho(\mathbf{r})$ used in the minimization

above results in:

$$\left[-\frac{1}{2}\nabla^2 + V_{\text{ext}} + \underbrace{\frac{\delta E_H[\rho]}{\delta\rho}}_{V_H(\mathbf{r})} + \underbrace{\frac{\delta E_{XC}[\rho]}{\delta\rho}}_{V_{XC}(\mathbf{r})}\right]\psi_a(\mathbf{r}) = \varepsilon_a\psi_a(\mathbf{r}) \tag{5.31}$$

where you can define an effective potential given by the sum of the external potential, Hartree potential, and exchange-correlation potential:

$$V_{\text{ef}} = V_{\text{ext}} + V_H + V_{XC} \tag{5.32}$$

The equation (5.31) is the so-called Kohn-Sham equation, which can be solved iteratively by an SCF method (Figure 4) similarly to the Hartree-Fock method. The SCF method in the context of Density Functional Theory consists of the following steps:

1. Specify coordinates, nuclear charges, and a base set $\phi_\nu(r_1)$;
2. Determine the electron density $\rho(\mathbf{r})$;
3. Construct the effective potential V_{ef};
4. Solve the Kohn-Sham equation in order to determine a new value for the electron density;
5. Repeat steps 2 to 5 until the convergence criterion is met.

After obtaining the final results, it is possible to proceed to the calculation of properties similarly to the Hartree-Fock approximation.

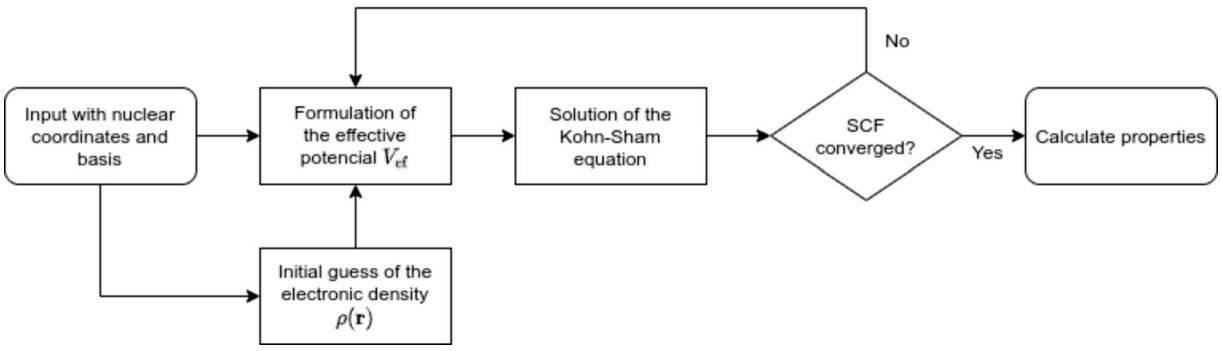

Figure 4 – Flowchart of the self-consistent field method in the context of Density Functional Theory.

The most challenging step in the description of the DFT is to determine the exchange-correlation functional, which has no analytical form except in the homogeneous

electron gas model. However, this term can be determined through local, or non-local approximations or even a combination of both. The main classes of approximations are (GROSS; DREIZLER, 2013):

- Local Density Approximation (LDA): Within this approximation, the exchange-correlation functional depends only on the electron density at each point in space. The LDA assumes that the density is the same at all points, hence, this approximation class tends to underestimate the exchange energy and overestimate the correlation energy. When dealing with systems governed by van der Waals interactions, in which dispersion terms are dominant, approximations of this class tend to overestimate bond energies;
- Generalized Gradient Approximation (GGA): Within this approximation, the inhomogeneity of the electron density is taken into account so that the exchange and correlation functional depends not only on the density at each point, but also of the density gradient. When dealing with systems governed by van der Waals interactions, approximations of this class tend to underestimate the binding energy, requiring the use of dispersion corrections;
- Meta-GGA approximation: Like GGA, this class of approximations is also non-local, with the difference that the terms of exchange and correlation also depend on the Laplacian of the electron density.

6 Nuclear Schrödinger Equation

The first step to solve the nuclear Schrödinger equation (3.16) is to plug in the analytical form adjusted for the PEC or PES, obtained from the solution of the electronic Schrödinger equation.

In this paper, the system comprised of the graphene quantum dot and the molecule to be adsorbed will be approximated by a two-body problem, in which the GQD will be treated as a body and the adsorbed molecule will be treated as a second body.

6.1 Two-Body Problem

To evaluate the two-body problem, consider a body of mass M_1, whose position relative to the origin is R_1, and a second body of mass M_2, whose position relative to the origin is R_2 , so that the relative position is given by R_{12} as illustrated in figure 5.

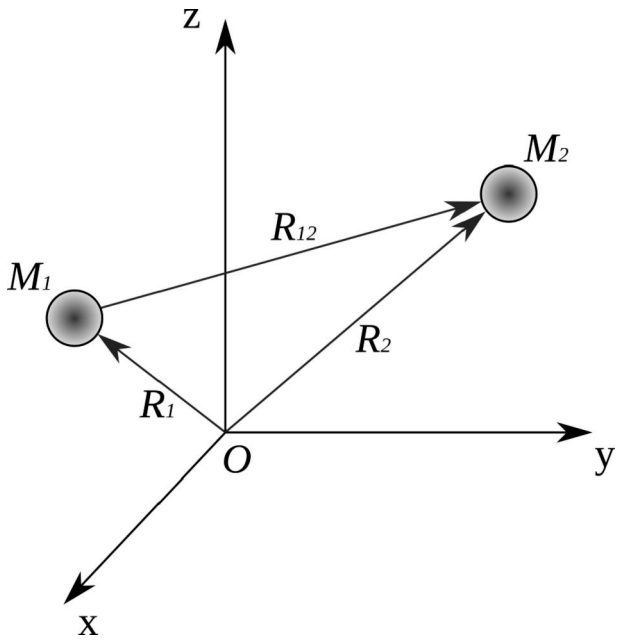

Figure 5 – Representation of a two-body system in Cartesian coordinates.

The Hamiltonian operator that describes this system is precisely the nuclear Hamiltonian (3.18) with $M = 2$. Due to the system's symmetry, a description in terms of the center of mass $\mathbf{R}_{CM}$ and the relative position $\mathbf{R}_{12}$ is more convenient. The classic Hamiltonian for this problem is given by:

$$H = \frac{1}{2M_1}\mathbf{P}_1^2 + \frac{1}{2M_2}\mathbf{P}_2^2 + V(\mathbf{R}_1, \mathbf{R}_2) \tag{6.1}$$

where $\mathbf{P}_1 = M_1\dot{\mathbf{R}}_1$ and $\mathbf{P}_2 = M_2\dot{\mathbf{R}}_2$ are the linear momenta of M_1 and M_2, respectively. The coordinate of the center of mass $\mathbf{R}_{CM}$ and the relative position $\mathbf{R}_{12}$ are described by:

$$\mathbf{R}_{CM} = \frac{M_1\mathbf{R}_1 + M_2\mathbf{R}_2}{M_1 + M_2} \tag{6.2}$$

$$\mathbf{R}_{12} = \mathbf{R}_2 - \mathbf{R}_1 \tag{6.3}$$

Thus, the positions $\mathbf{R}_1$ and $\mathbf{R}_2$ can be rewritten as:

$$\mathbf{R}_1 = \mathbf{R}_{CM} - \frac{M_2}{M_1 + M_2}\mathbf{R}_{12} \tag{6.4}$$

$$\mathbf{R}_2 = \mathbf{R}_{CM} + \frac{M_1}{M_1 + M_2}\mathbf{R}_{12} \tag{6.5}$$

Plugging the equations (6.4) and (6.5) into the equation (6.1) one obtains the Hamiltonian as a function of the center of mass and the relative coordinate:

$$H = \frac{1}{2(M_1 + M_2)}\mathbf{P}_{CM}^2 + \frac{1}{2\mu}\mathbf{P}_{12}^2 + V(\mathbf{R}_1, \mathbf{R}_2) \tag{6.6}$$

where $\mu \equiv M_1M_2/(M_1 + M_2)$ is the reduced mass of the system, $\mathbf{P}_{CM} \equiv (M1 + M_2)\dot{\mathbf{R}}_{CM}$ is the linear momentum of the center of mass, and $\mathbf{P}_{12} \equiv \mu\dot{\mathbf{R}}_{12}$ is the linear momentum associated with the relative motion of the bodies.

Therefore, in the context of quantum mechanics, the Hamiltonian operator that describes the two-body system as a function of R_{CM} and R_{12} is:

$$\hat{H} = \overbrace{-\frac{1}{2(M_1 + M_2)}\nabla_{CM}^2}^{\hat{H}_{CM}} \underbrace{-\frac{1}{2\mu}\nabla_{12}^2 + V(\mathbf{R}_{12})}_{\hat{H}_{\text{rel}}} \tag{6.7}$$

Note that this operator can be separated into one part regarding the movement of the center of mass, $\hat{H}_{CM}$, and another part regarding the relative movement of bodies, $\hat{H}_{\text{rel}}$. Thus, the nuclear Schödinger equation in the context of two bodies can be written as:

$$(\hat{H}_{CM} + \hat{H}_{\text{rel}})\Psi_N(\mathbf{R}_{CM}, \mathbf{R}_{12}) = E\Psi_N(\mathbf{R}_{CM}, \mathbf{R}_{12}) \tag{6.8}$$

Employing separation of variables, the nuclear wave function can be separated into two parts, one dependent on $\mathbf{R}_{CM}$ and another dependent on $\mathbf{R}_{12}$:

$$\Psi_N(\mathbf{R}_{CM}, \mathbf{R}_{12}) = \Phi_{CM}(\mathbf{R}_{CM})\Phi_{\text{rel}}(\mathbf{R}_{12}) \tag{6.9}$$

Plugging (6.9) into (6.8):

$$(\hat{H}_{CM} + \hat{H}_{\text{rel}})\Phi_{CM}(\mathbf{R}_{CM})\Phi_{\text{rel}}(\mathbf{R}_{12}) = E\Phi_{CM}(\mathbf{R}_{CM})\Phi_{\text{rel}}(\mathbf{R}_{12}) \tag{6.10}$$

Applying the distributive property:

$$\Phi_{\text{rel}}(\mathbf{R}_{12})\hat{H}_{CM}\Phi_{CM}(\mathbf{R}_{CM}) + \Phi_{CM}(\mathbf{R}_{CM})\hat{H}_{\text{rel}}\Phi_{\text{rel}}(\mathbf{R}_{12}) = E\Phi_{CM}(\mathbf{R}_{CM})\Phi_{\text{rel}}(\mathbf{R}_{12}) \quad (6.11)$$

Dividing (6.11) by $\Phi_{CM}(\mathbf{R}_{CM})\Phi_{\text{rel}}(\mathbf{R}_{12})$:

$$\overbrace{\frac{1}{\Phi_{CM}(\mathbf{R}_{CM})}\hat{H}_{CM}\Phi_{CM}(\mathbf{R}_{CM})}^{=E_{\text{trans}}} + \underbrace{\frac{1}{\Phi_{\text{rel}}(\mathbf{R}_{12})}\hat{H}_{\text{rel}}\Phi_{\text{rel}}(\mathbf{R}_{12})}_{=E_{\text{rov}}} = E \quad (6.12)$$

Note that the total energy is given by the sum of the translational energy, E_{trans}, associated with the movement of the center of mass, and the rovibrational energy, E_{rov}, associated with the relative movement between the bodies:

$$E = E_{\text{trans}} + E_{\text{rov}} \quad (6.13)$$

Hence, the following equations are obtained:

$$\hat{H}_{CM}\Phi_{CM}(\mathbf{R}_{CM}) = E_{\text{trans}}\Phi_{CM}(\mathbf{R}_{CM}) \quad (6.14)$$

$$\hat{H}_{\text{rel}}\Phi_{\text{rel}}(\mathbf{R}_{12}) = E_{\text{rov}}\Phi_{\text{rel}}(\mathbf{R}_{12}) \quad (6.15)$$

Thus, to solve the nuclear Schrödinger equation of a two-body system (6.8), one can simply solve the equations (6.14) and (6.15) separately.

Note that the equation (6.14) is analogous to the Schrödinger equation of a free particle. Provided that the system is not subject to external forces, then the translational energy is constant. Thereby, from a frame of reference that follows the center of mass, the translational energy is zero, $E_{\text{trans}} = 0$, so that the total energy will be given by E_{rov}.

6.2 Central-Force Problem

Given a coordinate system whose origin is fixed at the center of mass of the two bodies, the problem is simplified to a problem of following the relative position $\mathbf{R}_{12}$ (Figure 6).

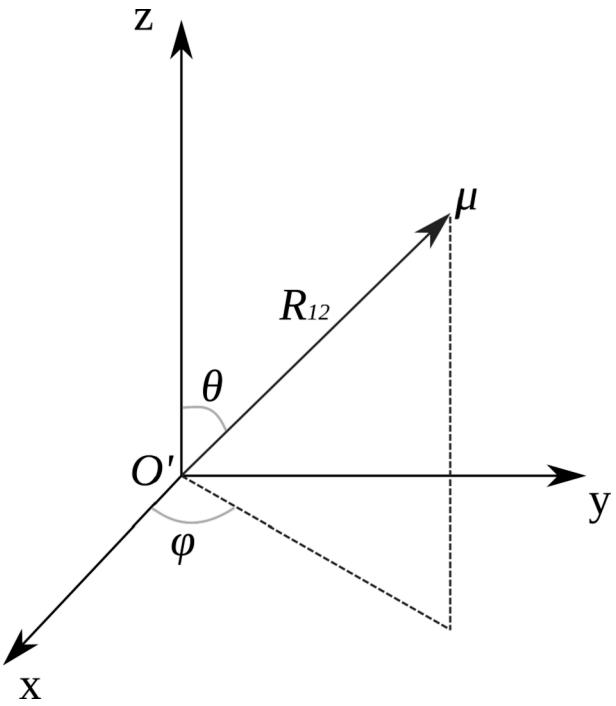

Figure 6 – Relative position between two bodies in the center-of-mass frame.

Writing the $\hat{H}_{\text{rel}}$ operator explicitly in the equation (6.15), one finds the mathematical statement that describes the system in the center-of-mass frame (in atomic units):

$$-\frac{1}{2\mu}\nabla_{12}^2\Phi_{\text{rel}}(\mathbf{R}_{12}) + V(R_{12})\Phi_{\text{rel}}(\mathbf{R}_{12}) = E_{\text{rov}}\Phi_{\text{rel}}(\mathbf{R}_{12}) \tag{6.16}$$

Since the interaction potential depends only on the relative coordinate R_{12}, the problem of following the movement of the reduced mass, in the fixed coordinate system at the center of mass, corresponds exactly to a central-force problem. For this reason, the mathematical treatment of the equation (6.16) will be in spherical coordinates due to the symmetry of the system. Expanding the Laplacian in terms of spherical coordinates in the equation (6.16):

$$\begin{aligned}&-\frac{1}{2\mu}\left[\frac{1}{R_{12}^2}\frac{\partial}{\partial R_{12}}\left(R_{12}^2\frac{\partial}{\partial R_{12}}\right) + \frac{1}{R_{12}^2\sin\theta}\frac{\partial}{\partial\theta}\left(\sin\theta\frac{\partial}{\partial\theta}\right) + \frac{1}{R_{12}^2\sin^2(\theta)}\frac{\partial^2}{\partial\varphi^2}\right]\Phi_{\text{rel}}(\mathbf{R}_{12}) + \\ &+ V(R_{12})\Phi_{\text{rel}}(\mathbf{R}_{12}) = E_{\text{rov}}\Phi_{\text{rel}}(\mathbf{R}_{12})\end{aligned} \tag{6.17}$$

Separating the radial part from the angular part will simplify the mathematical treatment. For that purpose, the squared angular momentum operator $\hat{J}^2$ in atomic units is used:

$$\hat{J}^2 \equiv -\frac{1}{\sin\theta}\frac{\partial}{\partial\theta}\left(\sin\theta\frac{\partial}{\partial\theta}\right) - \frac{1}{\sin^2\theta}\frac{\partial^2}{\partial\varphi^2}$$

Thus, the equation (6.17) can be rewritten as:

$$-\frac{1}{2\mu}\left[\frac{\partial^2}{\partial R_{12}^2}+\frac{2}{R_{12}}\frac{\partial}{\partial R_{12}}-\frac{\hat{J}^2}{R_{12}^2}-2\mu V(R_{12})\right]\Phi_{\text{rel}}(\mathbf{R}_{12})=E_{\text{rov}}\Phi_{\text{rel}}(\mathbf{R}_{12}) \tag{6.18}$$

Since the effective potential $V(R_{12})$ does not depend on the angular variables, one can separate the radial from the angular variables in the wave function $\Phi_{\text{rel}}(\mathbf{R}_{12})$:

$$\Phi_{\text{rel}}(\mathbf{R}_{12})=\zeta(R_{12})Y_j^m(\theta,\varphi) \tag{6.19}$$

where $Y_j^m(\theta,\varphi)$ are the spherical harmonics, which in turn are eigenfunctions of the $\hat{J}^2$ operator:

$$\hat{J}^2Y_j^m(\theta,\varphi)=j(j+1)Y_j^m(\theta,\varphi) \tag{6.20}$$

Applying the $\hat{J}^2$ operator on both sides of (6.18):

$$\begin{aligned}&-\frac{1}{2\mu}\left[Y_j^m(\theta,\varphi)\frac{d^2\zeta(R_{12})}{dR_{12}^2}+\frac{2Y_j^m(\theta,\varphi)}{R_{12}}\frac{d\zeta(R_{12})}{dR_{12}}-\zeta(R_{12})\frac{j(j+1)Y_j^m(\theta,\varphi)}{R_{12}^2}\right]+\\&+Y_j^m(\theta,\varphi)V(R_{12})\zeta(R_{12})=E_{\text{rov}}\zeta(R_{12})Y_j^m(\theta,\varphi)\end{aligned} \tag{6.21}$$

Dividing (6.21) by $Y_j^m(\theta,\varphi)$:

$$-\frac{1}{2\mu}\left[\frac{d^2\zeta(R_{12})}{dR_{12}^2}+\frac{2}{R_{12}}\frac{d\zeta(R_{12})}{dR_{12}}-\frac{j(j+1)}{R_{12}^2}\zeta(R_{12})\right]+V(R_{12})\zeta(R_{12})=E_{\text{rov}}\zeta(R_{12}) \tag{6.22}$$

Defining $\xi(R_{12})\equiv R_{12}\zeta(R_{12})$, the equation above can be rewritten as:

$$-\frac{1}{2\mu}\frac{d^2\xi(R_{12})}{dR_{12}^2}+U(R_{12})\xi(R_{12})=E_{\text{rov}}\xi(R_{12}) \tag{6.23}$$

where $U\equiv\frac{j(j+1)}{2\mu R_{12}^2}+V(R_{12})$ is the effective potential perceived by the system.

The equation (6.23) compensates all the mathematical treatment done to reach it, since it was possible to reduce the Schrödinger Nulear equation to a one-dimensional problem that depends only on the relative position R_{12}. Thus, it is enough to solve this one-dimensional equation to completely determine the nuclear wave function $\Psi_N(\mathbf{R}_{CM},\mathbf{R}_{12})$. However, it is not possible to solve the equation (6.23) analytically, therefore, one must resort to approximation methods. The present work will employ the variational method in conjunction with the Discrete Variable Representation Method (DVR) (PRUDENTE; COSTA; NETO, 1997) in order to solve the equation (6.23).

6.3 Discrete Variable Representation Method

The current goal is to find a trial function that can approximate $\xi(R_{12})$ so that the variational energy approaches the true energy value, $E_{\text{trial}}\approx E_{\text{rov}}$.

As seen in the linear variational method, to solve the Schrödinger equation $\hat{H}|\psi\rangle = E|\psi_i\rangle$, one can expand the state vector $|\psi_i\rangle$ using orthonormal basis functions $\{|\phi\rangle\}$ so that:

$$|\psi\rangle = \sum_i a_i |\phi_i\rangle \tag{6.24}$$

For non-integrable Hamiltonians, such as the Hamiltonian of (6.23), it is necessary to resort to numerical methods. This means that an infinite number of basis functions would be needed to solve the system exactly. Thus, the solution $\xi(R_{12})$ must be approximated by a finite basis expansion, which is equivalent to truncating the representation matrix, so that the parameters a_i can be obtained through diagonalization (SCHWEIZER, 2001).

Within the basis representation, matrix elements are calculated by numerical quadrature rather than continuous integration. If a quadrature rule, consisting of a set of quadrature points and weights, is used to calculate the elements of the matrix, there is an isomorphism between the finite base representation and a discrete representation of the eigenfunctions based on the quadrature points. This equivalence was first pointed out by Dickinson and Certain (DICKINSON; CERTAIN, 1968).

Summarily, the discrete variable method is viable provided that there is an expansion of the basis set and that a quadrature rule can be used to calculate the elements of the matrix in that expansion. The purpose of this method is to determine, from a known set of base functions, a new set of base functions that satisfy:

$$f_i(R_l) = \delta_{il} \tag{6.25}$$

where R_l $(l = 1, 2 \ldots, n)$ are quadrature points.

A set of basis functions that satisfy (6.25) is called a discrete variable representation. This representation diagonalizes the potential matrix.

6.4 Changing the Basis Representation of $\xi(R_{12})$

Firstly, the solution $\xi(R_{12})$ is written as a linear combination of square-integrable basis functions $\{\phi_j\}$:

$$\xi(R_{12}) \approx \sum_{j=1}^{n} c_j \phi_j(R_{12}) \tag{6.26}$$

To simplify the notation, the index of R will be subsumed throughout this section, that is, $R_{12} = R$.

The set of functions $\{\phi_j(R)\}$ obeys the completeness relation $\sum_{j=1}^{n} |\phi_j\rangle \langle\phi_j| = 1$. Thus:

$$f_i(R) = \sum_{j=1}^{n} \langle R|\phi_j\rangle \langle\phi_j|f_i\rangle = \sum_{j=1}^{n} \phi_j(R) \langle\phi_j|f_i\rangle \tag{6.27}$$

The integral $\langle\phi_i|f_i\rangle$ can be evaluated through a quadrature with points R_l and weights ω_l:

$$\langle\phi_j|f_i\rangle \approx \sum_{l=1}^{n} \omega_l \phi_j^*(R_l) f_i(R_l) \tag{6.28}$$

Plugging (6.28) into (6.27):

$$f_i(R) = \sum_{j=1}^{n}\sum_{l=1}^{n} \phi_j(R)\omega_l\phi_j^*(R_l) f_i(R_l) \tag{6.29}$$

Using the property (6.25) the equation above is reduced to:

$$f_i(R) = \omega_i \sum_{j=1}^{n} \phi_j^*(R_i)\phi_j(R) \tag{6.30}$$

For a given quadrature point R_l, the weight is given by:

$$\omega_l = \frac{1}{\sum\limits_{j=1}^{n} \phi_j(R_l)\phi_j^*(R_l)} \tag{6.31}$$

The points R_l of the quadrature correspond to the eigenvalues of the position matrix whose elements are given by:

$$R_{ij} = \langle\phi_i|\,\hat{R}\,|\phi_j\rangle \tag{6.32}$$

where $\hat{R}$ is the position operator. Rewriting the solution $\xi(R_{12})$ with respect to the representation of the discrete variable:

$$\xi(R) \approx \sum_{i=1}^{n} c_i f_i(R) \tag{6.33}$$

Thus, the matrix representation of the potential part of the Hamiltonian of the Schrödinger equation for the two-body problem (6.23) is:

$$U = \begin{bmatrix} \int_a^b f_1^*(R)U(R)f_1(R)dr & \dots & \int_a^b f_1^*(R)U(R)f_n(R)dr \\ \vdots & \ddots & \vdots \\ \int_a^b f_n^*(R)U(R)f_1(R)dr & \dots & \int_a^b f_n^*(R)U(R)f_n(R)dr \end{bmatrix} \tag{6.34}$$

where "a" represents the position of strong nuclear interaction and "b" the position where the potential energy curve asymptotes, in other words, where there is no more interaction between the nuclei. Using the quadrature method to calculate the matrix elements, one obtains:

$$U = \begin{bmatrix} \sum\limits_{k=1}^{n} \omega_k f_1^*(R_k)U(R_k)f_1(R_k) & \dots & \sum\limits_{k=1}^{n} \omega_k f_1^*(R_k)U(R_k)f_n(R_k) \\ \vdots & \ddots & \vdots \\ \sum\limits_{k=1}^{n} \omega_k f_n^*(R_k)U(R_k)f_1(R_k) & \dots & \sum\limits_{k=1}^{n} \omega_k f_n^*(R_k)U(R_k)f_n(R_k) \end{bmatrix} \tag{6.35}$$

Using the property (6.25), the matrix representation of the potential part can finally be diagonalized:

$$U = \begin{bmatrix} \omega_1 f_1^*(R_1)U(R_1)f_1(R_1) & \dots & 0 \\ \vdots & \ddots & \vdots \\ 0 & \dots & \omega_n f_n^*(R_n)U(R_n)f_n(R_n) \end{bmatrix} \tag{6.36}$$

Therefore, the DVR method allowed diagonalizing the potential part of the Hamiltonian.

6.5 Obtaining the Elements of the Kinetic Matrix

The matrix elements of the kinetic energy operator will finally be calculated. Firstly, one must choose points equally spaced in an interval $[\mathrm{a}, b]$ to enable the use of quadrature methods:

$$R_i = \mathrm{a} + \frac{b-\mathrm{a}}{N} i \tag{6.37}$$

where $i = 1, 2, \dots, N$.

Considering that the base functions vanish outside this range, this problem is analogous to the infinite square well. Hence, the base functions can be described by:

$$\phi_n(R_i) = \sqrt{\frac{2}{b-\mathrm{a}}} \sin\left[\frac{n\pi(R_i - \mathrm{a})}{b-\mathrm{a}}\right] \tag{6.38}$$

where $n = 1, 2, \dots, N-1$.

To calculate the elements of the kinetic energy matrix, one must find the expected values of the kinetic energy at the points R_i:

$$T_{ij} = \langle R_i | \hat{T} | R_j \rangle \tag{6.39}$$

where $\hat{T} = -\frac{1}{2\mu}\frac{d^2}{dR^2}$. Inserting the completeness relation:

$$T_{ij} = \sum_{n=1}^{N-1} \langle R_i | \hat{T} | \phi_n \rangle \langle \phi_n | R_j \rangle \tag{6.40}$$

Solving $\langle R_i | \hat{T} | \phi_n \rangle$ using a quadrature method:

$$T_{ij} = -\frac{1}{2\mu}\frac{b-\mathrm{a}}{N} \sum_{n=1}^{N-1} \frac{d^2\phi_n(R_i)}{dR_i^2} \phi_n^*(R_j) \tag{6.41}$$

Plugging (6.38) into (6.41):

$$T_{ij} = \frac{1}{2\mu}\left(\frac{\pi}{b-\mathrm{a}}\right)^2 \frac{2}{N} \sum_{n=1}^{N-1} n^2 \sin\left(\frac{n\pi i}{N}\right) \sin\left(\frac{n\pi j}{N}\right) \tag{6.42}$$

Solving the sum over n in the equation above results in:

$$T_{ij} = \frac{1}{2\mu}\frac{(-1)^{i-j}}{(b-\mathrm{a})^2}\frac{\pi^2}{2}\left[\sin^{-2}\left(\frac{\pi(i-j)}{N}\right) - \sin^{-2}\left(\frac{\pi(i+j)}{N}\right)\right], \text{ for } i \neq j \tag{6.43}$$

$$T_{ii} = \frac{1}{2\mu}\frac{1}{(b-\mathrm{a})^2}\frac{\pi^2}{2}\left[\frac{2N^2+1}{3} - \sin^{-2}\left(\frac{\pi i}{N}\right)\right], \text{ for } i = j \tag{6.44}$$

Therefore, the equation (6.43) produces the off-diagonal elements while (6.44) produces the diagonal elements of the kinetic energy matrix.

7 Spectroscopic Constants

The nuclei of a molecular system carry out two types of internal movement: rotation and vibration. Since the time and energy scales of these types of movement are distinct, rotation and vibration can be treated separately at first.

7.1 Pure Rotational Spectrum

The rotational motion of a two-body system can be approximated using a quantum approach to the classical rigid rotor model. In such an approach, the distance between the bodies is considered constant, and the treatment is conducted in the center-of-mass frame, then the mathematics is simplified to a one-body problem symbolized by the reduced mass position. Thus, the Hamiltonian that describes the rotational movement is:

$$\hat{H}_{\text{rot}} = \frac{\hbar^2}{2I}\hat{J}^2 \tag{7.1}$$

where $I \equiv \mu R_{eq}^2$ is the moment of inertia, $\mu \equiv M_1 M_2/(M_1 + M_2)$ is the reduced mass, R_{eq} is the equilibrium distance and $\hat{J}^2$ is the square angular momentum operator that satisfies the following eigenvalue equation:

$$\hat{J}^2\psi_j = \hbar^2 j(j+1)\psi_j \tag{7.2}$$

where $j = 0, 1, 2\ldots$ is the rotational quantum number.

Applying the Hamiltonian to the nuclear wave function, the following expression for the rotational energy is obtained:

$$E_{\text{rot}} = Bj(j+1) \tag{7.3}$$

where, $B \equiv \frac{\hbar^2}{2I}$ is the rotational constant.

A two-body system undergoing transitions from one rotational state to another obeys the selection rules for electric dipole-induced transitions, so that only transitions between adjacent states are allowed, $\Delta j = \pm 1$. Thus, the energy difference between two consecutive rotational levels is:

$$\begin{aligned} \Delta E &= E_{j+1} - E_j \\ &= \hbar^2 \frac{(j+1)(j+2)}{2I} - \hbar^2 \frac{j(j+1)}{2I} \\ &= \hbar^2 \frac{j+1}{I} \end{aligned} \tag{7.4}$$

The equation (7.4) reveals that the spacing between consecutive levels increases as j increases.

Spectroscopy studies are generally performed in units of cm^{-1}. The rotational constant B, in cm^{-1}, is given by:

$$B = \frac{\hbar^2}{2Ihc} \tag{7.5}$$

Plugging in the moment of inertia and considering the system in its equilibrium configuration, the rotational equilibrium constant is obtained:

$$B_e = \frac{\hbar^2}{2\mu R_{eq}^2 hc} \tag{7.6}$$

7.2 Pure Vibrational Spectrum

Once again the frame is fixed at the center-of-mass, so the problem is simplified to an one-body problem. Hence, the system can be approximated by a quantum harmonic oscillator.

The energies of a quantum harmonic oscillator, in units of inverse length, have the well known format:

$$E_v = \left(v + \frac{1}{2}\right) hc\omega_e \tag{7.7}$$

where $v = 0.1, 2, \ldots$ is the vibrational quantum number and ω_e is the harmonic frequency in inverse of lenght units.

Analogous to the rotational case, the system obeys the selection rules for electric dipole-induced transitions when undergoing transistions from one vibrational state to another, which only allow transitions between adjacent states, $\Delta v = \pm 1$. Thus, the energy difference between two consecutive vibrational levels is:

$$\begin{aligned} \Delta E &= E_{v+1} - E_v \\ &= \left(v + \frac{3}{2}\right) hc\omega_e - \left(v + \frac{1}{2}\right) hc\omega_e \\ &= hc\omega_e \end{aligned} \tag{7.8}$$

Note that the spacing between adjacent levels is always constant, that is, it does not depend on the value of v. However, this approximation is only efficient for the lower vibrational states, for internuclear distances much larger than the equilibrium, the space between the levels progressively decreases due to the anharmonicity of the potential energy curve. To describe both the harmonic and anharmonic parts of the PEC, one can resort to the Morse potential (PRUDENTE, 1999). This empirical potential is described by:

$$V(R) = D_e(1 - e^{-\beta(R-R_e)})^2 \tag{7.9}$$

where D_e is the dissociation energy, β is a parameter that determines whether the potential is short-range or long-range. Expanding (7.9) in a Taylor series around $R = R_e$:

$$V(R) \approx D_e\beta^2(R - R_e)^2 \tag{7.10}$$

Inserting the potential above into the Schrödinger equation of the harmonic oscillator, one finds the energies with corrections due to anharmonicity:

$$E_v = \left(v + \frac{1}{2}\right)^2 hc\omega_e - \left(v + \frac{1}{2}\right)^2 hc\omega_e x_e + \left(v + \frac{1}{2}\right)^3 hc\omega_e y_e + \dots \tag{7.11}$$

where $\omega_e x_e$ and $\omega_e y_e$ are anharmonic vibrational constants. Rewriting (7.11) in cm^{-1}:

$$E_v = \left(v + \frac{1}{2}\right)^2 \omega_e - \left(v + \frac{1}{2}\right)^2 \omega_e x_e + \left(v + \frac{1}{2}\right)^3 \omega_e y_e + \dots \tag{7.12}$$

7.3 Rovibrational Spectrum

Although the mathematical treatment of rotational and vibrational movements was done separately in the previous sections, they occur simultaneously, which causes a fine structure in the vibrational bands to arise. Therefore, a more accurate description of these coupled movements (Figure 7) will be made in this section.

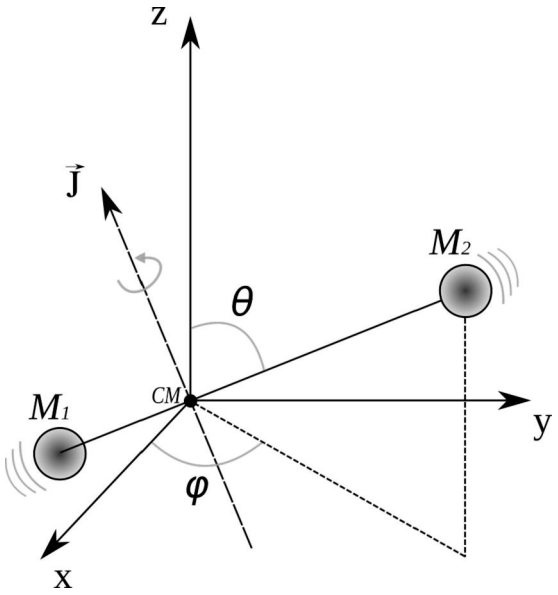

Figure 7 – Rovibrational movement of a two-body system.

To study the rovibrational spectrum, one can join the harmonic oscillator model with the rigid rotor model, so the system Hamiltonian will be the sum of both contributions:

$$\hat{H}_{\mathrm{rov}} = \hat{H}_{\mathrm{rot}} + \hat{H}_{\mathrm{vib}} \tag{7.13}$$

However, there is a rovibrational coupling that appears due to the vibrational dependence of the rotational constant, since vibrations that cause oscillations in the internuclear distance occur concomitantly with the rotational movement, these oscillations are dependent on the vibrational wave function and the quantum number v. Consequently,

the rotational constant B takes into account these oscillations within the definition of the moment of inertia. Thus, the rotational constant has a dependency on ν. Taylor expanding around $\left(v+\frac{1}{2}\right)$:

$$B_v = B_e - \alpha_e\left(v+\frac{1}{2}\right) - \gamma_e\left(v+\frac{1}{2}\right)^2 + \dots \tag{7.14}$$

where B_v represents the rotational constant with rovibration correction, α_e and γ_e are called rovibrational spectroscopic constants.

Thereby, the rovibration energy of a level (v, j) can be obtained through all vibrational, harmonic and anharmonic, and rigid and non-rigid rotational contributions:

$$\begin{aligned} E_{v,j} = &\left(v+\frac{1}{2}\right)\omega_e - \left(v+\frac{1}{2}\right)^2\omega_e x_e + \left(v+\frac{1}{2}\right)^3\omega_e y_e + \\ &\cdots + \left[B_e - \alpha_e\left(v+\frac{1}{2}\right) - \gamma_e\left(v+\frac{1}{2}\right)^2 + \dots\right] j(j+1) + \dots \end{aligned} \tag{7.15}$$

The rovibrational levels described by the equation (7.15) can be evaluated from the solution of the equation (6.23), with $V(R)$ given by the Morse Potential. Thus, to calculate the rovibrational spectroscopic constants, it is possible to plug in the values of the rovibrational energies $E_{v,j}$ calculated by solving the nuclear Schrödinger equation so that the following system of equations is obtained:

$$\begin{aligned} \omega_e &= \frac{1}{24}\left[141\left(E_{1,0}-E_{0,0}\right) - 93\left(E_{2,0}-E_{0,0}\right) + 23\left(E_{3,0}-E_{1,0}\right)\right] \\ \omega_e x_e &= \frac{1}{4}\left[13\left(E_{1,0}-E_{0,0}\right) - 11\left(E_{2,0}-E_{0,0}\right) + 3\left(E_{3,0}-E_{1,0}\right)\right] \\ \omega_e y_e &= \frac{1}{6}\left[3\left(E_{1,0}-E_{0,0}\right) - 3\left(E_{2,0}-E_{0,0}\right) + \left(E_{3,0}-E_{1,0}\right)\right] \\ \alpha_e &= \frac{1}{8}\left[-12\left(E_{1,1}-E_{0,1}\right) + 4\left(E_{2,1}-E_{0,1}\right) + 4\omega_e - 23\omega_e y_e\right] \\ \gamma_e &= \frac{1}{4}\left[-2\left(E_{1,1}-E_{0,1}\right) + \left(E_{2,1}-E_{0,1}\right) + 2\omega_e x_e - 9\omega_e y_e\right], \end{aligned} \tag{7.16}$$

The equation (7.16) constitutes the first methodology employed by the present paper to determine the rovibrational spectroscopic constants.

7.4 Dunham Expansion

Dunham solved the equation (6.23) using the Wentzel-Brillouin-Kramers method (WBK) (DUNHAM, 1932). However, instead of using the Morse potential to describe the potential $V(R)$ under which the nuclei of the diatomic system move, Dunham assumed that $V(R)$ is an analytic function that can be described by the series (DUNHAM, 1932; MITIN, 1998):

$$V(R) = c_0\left(\frac{R-R_e}{R_e}\right)^2\left[1+\sum_{n=1}^{\infty} c_n\left(\frac{R-R_e}{R_e}\right)^n\right] \tag{7.17}$$

where $c_0 = \frac{\omega_e^2}{4B_e}$, and B_e is the equilibrium rotational constant given by the equation (7.6).

Thereby, Dunham was able to express the rovibrational energy levels as follows:

$$E_{v,j} = \sum_{k=0}^{\infty}\sum_{l=0}^{\infty} Y_{kl}\left(v+\frac{1}{2}\right)^k [j(j+1)]^l \tag{7.18}$$

where Y_{kl} are coefficients called Dunham parameters.

Comparing this expansion with the equation (7.15), it can be noted that the coefficients Y_{kl} are related to the spectroscopic constants:

$$Y_{10} \approx \omega_e \quad Y_{20} \approx -\omega_e x_e \quad Y_{30} \approx \omega_e y_e$$

$$Y_{01} \approx B_e \quad Y_{11} \approx -\alpha_e \quad Y_{21} \approx \gamma_e$$

Thus, the coefficients Y_{kl} can be written in terms of the parameters c_n. The first six coefficients Y_{kl} are:

$$\begin{aligned}
Y_{10} &= \omega_e\left[1+\left(\frac{B_e^2}{4\omega_e^2}\right)\left(25c_4-\frac{95}{2}c_1c_3-\frac{67}{4}c_2^2+\frac{459}{8}c_1^2c_2-\frac{1155}{64}c_1^4\right)\right]\\
Y_{20} &= \left(\frac{B_e}{2}\right)\left[3\left(c_2-\frac{5}{4}c_1^2\right)+\left(\frac{B_e^2}{2\omega_e^2}\right)\left(245c_6-\frac{1365}{2}c_1c_5-\frac{885}{2}c_2c_4-\frac{1085}{4}c_3^2\right.\right.\\
&+\frac{8535}{8}c_1^2c_4+\frac{1707}{8}c_2^3+\frac{7335}{4}c_1c_2c_3-\frac{23865}{16}c_1^3c_3-\frac{62013}{32}c_1^2c_2^2\\
&\left.\left.+\frac{239985}{128}c_1^4c_2-\frac{209055}{512}c_1^6\right)\right]\\
Y_{30} &= \left(\frac{B_e^2}{2\omega_e}\right)\left(10c_4-35c_1c_3-\frac{17}{2}c_2^2+\frac{225}{4}c_1^2c_2-\frac{705}{32}c_1^4\right)\\
Y_{01} &= B_e\left[1+\left(\frac{B_e^2}{2\omega_e^2}\right)\left(15+14c_1-9c_2+15c_3-23c_1c_2+\frac{21}{2}(c_1^2+c_1^3)\right)\right]\\
Y_{11} &= \left(\frac{B_e^2}{\omega_e}\right)\left[6(1+c_1)+\left(\frac{B_e^2}{\omega_e^2}\right)\left(175+285c_1-\frac{335}{2}c_2+175c_5+\frac{2295}{8}c_1^2\right.\right.\\
&-459c_1c_2+\frac{1425}{4}c_1c_3-\frac{7955}{2}c_1c_4+\frac{1005}{8}c_2^2-\frac{715}{2}c_2c_3+\frac{1155}{4}c_1^3-\frac{9639}{16}c_1^2c_2\\
&\left.\left.+\frac{5145}{8}c_1^2c_3+\frac{4677}{8}c_1c_2^2-\frac{14259}{16}c_1^3c_2+\frac{31185}{128}(c_1^4+c_1^5)\right)\right]\\
Y_{21} &= \left(\frac{6B_e^3}{\omega_e^2}\right)\left(5+10c_1-3c_2+5c_3-13c_1c_2+\frac{15}{2}(c_1^2+c_1^3)\right)
\end{aligned} \tag{7.19}$$

Summarily, Dunham's approach to calculating rovibrational energy levels consists of three steps: defining the limits of the sums in (7.18), finding the system's potential energy curve, and finally, calculating the coefficients Y_{kl} using the equations (7.19).

The final two steps are closely related. Within the Dunham method, to calculate the coefficients Y_{kl} one just need to find the parameters c_n of the potential $V(R)$ in (7.17). Since the series (7.17) is nothing more than a Taylor expansion of $V(R)$ around the point

R_e, the problem of finding c_n leads to the calculation of derivatives at the minimum value of the PEC. Thus:

$$c_0 = \frac{R_e}{2}\left(\frac{d^2V(R)}{dR^2}\right) \tag{7.20}$$

$$c_n = \frac{R_e^{n+1}}{c_0(n+2)!}\left(\frac{d^{n+2}V(R)}{dR^{n+2}}\right) \tag{7.21}$$

Calculating the potential derivatives does not represent a problem since the potential $V(R)$ is assumed to belong to the function space $C^\infty(0,+\infty)$, which is infinitely differentiable within its limits. However, in the case of *ab initio* calculations, such as the ones performed in this paper, this assumption cannot be made, since the PEC will be obtained in the form of a table with pairs of points associating energies and distances. Therefore, to calculate the derivative of tabulated functions, such as the PEC obtained by *ab initio* calculations, the potential energy curve must first be fitted by an analytical function.

7.5 Lifetime

Once the spectroscopic constants, the dissociation energy, D_e, and the ground state energy $E_{0,0}$ are calculated, it is possible to determine the lifetime of the system. The thermal rate within Slater's theory (SLATER, 1929; MENEZES et al., 2021) is defined as:

$$k(T) = \omega_e e^{-\frac{D_e - E_{0,0}}{RT}} \tag{7.22}$$

Therefore, the inverse of the equation above expresses the lifetime as a function of temperature:

$$\tau(T) = \frac{1}{\omega_e} e^{\frac{D_e - E_{0,0}}{RT}} \tag{7.23}$$

It is important to note that the lifetime for the dissociation of the complexes is a purely dynamic description with a vibrational analysis of the compounds and, therefore, refers to the low or high rate of unimolecular decay. According to this formulation, the unimolecular aggregate dissociation must occur when the interaction coordinate reaches the dissociation threshold defined by the dissociation parameter D_e. Furthermore, the applicability of such an approach is suitable for regions of intermediate pressure due to the kinetic behavior of the system.

8 Natural Bond Orbital Analysis

To better understand the origin of the electronic rearrangements that occur during the adsorption process of the pollutant molecules, the distribution of electron density in atoms and bonds between atoms were calculated by the Natural Bond Orbital Analysis (NBO) (REED; WEINSTOCK; WEINHOLD, 1985; WEINHOLD, 2012) implemented by the computational package Gaussian09 (FRISCH et al., 2009), which contains the NBO program by F. Weinhold and coworkers (GLENDENING; LANDIS; WEINHOLD, 2013).

The NBO method uses the electron density matrix to construct the shape of atomic orbitals in a molecular environment. The density matrix can be written in terms of basic function blocks belonging to a specific center:

$$\begin{bmatrix} D^{AA} & D^{AB} & D^{AC} & \dots \\ D^{BA} & D^{BB} & D^{BC} & \dots \\ D^{CA} & D^{CB} & D^{CC} & \dots \\ \vdots & \vdots & \vdots & \ddots \end{bmatrix} \tag{8.1}$$

The natural atomic orbital for atom X is defined as the one that diagonalizes the D^{XX} block in the molecular environment. Generally, these natural atomic orbitals are not orthogonal, which results in a total number of electrons that do not correspond to the number of occupied orbitals.

To fully divide the electrons, the orbitals must be orthogonalized maintaining the shape of the strongly occupied orbitals, which is possible using an Occupancy-Weighted Symmetric Orthogonalization. As a result, the charge donors and acceptors can be identified.

9 Symmetry Adapted Perturbation Theory

Symmetry-adapted perturbation theory (SAPT) provides a means of directly computing the non-covalent interaction between two moieties that compose a dimer. In other words, the interaction energy is determined without computing the total energy of the monomers or dimer. Moreover, SAPT provides a decomposition of the interaction energy into physically meaningful components, *i.e.*, electrostatic (E_{elst}), induction (E_{ind}), dispersion (E_{disp}), and exchange (E_{exch}) terms.

Within the SAPT methodology, the Hamiltonian of the dimer is partitioned into contributions from each monomer and the interaction:

$$H = F_A + W_A + F_B + W_B + V \tag{9.1}$$

where F_A and F_B are the Fock operators of each monomer. W_A and W_B are the fluctuation potential of each monomer, and V is the interaction potential.

The monomer Fock operators, F_A+F_B, are treated as the zeroth-order Hamiltonian and the interaction energy is evaluated through a perturbative expansion of V, W_A, and W_B. Through first-order in V, electrostatic and exchange interactions are included; induction and dispersion first appear at second-order in V (JEZIORSKI; MOSZYNSKI; SZALEWICZ, 1994). The simplest truncation of SAPT is denoted SAPT0 and it is defined as:

$$\mathrm{E}_{\mathrm{SAPT0}} = \mathrm{E}^{(10)}_{elst} + \mathrm{E}^{(10)}_{exch}\mathrm{E}^{(20)}_{ind,resp} + \mathrm{E}^{(20)}_{exch-ind,resp}\mathrm{E}^{(20)}_{disp} + \mathrm{E}^{(20)}_{exch-disp} + \delta^{(2)}_{HF}. \tag{9.2}$$

where $\mathrm{E}^{v,w}$ defines the order in V and in $W_A + W_B$. The subscript "$resp$" indicates that orbital relaxation effects are included.

Part III

Computational Details

10 Theory Level (DFT Functional)

To obtain the PECs, the distance between the GQD and the molecule was systematically varied with a step of 0.1Å, performing a single point calculation in each iteration. After determining the equilibrium distance R_e, ten additional single points, with a step of 0.01Å, were calculated around the equilibrium value seeking to improve the accuracy of the results. The potential energy curves were fitted by the ten-coefficient extended-Rydberg function (Equation 13.1) using Powell's method (POWELL, 1965).

The electronic structure calculations were performed by the Gaussian 09 (FRISCH et al., 2009) software using the ωB97XD functional, which is the latest functional from Head-Gordon and collaborators (CHAI; HEAD-GORDON, 2008) and includes a version of the Grimme D2 empirical dispersion model (GRIMME et al., 2010). The ωB97XD is a hybrid functional capable of describing both short-range and long-range interactions, and the fact that it already includes dispersion corrections is essential to accurately describe the systems composed by the GQD and the adsorbed molecule (CO, NO_2, SO_2, NH_3). Studies comparing this functional with other popular DFT functionals indicate that the ωB97XD functional delivers the best results when compared to experimental data for systems governed by van der Waals interactions (MINENKOV et al., 2012).

11 Basis Functions

Choosing the basis functions in electronic structure calculations has a big impact on the quality of the results. Although Slater functions provide a good description of monoelectronic orbitals, their integrals are difficult to solve, therefore, the applicability of Slater-type orbitals (STO) is restricted to monoatomic and diatomic systems. For larger molecules, it is customary to use Gaussian-type Orbitals (GTO). Despite being necessary to combine several GTOs to describe an atomic orbital with a format similar to that of an STO, the integrals are more easily solved, generating a gain in computational performance.

Another option to improve computational efficiency is the use of a linear combination of primitive Gaussians called contracted Gaussian-type Orbitals (CGTO). This approach reduces the disk space required for the calculation since only the contractions are stored in the computer's memory at each SCF cycle. The main benefit of using CGTO lies in the description of inner-shell electrons. Such electrons have a lesser relevance in the formation of chemical interactions, hence, they can be treated by only one contraction of several primitive Gaussians. On the other hand, valence orbitals, being more diffuse and, consequently, more affected by the molecular environment, need to be treated by two or more contractions.

Within the CGTO basis sets, the 6-31G basis set created by Pople's group (HEHRE; DITCHFIELD; POPLE, 1972) stands out. Within this basis, the inner-shell electrons are described by one CGTO formed by 6 primitive Gaussians, whereas the valence orbitals are represented by two CGTOs each, the first composed of 3 primitives and the second of 1 primitive. The name 6-31G precisely reflects this structure. This basis is applicable in the description of systems involving atoms with an atomic number up to 36, that is, from H to Kr.

Within a molecular system, adjacent atoms distort each other's atomic orbitals. Thus, in addition to the basis set, additional polarization functions can be introduced providing more accurate results since the effect of polarization is taken into account. These additional functions describe atomic orbitals through angular moments higher than those of the valence electrons. For a hydrogen atom, for example, which only requires s-type functions, the p, d, and f-type functions are also added, thereby improving the accuracy of molecular properties such as dissociation energy and dipole moment (ARRUDA, 2009).

Thus, the basis set chosen to be used in the electronic structure calculations of this paper was the base 6-31G(d,p) (RASSOLOV et al., 2001), where the term (d,p) indicates the addition of polarization functions.

12 Functionalization Designs

For the adsorbates CO, SO_2 and NH_3, the doping approach of the GQDs consisted of swapping the 22th and the 44th carbons within the nanoflake (see Figure 8) three times, once with every heteroatom (B, N and Al). On the other hand, for the systems with NO_2, only the 44th carbon (C44) was swapped with the heteroatoms. Hence, the multiplicity of the systems would be equal to one. CO, NH_3 and SO_2 exhibit an electron lone pair on C, N, and S atom, respectively, while NO2 is a free radical with an unpaired electron on N atom. A number of different approaches were also tested, but none was as effective as the one reported in this paper. The following notation was used to identify each system:

$$\text{Adsorbate} - \underbrace{\text{Adsorbent}}_{\text{GQD}} @nX \tag{12.1}$$

where n is the number heteroatoms and X is the dopant chemical symbol.

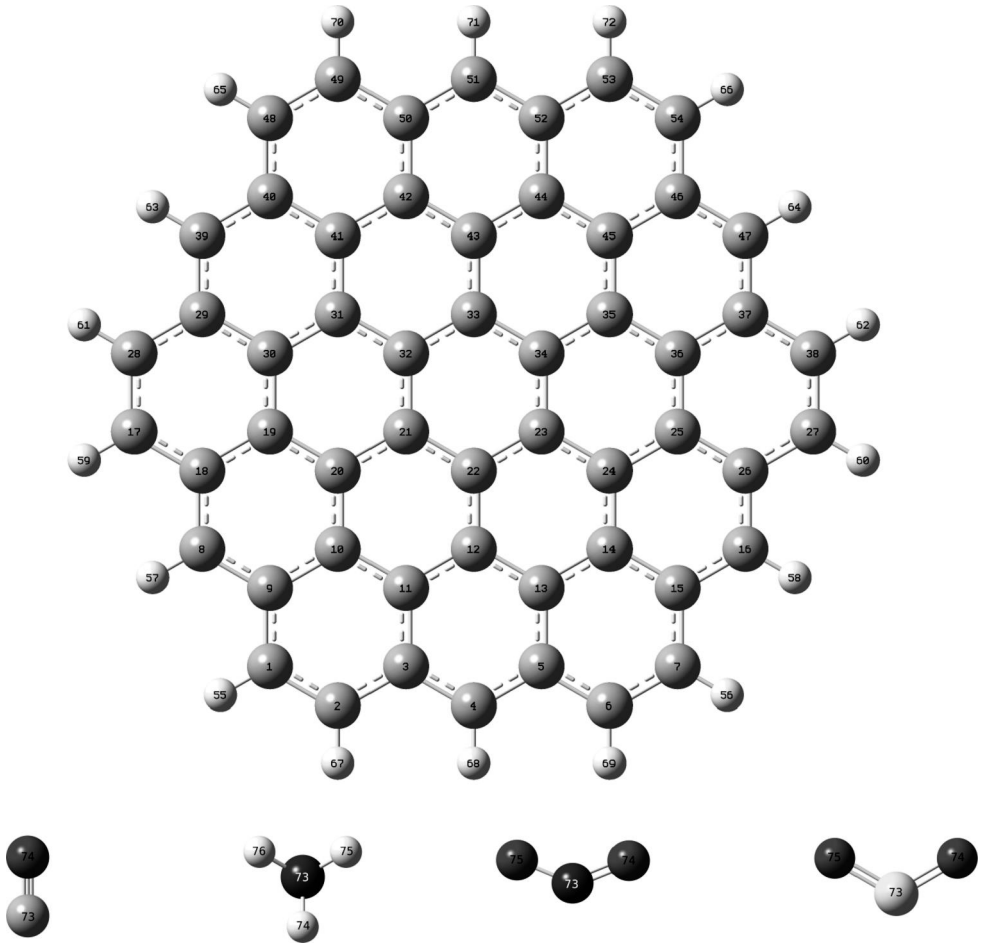

Figure 8 – Schematic representation of a graphene quantum dot (composed by 54 carbons and 18 hydrogens) and the CO, NH_3, NO_2, and SO_2 adsorbates. The grey, red, white, blue, and yellow colors stand for carbon, oxygen, hydrogen, nitrogen, and sulfur, respectively.

Moreover, the adsorbates can approach the quantum dot in many ways. For example, the carbon monoxide can approach the GQD with a C-O bond that is parallel, perpendicular or any angle in between, with respect to the quantum dot's plane. In this work, the adsorbates approached the quantum dot through its 22th atom, which is the one swapped with heteroatoms, so depending on the functionalization, the adsorbate will either approach a carbon, a boron, a nitrogen or an aluminum. The geometries that presented the most promising results, and thus reported in this paper, were the following: the CO approaching the GQD perpendicularly with its carbon facing the quantum dot; the NH_3 approaching with its nitrogen facing the quantum dot; the NO_2 with with its nitrogen facing the quantum dot; and the SO_2 with its sulfur facing the quantum dot (see Figure 9).

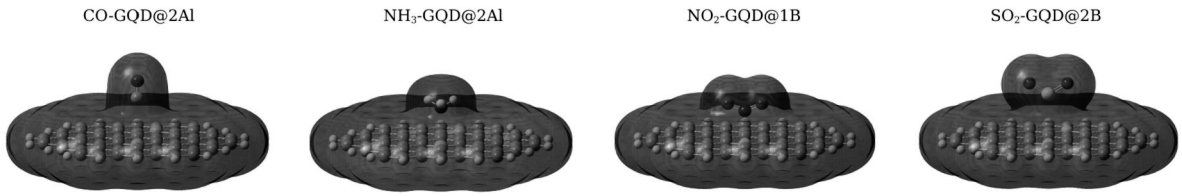

Figure 9 – Electronic density of the most promising system for each adsorbate.

13 Rydberg's Analytical Function

After obtaining the potential energy curves, they were fitted by Rydberg's analytical function (RYDBERG, 1932):

$$V(R) = -D_e \left[1 + \sum_{i=1}^{k} c_i (R - R_e)^i\right] e^{-c_1(R-R_e)} \tag{13.1}$$

where D_e is the dissociation energy, R is the distance between GQD and the adsorbed molecule, and R_{eq} is the equilibrium distance of the system. The fitting of the *ab initio* points was performed employing the Powell method (POWELL, 1965), which consists of a search over the parameters c_i to minimize the deviation between the values *ab initio* and the values generated by the analytic form.

The next step was to plug in the resulting analytic function into the nuclear Hamiltonian and then solve the nuclear Schrödinger equation. Finally, the spectroscopic constants are obtained either by utilizing Dunham's method or utilizing the equations (7.16), enabling the calculation of the system's lifetime. The aforementioned steps were performed by programs in Fortran written by the professors of the Atomic and Molecular group of the University of Brasilia. These programs employed the equations and steps described in the sections 6 and 7.

Part IV

Results

14 Potential Energy Curves

The electronic energies for a set of different internuclear distances, that ranges from the strong interaction region to the asymptotic region (weak interaction), were calculated at ωB97XD/6-31G(d,p) level for every system investigated and they are shown in the Appendix A (Tables 7, 8, 9, and 10). These energies were adjusted to the analytical form given by Equation 13.1 and the fitted parameters (c_i) are presented in Table 1. The Dissociation energies D_e, the equilibrium distances R_e, and the reduced mass for each system are given in Table 2. It follows from the PECs (Figure 10) that the doping schemes were effective in increasing the well's depth and, thus, increasing D_e.

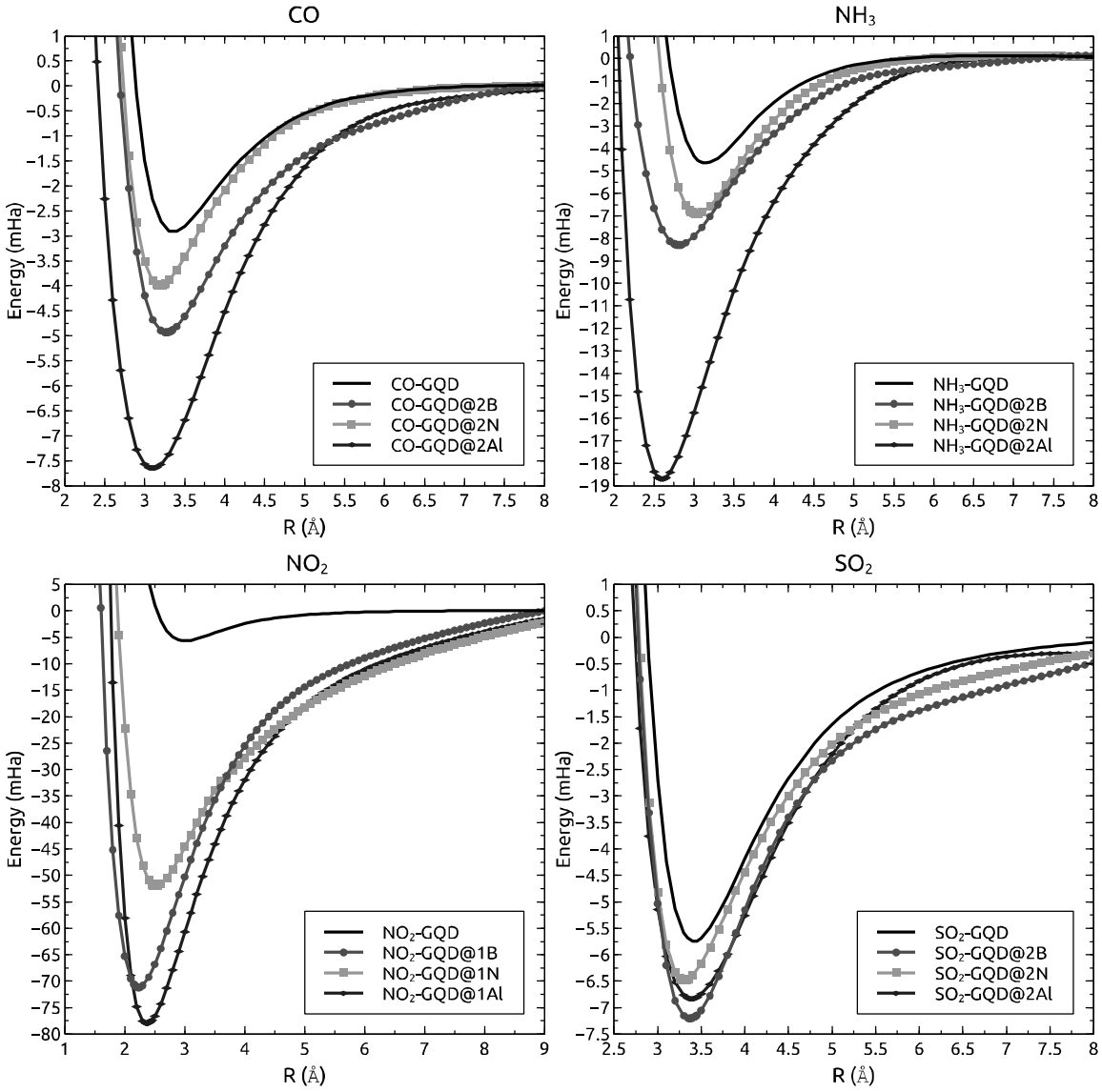

Figure 10 – Potential energy curves of all systems.

Concerning the systems with CO, the most effective functionalization was the one made with two atoms of Al, more than doubling the dissociation energy when compared to a system with the pristine GQD. Additionally, evaluating the systems with NH_3 shows that the greatest improvement in the well's depth was once again due to the doping with two atoms of Al, which entailed a gain of approximately 14 mHa within the D_e. Furthermore, the systems with NO_2 were the most impacted by the functionalizations, with the boron and aluminum doping increasing more than twelve times the dissociation energy of the not functionalized system, which indicates a huge gain on the strength of interaction. On the other hand, the systems with SO_2 had the lowest increases with the functionalizations.

Table 1 – Fitting coefficients and root-mean-square deviation (RMSD) associated.

Complex	C1	C2	C3	C4	C5	C6	C7	C8	C9	C10	RMSD (Ha)
CO-GQD	2.78	1.87	2.33×10^{-1}	-4.72×10^{-1}	6.32×10^{-1}	7.33×10^{-1}	-3.39×10^{-1}	-1.72×10^{-1}	1.10×10^{-1}	-1.19×10^{-2}	9.7×10^{-6}
CO-GQD@2B	1.79	3.94×10^{-3}	9.76×10^{-2}	2.97×10^{-1}	-5.35×10^{-2}	-4.45×10^{-2}	1.75×10^{-2}	9.26×10^{-3}	-4.48×10^{-3}	4.46×10^{-4}	9.9×10^{-6}
CO-GQD@2N	2.16	8.71×10^{-2}	1.58×10^{-1}	1.50×10^{-1}	3.16×10^{-2}	-2.48×10^{-2}	-7.17×10^{-3}	6.00×10^{-3}	-1.10×10^{-3}	4.76×10^{-5}	9.8×10^{-6}
CO-GQD@2Al	1.37	-1.76×10^{-1}	-1.56×10^{-1}	1.69×10^{-2}	8.83×10^{-2}	-2.29×10^{-2}	-1.77×10^{-2}	9.98×10^{-3}	-1.77×10^{-3}	1.07×10^{-4}	1.3×10^{-5}
NH_3-GQD	2.28	1.69×10^{1}	-2.27×10^{1}	-2.25×10^{3}	4.00×10^{2}	2.47×10^{2}	-2.08×10^{2}	-5.51×10^{4}	-4.47×10^{4}	1.07×10^{4}	9.7×10^{6}
NH_3-GQD@2B	1.83	1.42×10^{1}	-2.00×10^{1}	2.87×10^{1}	1.83×10^{1}	-1.80×10^{1}	-4.66×10^{2}	6.37×10^{2}	-1.58×10^{2}	1.18×10^{3}	9.1×10^{6}
NH_3-GQD@2N	2.01	-2.78×10^{-1}	6.99×10^{-2}	5.48×10^{-2}	1.69×10^{-2}	-3.95×10^{-2}	-1.90×10^{-2}	2.19×10^{-2}	-6.23×10^{-3}	5.45×10^{-4}	9.5×10^{-6}
NH_3-GQD@2Al	2.35	1.20	4.22×10^{-1}	5.99×10^{-2}	2.50×10^{-1}	4.85×10^{-2}	-4.70×10^{-2}	-5.96×10^{-3}	4.10×10^{-3}	-3.95×10^{-4}	1.9×10^{-5}
NO_2-GQD	1.73	-6.77×10^{-1}	2.69×10^{-1}	1.59×10^{-1}	-1.26×10^{-1}	3.76×10^{-2}	-6.24×10^{-3}	1.56×10^{-3}	-4.46×10^{-4}	4.30×10^{-5}	5.6×10^{-6}
NO_2-GQD@1B	1.72	3.22×10^{-1}	2.53×10^{-1}	1.19×10^{-1}	-3.03×10^{-2}	-1.97×10^{-2}	1.21×10^{-2}	-1.77×10^{-2}	3.35×10^{-3}	-2.33×10^{-4}	2.3×10^{-5}
NO_2-GQD@1N	1.56	7.09×10^{-2}	2.95×10^{-1}	2.71×10^{-1}	-6.31×10^{-2}	-1.76×10^{-2}	2.73×10^{-2}	-9.43×10^{-3}	1.60×10^{-3}	-1.03×10^{-4}	1.8×10^{-5}
NO_2-GQD@1Al	1.65	1.85×10^{-1}	3.78×10^{-1}	1.81×10^{-2}	-7.48×10^{-3}	-1.18×10^{-2}	3.19×10^{-2}	-1.32×10^{-2}	2.38×10^{-3}	-1.54×10^{-4}	6.8×10^{-5}
SO_2-GQD	1.88	1.41×10^{-1}	1.65×10^{-1}	9.82×10^{-3}	1.63×10^{-2}	4.07×10^{-2}	-1.21×10^{-2}	-3.77×10^{-3}	1.99×10^{-3}	-2.14×10^{-4}	2.2×10^{-5}
SO_2-GQD@2B	2.06	6.81×10^{-1}	1.04×10^{-1}	1.22×10^{-1}	1.25×10^{-1}	6.00×10^{-2}	-2.57×10^{-2}	-5.53×10^{-3}	6.20×10^{-3}	-8.30×10^{-4}	1.5×10^{-5}
SO_2-GQD@2N	2.08	4.31×10^{-1}	5.00×10^{-1}	3.22×10^{-1}	2.51×10^{-2}	-5.38×10^{-2}	3.21×10^{-3}	1.34×10^{-2}	-2.03×10^{-3}	9.67×10^{-9}	2.0×10^{-5}
SO_2-GQD@2Al	1.76	4.82×10^{1}	1.26×10^{1}	-1.59×10^{1}	5.10×10^{3}	9.41×10^{2}	-1.22×10^{2}	-1.88×10^{2}	6.60×10^{3}	-5.87×10^{4}	2.8×10^{5}

Overall, the PECs suggest that the most promising systems regarding gas sensing applications are NO_2-GQD@1Al, NO_2-GQD@1B, and NH_3-GQD@2Al.

Table 2 – Equilibrium distance R_e (Å), dissociation energies D_e (mHa), and reduced mass (μ) of all systems.

Complexo	R_e (Å)	D_e (mHa)	μ (a.u)
CO-GQD	3.40	2.9104	48999.9678
CO-GQD@2B	3.26	4.9339	48992.8335
CO-GQD@2N	3.20	3.9922	49011.7306
CO-GQD@2Al	3.11	7.6454	49085.0247
NH_3-GQD	3.15	4.6374	30271.4659
NH_3-GQD@2B	2.81	8.2999	30268.7429
NH_3-GQD@2N	3.03	6.9029	30275.9549
NH_3-GQD@2Al	2.60	18.7071	30303.9071
NO_2-GQD	3.01	5.6512	78448.7861
NO_2-GQD@1B	2.23	71.1702	78439.6590
NO_2-GQD@1N	2.52	51.9858	78463.9056
NO_2-GQD@1Al	2.36	77.9882	78560.1536
SO_2-GQD	3.43	5.7452	106534.6981
SO_2-GQD@2B	3.37	7.2039	106500.9797
SO_2-GQD@2N	3.30	6.4794	106590.3176
SO_2-GQD@2Al	3.39	6.8354	106937.5883

15 Spectroscopic Properties

Using the adjusted PECs for each system, the rovibrational energies were calculated (Tables 11, 12, 13, and 14 of Appendix B). The data reveal that the system NO_2-GQD@1B has the highest number of energy levels with 221, representing a gain of 183 energy levels in comparison with the not functionalized system. On the other hand, the system NH_3-GQD has the lowest number of energy levels with 17. The highest number of energy levels for each adsorbate was obtained by a functionalization with either boron or aluminum, implying that those are the most auspicious dopants, especially for NO_2.

Additionally, the spectroscopy constants of each system are presented in Table 3. Comparing the numerical values obtained by both methods, one can verify that they are in incredible consonance with each other, thus suggesting that the data are reliable. Moreover, the lifetime of the systems was calculated within the Slater theory (Equation 7.23) and indicated that the functionalization can greatly improve the stability of the systems (see Table 4).

Table 3 – Spectroscopic constants (cm^{-1}) calculated for all systems.

Complex	Method	ω_e	$\omega_e x_e$	$\omega_e y_e$	α_e	γ_e
CO-GQD	Equation (7.16)	56.40	0.78	3.85×10^{-2}	8.45×10^{-4}	4.13×10^{-5}
	Dunham	56.40	0.78	3.86×10^{-2}	8.50×10^{-4}	3.79×10^{-5}
CO-GQD@2B	Equation (7.16)	65.69	1.16	2.01×10^{-3}	9.73×10^{-4}	1.62×10^{-5}
	Dunham	65.68	1.16	3.45×10^{-3}	9.73×10^{-4}	1.60×10^{-5}
CO-GQD@2N	Equation (7.16)	70.10	1.44	3.11×10^{-3}	1.20×10^{-3}	1.78×10^{-5}
	Dunham	70.10	1.44	3.93×10^{-3}	1.20×10^{-3}	1.64×10^{-5}
CO-GQD@2Al	Equation (7.16)	68.58	0.53	4.72×10^{-3}	5.99×10^{-4}	9.05×10^{-6}
	Dunham	68.57	0.53	4.64×10^{-3}	6.00×10^{-4}	8.75×10^{-6}
NH_3-GQD	Equation (7.16)	100.07	2.06	1.57×10^{-2}	2.07×10^{-3}	4.08×10^{-5}
	Dunham	100.07	2.07	1.35×10^{-2}	2.08×10^{-3}	3.46×10^{-5}
NH_3-GQD@2B	Equation (7.16)	106.75	1.53	1.08×10^{-2}	1.77×10^{-3}	4.88×10^{-5}
	Dunham	106.73	1.53	1.26×10^{-2}	1.77×10^{-3}	4.80×10^{-5}
NH_3-GQD@2N	Equation (7.16)	118.94	2.23	4.51×10^{-3}	2.09×10^{-3}	2.59×10^{-5}
	Dunham	118.92	2.23	5.66×10^{-3}	2.09×10^{-3}	2.42×10^{-5}
NH_3-GQD@2Al	Equation (7.16)	161.70	1.51	1.02×10^{-2}	1.85×10^{-3}	1.49×10^{-5}
	Dunham	161.69	1.51	1.02×10^{-2}	1.85×10^{-3}	1.41×10^{-5}
NO_2-GQD	Equation (7.16)	65.11	0.90	9.43×10^{-4}	5.86×10^{-4}	5.62×10^{-6}
	Dunham	65.10	0.90	1.18×10^{-3}	5.84×10^{-4}	5.40×10^{-6}
NO_2-GQD@1B	Equation (7.16)	168.83	0.60	5.02×10^{-4}	3.71×10^{-4}	2.67×10^{-7}
	Dunham	168.82	0.60	4.80×10^{-4}	3.73×10^{-4}	2.99×10^{-7}
NO_2GQD@1N	Equation (7.16)	143.52	0.74	6.07×10^{-4}	3.52×10^{-4}	1.60×10^{-6}
	Dunham	143.51	0.74	6.79×10^{-4}	3.49×10^{-4}	1.60×10^{-6}
NO_2-GQD@2Al	Equation (7.16)	177.42	0.67	1.04×10^{-3}	3.58×10^{-4}	1.45×10^{-7}
	Dunham	177.40	0.67	1.02×10^{-3}	3.59×10^{-4}	1.21×10^{-7}
SO_2-GQD	Equation (7.16)	48.53	0.48	3.66×10^{-4}	2.56×10^{-4}	1.16×10^{-6}
	Dunham	48.52	0.48	2.42×10^{-4}	2.57×10^{-4}	1.05×10^{-6}
SO_2-GQD@2B	Equation (7.16)	51.41	0.41	2.11×10^{-3}	2.11×10^{-4}	1.95×10^{-6}
	Dunham	51.41	0.41	2.01×10^{-3}	2.10×10^{-4}	1.81×10^{-6}
SO_2-GQD@2N	Equation (7.16)	53.29	0.69	5.58×10^{-4}	3.12×10^{-4}	2.54×10^{-6}
	Dunham	53.28	0.69	9.06×10^{-5}	3.12×10^{-4}	2.60×10^{-6}
SO_2-GQD@2Al	Equation (7.16)	42.90	0.23	1.23×10^{-3}	2.16×10^{-4}	3.88×10^{-7}
	Dunham	42.89	0.23	9.58×10^{-4}	2.17×10^{-4}	7.04×10^{-7}

Table 4 – Lifetime (in seconds) as a function of the temperature within the Slater theory.

Complex	Lifetime (s)			
	200 K	300 K	400 K	500 K
CO-GQD	4.8×10^{-11}	1.1×10^{-11}	5.3×10^{-12}	3.4×10^{-12}
CO-GQD@2B	9.7×10^{-10}	7.8×10^{-11}	2.2×10^{-11}	1.0×10^{-11}
CO-GQD@2N	2.0×10^{-10}	2.7×10^{-11}	9.8×10^{-12}	5.4×10^{-12}
CO-GQD@2Al	6.7×10^{-8}	1.3×10^{-9}	1.8×10^{-10}	5.5×10^{-11}
NH_3-GQD	3.5×10^{-10}	3.5×10^{-11}	1.1×10^{-11}	5.4×10^{-12}
NH_3-GQD@2B	1.0×10^{-7}	1.5×10^{-9}	1.8×10^{-10}	5.1×10^{-11}
NH_3-GQD@2N	9.9×10^{-9}	3.0×10^{-10}	5.3×10^{-11}	1.9×10^{-11}
NH_3-GQD@2Al	7.8×10^{-1}	5.0×10^{-5}	4.0×10^{-7}	2.2×10^{-8}
NO_2-GQD	3.0×10^{-9}	1.7×10^{-10}	4.0×10^{-11}	1.7×10^{-11}
NO_2-GQD@1B	6.8×10^{35}	4.5×10^{19}	3.7×10^{11}	5.1×10^{6}
NO_2-GQD@1N	6.2×10^{22}	9.6×10^{10}	1.2×10^{5}	3.4×10
NO_2-GQD@1Al	6.0×10^{40}	1.1×10^{23}	1.5×10^{14}	7.2×10^{8}
SO_2-GQD	5.0×10^{-9}	2.6×10^{-10}	5.9×10^{-11}	2.4×10^{-11}
SO_2-GQD@2B	4.7×10^{-8}	1.1×10^{-9}	1.7×10^{-10}	5.7×10^{-11}
SO_2-GQD@2N	1.4×10^{-8}	5.1×10^{-10}	9.5×10^{-11}	3.5×10^{-11}
SO_2-GQD@2Al	3.2×10^{-8}	9.3×10^{-10}	1.6×10^{-10}	5.5×10^{-11}

Thereby, the spectroscopy properties endorse the idea that the systems NO_2-GQD@1Al, NO_2-GQD@1B and NH_3-GQD@2Al are the most promising in regards to gas sensing.

16 Charge Displacement and Energy Decomposition

To better understand the charge displacement process between the adsorbates (CO, NH_3, NO_2, SO_2) and the adsorbent, second-order perturbation energies (E^2), obtained via NBO analysis were calculated and reported in Table 5.

Table 5 – Main NBO population donation at ωB97XD/6-31G(d,p) level of each system. E^2 stands for second-order perturbation energies obtained via NBO analysis.

Complex	Donor	Acceptor	E^2(mHa)
CO-GQD	BD (1) C73 - O74	RY* (3) C22	0.19
CO-GQD@2B	LP (1) C73	LP* (1) B22	5.47
CO-GQD@2N	LP (1) C73	BD* (1) N22 - C23	0.11
CO-GQD@2Al	LP (1) C73	LP* (4) Al22	21.66
NH_3-GQD	LP (1) N73	BD* (2) C21 - C22	0.49
NH_3-GQD@2B	LP (1) N73	LP* (1) B22	18.41
NH_3-GQD@2N	LP (1) N73	RY* (6) N22	0.30
NH_3-GQD@2Al	LP (1) N73	LP* (4) Al22	37.45
NO_2-GQD	BD (2) C21 - C22	LP* (2) N73	7.19
NO_2-GQD@1B	BD* (2) C11 - C12	BD* (1) B22 - N73	163.20
NO_2-GQD@1N	LP (2) O75	BD* (2) C21 - N22	4.49
NO_2-GQD@1Al	LP (1) N73	LP* (4) Al22	51.55
SO_2-GQD	BD (2) C11 - C12	LP* (2) S73	1.86
SO_2-GQD@2B	LP (1) S73	LP* (1) B22	5.08
SO_2-GQD@2N	LP (1) S73	RY* (1) N22	0.10
SO_2-GQD@2Al	LP (1) S73	LP* (4) Al22	14.20

Analyzing the systems with CO, it can be noted that when the adsorption occurs with the pristine GQD or the quantum dot doped with nitrogen, the charge displacement between the interacting components is negligible. Contrarily, when the interaction occurs with the GQD@2B or GQD@2Al, a significant charge displacement occurs from the 1-center valence lone pair C73 (the carbon of the CO) to the 1-center valence lone pair antibond B22 or Al22, when doped with boron or aluminum respectively.

The charge displacements within the system with NH_3 follow a similar pattern to those with carbon monoxide, the difference being that the charge displacements are now larger.

Once again, the systems with NO_2 present exciting results. The strength of the interaction is so high between the nitrogen dioxide and the quantum dot doped with boron, that a 2-center antibond is formed between the nitrogen from NO_2 and the boron

used in the functionalization (BD* B22-N73). This antibond receives charge from the 2-center antibond C11-C12.

When it comes to systems with SO_2, they also follow a similar pattern to those with carbon monoxide and ammonia, however, the charge displacement increase due to functionalizations with boron or aluminum is the smallest of all the systems.

In short, the functionalization with boron and aluminum implies an appreciable increase in the charge displacement between the adsorbates and the adsorbent, especially in the adsorption of NO_2, but when doped with nitrogen, the charge displacement reduces.

The results obtained by SAPT0 (Table 6) reveal the nature of the interactions of each system. For the majority of the systems, the dispersion term E_{disp} dominates, exposing the non-covalent character of these interactions. Nonetheless, the functionalizations with boron and aluminum seem to diminish the influence of the dispersion term and increase the significance of the electrostatic term E_{elst}. In the systems NH_3-GQD@2B, NH_3-GQD@2Al, and NO_2-GQD@1B, this increase of the electrostatic term is so great that it starts to dominate the interaction.

Table 6 – SAPT0/cc-pVDZ percentages of each contribution of the interaction energies for all systems. E_{elst}, E_{ind} , and E_{disp} refer to attractive electronic, induction, and attractive dispersion terms of interaction energy, respectively.

Systems	$\%E_{elst}$	$\%E_{ind}$	$\%E_{disp}$
CO-GQD	23.2	5.0	71.8
CO-GQD@2B	30.4	7.6	62.0
CO-GQD@2N	28.6	4.5	66.9
CO-GQD@2Al	42.2	11.6	46.2
NH_3-GQD	22.3	18.9	58.8
NH_3-GQD@2B	40.7	21.5	37.8
NH_3-GQD@2N	36.0	14.5	49.5
NH_3-GQD@2Al	57.5	19.6	22.9
NO_2-GQD	26.4	10.4	63.2
NO_2-GQD@1B	42.1	17.1	40.8
NO_2-GQD@1N	27.2	35.1	37.7
NO_2-GQD@1Al	30.2	42.1	27.7
SO_2-GQD	33.3	9.6	57.1
SO_2-GQD@2B	35.9	10.6	53.5
SO_2-GQD@2N	27.3	10.5	62.2
SO_2-GQD@2Al	32.3	13.1	54.6

Conclusions

The adsorbing capabilities of graphene quantum dots (GQDs) were investigated alongside functionalizations schemes with heteroatoms (boron, nitrogen, and aluminum). Hence, electronic and dynamic properties of systems comprised of a GQD and the most common pollutant gas molecules (CO, NH_3, NO_2, and SO_2), whose monitoring of emissions is crucial to sustainable development, were calculated.

The potential energy curves revealed that doping the GQD with boron or aluminum was very effective in increasing the well's depth and, thus, increasing the dissociation energy of the system. For example, the dissociation energy for the complex with NO_2 increased more than twelve times due to those functionalizations.

Moreover, the number of energy levels of each system also increased as a result of the functionalization, providing even more evidence that interaction becomes stronger. Therefore, the pollutant gas molecules are more easily captured by the functionalized quantum dot. Furthermore, the spectroscopic constants were calculated by two different and independent methodologies (Equation 7.16 and Dunham Method). Comparing the results show that there is an agreement between them, which suggests their reliability.

Regarding the energy decomposition in physically significant terms, the SAPT0 results show that the functionalizations induce a transition from systems dominated by the dispersion term to systems dominated by the electrostatic term. Consequently, doping graphene quantum dots with heteroatoms strengthens the bond with gas molecules. Finally, the NBO analysis helps to better understand the charge displacement process. The data suggest that these charge displacements have a key role in strengthening the bond between adsorbent and adsorbate.

In summary, doping graphene quantum dots with heteroatoms can drastically improve their adsorbing capabilities. For both carbon monoxide and ammonia, functionalizations with aluminum are the most effective, while the adsorption of sulfur dioxide was not very affected by any of the doping schemes. Particularly, doping quantum dots with either aluminum or boron is very promising regarding the application in nitrogen dioxide gas sensors. Therefore, an experimental study on the adsorption of NO_2, NH_3, and CO is highly encouraged due to the possibility of the formulation of an accurate, and resilient gas sensor for these molecules.

Bibliography

ARRUDA, P. Algumas considerações sobre conjuntos de bases para cálculos de propriedades elétricas. *Univerisadade Federal do Espírito Santo. Vitória*, p. 107, 2009. Cited on page 73.

BIGGERI, A.; BELLINI, P.; TERRACINI, B. Meta-analysis of the italian studies on short-term effects of air pollution–misa 1996-2002. *Epidemiologia e prevenzione*, v. 28, n. 4-5 Suppl, p. 4–100, 2004. Cited on page 21.

BORN, M.; OPPENHEIMER, R. On the quantum theory of molecules. In: *Quantum Chemistry: Classic Scientific Papers*. [S.l.]: World Scientific, 2000. p. 1–24. Cited on page 32.

CHAI, J.-D.; HEAD-GORDON, M. Long-range corrected hybrid density functionals with damped atom–atom dispersion corrections. *Physical Chemistry Chemical Physics*, Royal Society of Chemistry, v. 10, n. 44, p. 6615–6620, 2008. Cited on page 71.

DAI, J.; YUAN, J.; GIANNOZZI, P. Gas adsorption on graphene doped with b, n, al, and s: A theoretical study. *Applied Physics Letters*, American Institute of Physics, v. 95, n. 23, p. 232105, 2009. Cited on page 27.

DICKINSON, A.; CERTAIN, P. Calculation of matrix elements for one-dimensional quantum-mechanical problems. *The Journal of Chemical Physics*, American Institute of Physics, v. 49, n. 9, p. 4209–4211, 1968. Cited on page 54.

DUNHAM, J. The energy levels of a rotating vibrator. *Physical Review*, APS, v. 41, n. 6, p. 721, 1932. Cited on page 62.

FANO, U. Effects of configuration interaction on intensities and phase shifts. *Physical Review*, APS, v. 124, n. 6, p. 1866, 1961. Cited on page 44.

FOCK, V. A. *Selected works: quantum mechanics and quantum field theory*. [S.l.]: Chapman & Hall/CRC, 2004. Cited on page 39.

FOWLER, J. D. et al. Practical chemical sensors from chemically derived graphene. *ACS nano*, ACS Publications, v. 3, n. 2, p. 301–306, 2009. Cited on page 21.

FRISCH, M. J. et al. *Gaussian~09 Revision A.02*. 2009. Gaussian Inc. Wallingford CT. Cited 2 times on pages 65 and 71.

GEIM, A. K. Graphene: status and prospects. *science*, American Association for the Advancement of Science, v. 324, n. 5934, p. 1530–1534, 2009. Cited on page 25.

GEIM, A. K.; NOVOSELOV, K. S. The rise of graphene. In: *Nanoscience and technology: a collection of reviews from nature journals*. [S.l.]: World Scientific, 2010. p. 11–19. Cited on page 25.

GLENDENING, E. D.; LANDIS, C. R.; WEINHOLD, F. Nbo 6.0: Natural bond orbital analysis program. *Journal of computational chemistry*, Wiley Online Library, v. 34, n. 16, p. 1429–1437, 2013. Cited on page 65.

GRIMME, S. et al. A consistent and accurate ab initio parametrization of density functional dispersion correction (dft-d) for the 94 elements h-pu. *The Journal of chemical physics*, American Institute of Physics, v. 132, n. 15, p. 154104, 2010. Cited on page 71.

GROSS, E. K.; DREIZLER, R. M. *Density functional theory*. [S.l.]: Springer Science & Business Media, 2013. v. 337. Cited on page 47.

HARTREE, D. R. The calculation of atomic structures. Wiley, 1957. Cited on page 39.

HEHRE, W. J.; DITCHFIELD, R.; POPLE, J. A. Self—consistent molecular orbital methods. xii. further extensions of gaussian—type basis sets for use in molecular orbital studies of organic molecules. *The Journal of Chemical Physics*, American Institute of Physics, v. 56, n. 5, p. 2257–2261, 1972. Cited on page 73.

HUANG, B. et al. Adsorption of gas molecules on graphene nanoribbons and its implication for nanoscale molecule sensor. *The Journal of Physical Chemistry C*, ACS Publications, v. 112, n. 35, p. 13442–13446, 2008. Cited on page 21.

III, G. D. P.; BARTLETT, R. J. A full coupled-cluster singles and doubles model: The inclusion of disconnected triples. *The Journal of Chemical Physics*, American Institute of Physics, v. 76, n. 4, p. 1910–1918, 1982. Cited on page 44.

JACKSON, J. D. *Classical electrodynamics*. [S.l.]: American Association of Physics Teachers, 1999. Cited on page 32.

JEZIORSKI, B.; MOSZYNSKI, R.; SZALEWICZ, K. Perturbation theory approach to intermolecular potential energy surfaces of van der waals complexes. *Chemical Reviews*, ACS Publications, v. 94, n. 7, p. 1887–1930, 1994. Cited 2 times on pages 21 and 67.

KOHN, W.; SHAM, L. J. Self-consistent equations including exchange and correlation effects. *Physical review*, APS, v. 140, n. 4A, p. A1133, 1965. Cited on page 45.

KOŁSOS, W. Adiabatic approximation and its accuracy. In: *Advances in Quantum Chemistry*. [S.l.]: Elsevier, 1970. v. 5, p. 99–133. Cited on page 32.

KRUPA, S. Effects of atmospheric ammonia (nh3) on terrestrial vegetation: a review. *Environmental pollution*, Elsevier, v. 124, n. 2, p. 179–221, 2003. Cited on page 21.

LIN, X.; NI, J.; FANG, C. Adsorption capacity of h2o, nh3, co, and no2 on the pristine graphene. *Journal of Applied Physics*, American Institute of Physics, v. 113, n. 3, p. 034306, 2013. Cited on page 22.

LIU, H.; LIU, Y.; ZHU, D. Chemical doping of graphene. *Journal of materials chemistry*, Royal Society of Chemistry, v. 21, n. 10, p. 3335–3345, 2011. Cited on page 27.

MENEZES, R. F. de et al. Investigation of strength and nature of the weak intermolecular bond in nh2 radical-noble gas atom adducts and evaluation of their basic spectroscopic features. *Chemical Physics Letters*, Elsevier, v. 769, p. 138386, 2021. Cited on page 64.

MINENKOV, Y. et al. The accuracy of dft-optimized geometries of functional transition metal compounds: a validation study of catalysts for olefin metathesis and other reactions in the homogeneous phase. *Dalton Transactions*, Royal Society of Chemistry, v. 41, n. 18, p. 5526–5541, 2012. Cited on page 71.

MITIN, A. V. Calculation of rovibrational energy levels of diatomic molecules by dunham method with potential obtained from ab initio calculations. *Journal of computational chemistry*, Wiley Online Library, v. 19, n. 1, p. 94–101, 1998. Cited on page 62.

MØLLER, C.; PLESSET, M. S. Note on an approximation treatment for many-electron systems. *Physical review*, APS, v. 46, n. 7, p. 618, 1934. Cited on page 44.

NOVOSELOV, K. S. et al. Electric field effect in atomically thin carbon films. *science*, American Association for the Advancement of Science, v. 306, n. 5696, p. 666–669, 2004. Cited on page 25.

PEEL, J. L. et al. Ambient air pollution and respiratory emergency department visits. *Epidemiology*, JSTOR, p. 164–174, 2005. Cited on page 21.

POWELL, M. A method for minimizing a sum of squares of non-linear functions without calculating derivatives. *The Computer Journal*, The British Computer Society, v. 7, n. 4, p. 303–307, 1965. Cited 2 times on pages 71 and 77.

PRUDENTE, F. *Superfícies de Energia Potencial e Dinâmica Molecular*. Tese (Doutorado) — Tese de Doutorado, Instituto de Física, UnB, 1999. Cited on page 60.

PRUDENTE, F.; COSTA, L.; NETO, J. S. Discrete variable representation and negative imaginary potential to study metastable states and photodissociation processes. application to diatomic and triatomic molecules. *Journal of Molecular Structure: THEOCHEM*, Elsevier, v. 394, n. 2-3, p. 169–180, 1997. Cited on page 53.

RAEYANI, D.; SHOJAEI, S.; AHMADI-KANDJANI, S. Optical graphene quantum dots gas sensors: Experimental study. *Materials Research Express*, IOP Publishing, v. 7, n. 1, p. 015608, 2020. Cited on page 27.

RASSOLOV, V. A. et al. 6-31g* basis set for third-row atoms. *Journal of Computational Chemistry*, Wiley Online Library, v. 22, n. 9, p. 976–984, 2001. Cited on page 73.

REED, A. E.; WEINSTOCK, R. B.; WEINHOLD, F. Natural population analysis. *The Journal of Chemical Physics*, American Institute of Physics, v. 83, n. 2, p. 735–746, 1985. Cited on page 65.

ROOTHAAN, C. C. J. New developments in molecular orbital theory. *Reviews of modern physics*, APS, v. 23, n. 2, p. 69, 1951. Cited on page 43.

RYDBERG, R. Graphische darstellung einiger bandenspektroskopischer ergebnisse. *Zeitschrift für Physik*, Springer, v. 73, n. 5, p. 376–385, 1932. Cited on page 77.

SCHWEIZER, W. *Numerical quantum dynamics*. [S.l.]: Springer Science & Business Media, 2001. v. 9. Cited on page 54.

SLATER, J. C. The theory of complex spectra. *Physical Review*, APS, v. 34, n. 10, p. 1293, 1929. Cited 2 times on pages 41 and 64.

SZABO, A.; OSTLUND, N. S. *Modern quantum chemistry: introduction to advanced electronic structure theory*. [S.l.]: Courier Corporation, 2012. Cited 3 times on pages 32, 40, and 41.

TIAN, P. et al. Graphene quantum dots from chemistry to applications. *Materials today chemistry*, Elsevier, v. 10, p. 221–258, 2018. Cited on page 27.

WANNO, B.; TABTIMSAI, C. A dft investigation of co adsorption on viiib transition metal-doped graphene sheets. *Superlattices and Microstructures*, Elsevier, v. 67, p. 110–117, 2014. Cited on page 22.

WEHLING, T. et al. Molecular doping of graphene. *Nano letters*, ACS Publications, v. 8, n. 1, p. 173–177, 2008. Cited on page 22.

WEINHOLD, F. Natural bond orbital analysis: a critical overview of relationships to alternative bonding perspectives. *Journal of computational chemistry*, Wiley Online Library, v. 33, n. 30, p. 2363–2379, 2012. Cited 2 times on pages 21 and 65.

ZHANG, Y.-H. et al. Improving gas sensing properties of graphene by introducing dopants and defects: a first-principles study. *Nanotechnology*, IOP Publishing, v. 20, n. 18, p. 185504, 2009. Cited on page 27.

APPENDIX A – Electronic Energies

Table 7 – Electronic energies (in Hartree) of the systems CO-GQD, CO-GQD@2B, CO-GQD@2N, and CO-GQD@2Al calculated at ωB97XD/6-31G(d,p) level.

CO-GQD		CO-GQD@2B		CO-GQD@2N		CO-GQD@2Al	
R(Å)	Energy (Ha)	R(Å)	Energy (Ha)	R(Å)	Energy (Ha)	R(Å)	Energy (Ha)
2.3	0.03226701	2.0	0.01482097	2.0	0.08061333	2.0	0.02211123
2.4	0.02212166	2.1	0.00985752	2.1	0.05654070	2.1	0.01444421
2.5	0.01449680	2.2	0.00567934	2.2	0.03857989	2.2	0.00852148
2.6	0.00881910	2.3	0.00234839	2.3	0.02534773	2.3	0.00398768
2.7	0.00470505	2.4	-0.00018335	2.4	0.01574625	2.4	0.00048537
2.8	0.00183803	2.5	-0.00204929	2.5	0.00887428	2.5	-0.00226173
2.9	-0.00016170	2.6	-0.00332364	2.6	0.00406669	2.6	-0.00428347
3.0	-0.00148996	2.7	-0.00419277	2.7	0.00078124	2.7	-0.00569087
3.1	-0.00227499	2.8	-0.00468034	2.8	-0.00139552	2.8	-0.00665096
3.2	-0.00270887	2.9	-0.00489400	2.9	-0.00274091	2.9	-0.00727948
3.3	-0.00290273	3.0	-0.00493230	3.0	-0.00351306	3.0	-0.00757062
3.4	-0.00291036	3.1	-0.00493388	3.1	-0.00390262	3.05	-0.00763481
3.5	-0.00280516	3.2	-0.00493373	3.15	-0.00397667	3.06	-0.00763964
3.6	-0.00264081	3.25	-0.00493195	3.16	-0.00398279	3.07	-0.00764238
3.7	-0.00244796	3.26	-0.00492865	3.17	-0.00398703	3.08	-0.00764367
3.8	-0.00224442	3.27	-0.00492389	3.18	-0.00398995	3.09	-0.00764431
3.9	-0.00203459	3.28	-0.00491779	3.19	-0.00399179	3.1	-0.00764491
4.0	-0.00183726	3.29	-0.00491045	3.2	-0.00399216	3.11	-0.00764537
4.1	-0.00164904	3.3	-0.00490200	3.21	-0.00399036	3.12	-0.00764474
4.2	-0.00147785	3.31	-0.00489255	3.22	-0.00398604	3.13	-0.00764187
4.3	-0.00132272	3.32	-0.00488216	3.23	-0.00397952	3.14	-0.00763612
4.4	-0.00118207	3.33	-0.00481566	3.24	-0.00397124	3.15	-0.00762778
4.5	-0.00105189	3.34	-0.00460984	3.25	-0.00396144	3.2	-0.00757314
4.6	-0.00092782	3.35	-0.00435155	3.3	-0.00389152	3.3	-0.00737088
4.7	-0.00081009	3.4	-0.00406741	3.4	-0.00368190	3.4	-0.00705186
4.8	-0.00070727	3.5	-0.00377599	3.5	-0.00342508	3.5	-0.00668867
4.9	-0.00062000	3.6	-0.00348005	3.6	-0.00313812	3.6	-0.00627555
5.0	-0.00054549	3.7	-0.00320031	3.7	-0.00284952	3.7	-0.00583484
5.1	-0.00047902	3.8	-0.00293924	3.8	-0.00257358	3.8	-0.00538769

5.2	-0.00041785	3.9	-0.00270212	3.9	-0.00231742	3.9	-0.00494176
5.3	-0.00036444	4.0	-0.00248453	4.0	-0.00208066	4.0	-0.00452200
5.4	-0.00031915	4.1	-0.00228662	4.1	-0.00185422	4.1	-0.00412076
5.5	-0.00027982	4.2	-0.00209961	4.2	-0.00165797	4.2	-0.00374240
5.6	-0.00024506	4.3	-0.00192621	4.3	-0.00148653	4.3	-0.00339858
5.7	-0.00021410	4.4	-0.00176967	4.4	-0.00132425	4.4	-0.00307705
5.8	-0.00018622	4.5	-0.00162982	4.5	-0.00116374	4.5	-0.00277852
5.9	-0.00016123	4.6	-0.00150571	4.6	-0.00101483	4.6	-0.00250196
6.0	-0.00013902	4.7	-0.00139464	4.7	-0.00088708	4.7	-0.00225146
6.1	-0.00011919	4.8	-0.00129278	4.8	-0.00077858	4.8	-0.00202452
6.2	-0.00010138	4.9	-0.00120129	4.9	-0.00068448	4.9	-0.00181592
6.3	-0.00008538	5.0	-0.00111889	5.0	-0.00060029	5.0	-0.00162296
6.4	-0.00007103	5.1	-0.00104582	5.1	-0.00052641	5.1	-0.00144401
6.5	-0.00005822	5.2	-0.00097957	5.2	-0.00046188	5.2	-0.00128422
6.6	-0.00004683	5.3	-0.00091802	5.3	-0.00040605	5.3	-0.00114268
6.7	-0.00003671	5.4	-0.00085953	5.4	-0.00035796	5.4	-0.00101729
6.8	-0.00002778	5.5	-0.00080359	5.5	-0.00031587	5.5	-0.00090526
6.9	-0.00001992	5.6	-0.00075051	5.6	-0.00027794	5.6	-0.00080537
7.0	-0.00001304	5.7	-0.00069940	5.7	-0.00024452	5.7	-0.00071728
7.1	-0.00000707	5.8	-0.00064970	5.8	-0.00021476	5.8	-0.00064056
7.2	-0.00000193	5.9	-0.00060114	5.9	-0.00018815	5.9	-0.00057390
7.3	0.00000241	6.0	-0.00055359	6.0	-0.00016423	6.0	-0.00051569
7.4	0.00000606	6.1	-0.00050703	6.1	-0.00014280	6.1	-0.00046424
7.5	0.00000901	6.2	-0.00046149	6.2	-0.00012356	6.2	-0.00041959
7.6	0.00001135	6.3	-0.00041703	6.3	-0.00010629	6.3	-0.00038040
7.7	0.00001309	6.4	-0.00037372	6.4	-0.00009086	6.4	-0.00034592
7.8	0.00001431	6.5	-0.00033165	6.5	-0.00007708	6.5	-0.00031538
7.9	0.00001501	6.6	-0.00029098	6.6	-0.00006479	6.6	-0.00028826
8.0	0.00001524	6.7	-0.00025183	6.7	-0.00005386	6.7	-0.00026407
8.3	0.00001337	6.8	-0.00021438	6.8	-0.00004414	6.8	-0.00024234
8.6	0.00000813	6.9	-0.00017878	6.9	-0.00003556	6.9	-0.00022272
8.9	0.00000000	7.0	-0.00014522	7.0	-0.00002799	7.0	-0.00020488
-	-	7.1	-0.00011382	7.1	-0.00002137	7.1	-0.00018849
-	-	7.2	-0.00008475	7.2	-0.00001563	7.2	-0.00017335
-	-	7.3	-0.00005813	7.3	-0.00001068	7.3	-0.00015934
-	-	7.4	-0.00003413	7.4	-0.00000646	7.4	-0.00014628
-	-	7.5	-0.00001282	7.5	-0.00000290	7.5	-0.00013397
-	-	7.6	0.00000563	7.6	0.00000005	7.6	-0.00012237
-	-	7.7	0.00002117	7.7	0.00000243	7.7	-0.00011141

-	-	7.8	0.00003371	7.8	0.00000432	7.8	-0.00010092
-	-	7.9	0.00004309	7.9	0.00000570	7.9	-0.00009093
-	-	8.0	0.00004932	8.0	0.00000669	8.0	-0.00008131
-	-	8.1	0.00005230	8.1	0.00000729	8.1	-0.00007204
-	-	8.2	0.00005197	8.2	0.00000750	8.2	-0.00006315
-	-	8.3	0.00004834	8.3	0.00000741	8.3	-0.00005450
-	-	8.4	0.00004132	8.4	0.00000701	8.4	-0.00004613
-	-	8.5	0.00003093	8.5	0.00000636	8.5	-0.00003797
-	-	8.6	0.00001716	8.6	0.00000546	8.6	-0.00003001
-	-	8.7	0.00000000	8.7	0.00000436	8.7	-0.00002227
-	-	8.8	-0.00001467	8.8	0.00000307	8.8	-0.00001467
-	-	8.9	-0.00000725	8.9	0.00000161	8.9	-0.00000725
-	-	9.0	0.00000000	9.0	0.00000000	9.0	0.00000000

Table 8 – Electronic energies (in Hartree) of the systems NH_3-GQD, NH_3-GQD@2B, NH_3-GQD@2N, and NH_3-GQD@2Al calculated at ωB97XD/6-31G(d,p) level.

NH_3-GQD		NH_3-GQD@2B		NH_3-GQD@2N		NH_3-GQD@2Al	
R(Å)	Energy (Ha)	R(Å)	Energy (Ha)	R(Å)	Energy (Ha)	R(Å)	Energy (Ha)
2.0	0.06492704	2.0	0.00925466	2.0	0.07600202	2.0	0.00611630
2.1	0.04723605	2.1	0.00405607	2.1	0.05087327	2.1	-0.00404572
2.2	0.03290507	2.2	0.00008967	2.2	0.03234561	2.2	-0.01072401
2.3	0.02175199	2.3	-0.00294978	2.3	0.01896834	2.3	-0.01482646
2.4	0.01330116	2.4	-0.00512324	2.4	0.00951191	2.4	-0.01720696
2.5	0.00709667	2.5	-0.00665691	2.5	0.00302090	2.5	-0.01837970
2.6	0.00265740	2.6	-0.00760393	2.6	-0.00129559	2.55	-0.01862463
2.7	-0.00040525	2.7	-0.00813355	2.7	-0.00406970	2.56	-0.01865206
2.8	-0.00239449	2.75	-0.00824444	2.8	-0.00571884	2.57	-0.01867390
2.9	-0.00363072	2.76	-0.00825933	2.9	-0.00656187	2.58	-0.01869044
3.0	-0.00432902	2.77	-0.00827235	2.95	-0.00678042	2.59	-0.01870158
3.05	-0.00452077	2.78	-0.00828323	2.96	-0.00681044	2.6	-0.01870710
3.06	-0.00454793	2.79	-0.00829162	2.97	-0.00683598	2.61	-0.01870658
3.07	-0.00457117	2.8	-0.00829725	2.98	-0.00685717	2.62	-0.01869965
3.08	-0.00459051	2.81	-0.00829992	2.99	-0.00687408	2.63	-0.01868597
3.09	-0.00460609	2.82	-0.00829953	3.0	-0.00688683	2.64	-0.01866530
3.1	-0.00461807	2.83	-0.00829603	3.01	-0.00689563	2.65	-0.01863762
3.11	-0.00462674	2.84	-0.00828940	3.02	-0.00690084	2.7	-0.01840793
3.12	-0.00463249	2.85	-0.00827972	3.03	-0.00690291	2.8	-0.01771707
3.13	-0.00463584	2.9	-0.00819198	3.04	-0.00690226	2.9	-0.01678354
3.14	-0.00463733	3.0	-0.00790554	3.05	-0.00689915	3.0	-0.01576183
3.15	-0.00463740	3.1	-0.00751446	3.1	-0.00684777	3.1	-0.01462346
3.2	-0.00461455	3.2	-0.00702661	3.2	-0.00658423	3.2	-0.01350243
3.3	-0.00443917	3.3	-0.00650690	3.3	-0.00615633	3.3	-0.01240994
3.4	-0.00414773	3.4	-0.00598264	3.4	-0.00563014	3.4	-0.01136089
3.5	-0.00377920	3.5	-0.00547160	3.5	-0.00507588	3.5	-0.01033612
3.6	-0.00338169	3.6	-0.00498947	3.6	-0.00454252	3.6	-0.00941678
3.7	-0.00298765	3.7	-0.00453582	3.7	-0.00402290	3.7	-0.00855898
3.8	-0.00261107	3.8	-0.00411240	3.8	-0.00354689	3.8	-0.00777064
3.9	-0.00226340	3.9	-0.00372291	3.9	-0.00312186	3.9	-0.00704211
4.0	-0.00195462	4.0	-0.00335401	4.0	-0.00273780	4.0	-0.00637130
4.1	-0.00167925	4.1	-0.00301615	4.1	-0.00237685	4.1	-0.00577661
4.2	-0.00143381	4.2	-0.00269968	4.2	-0.00205107	4.2	-0.00523296

4.3	-0.00122036	4.3	-0.00240771	4.3	-0.00177205	4.3	-0.00472855
4.4	-0.00103332	4.4	-0.00214041	4.4	-0.00152434	4.4	-0.00426637
4.5	-0.00086920	4.5	-0.00189149	4.5	-0.00128997	4.5	-0.00383040
4.6	-0.00072342	4.6	-0.00166032	4.6	-0.00107841	4.6	-0.00342031
4.7	-0.00058942	4.7	-0.00145562	4.7	-0.00089877	4.7	-0.00303612
4.8	-0.00047584	4.8	-0.00127641	4.8	-0.00074729	4.8	-0.00267827
4.9	-0.00038094	4.9	-0.00112211	4.9	-0.00061957	4.9	-0.00234829
5.0	-0.00030151	5.0	-0.00099184	5.0	-0.00050677	5.0	-0.00204169
5.1	-0.00023333	5.1	-0.00088095	5.1	-0.00041047	5.1	-0.00175809
5.2	-0.00017214	5.2	-0.00078811	5.2	-0.00032680	5.2	-0.00150190
5.3	-0.00012058	5.3	-0.00070974	5.3	-0.00025602	5.3	-0.00127344
5.4	-0.00007687	5.4	-0.00064564	5.4	-0.00019515	5.4	-0.00107189
5.5	-0.00003966	5.5	-0.00059235	5.5	-0.00014229	5.5	-0.00089451
5.6	-0.00000795	5.6	-0.00054688	5.6	-0.00009619	5.6	-0.00073970
5.7	0.00001920	5.7	-0.00050653	5.7	-0.00005624	5.7	-0.00060670
5.8	0.00004256	5.8	-0.00047083	5.8	-0.00002162	5.8	-0.00049366
5.9	0.00006227	5.9	-0.00043811	5.9	0.00000828	5.9	-0.00039838
6.0	0.00007883	6.0	-0.00040722	6.0	0.00003395	6.0	-0.00031783
6.1	0.00009255	6.1	-0.00037734	6.1	0.00005590	6.1	-0.00025034
6.2	0.00010374	6.2	-0.00034777	6.2	0.00007452	6.2	-0.00019424
6.3	0.00011269	6.3	-0.00031801	6.3	0.00009012	6.3	-0.00014768
6.4	0.00011964	6.4	-0.00028775	6.4	0.00010301	6.4	-0.00010945
6.5	0.00012480	6.5	-0.00025678	6.5	0.00011344	6.5	-0.00007816
6.6	0.00012836	6.6	-0.00022506	6.6	0.00012166	6.6	-0.00005272
6.7	0.00013048	6.7	-0.00019262	6.7	0.00012787	6.7	-0.00003217
6.8	0.00013131	6.8	-0.00015962	6.8	0.00013227	6.8	-0.00001565
6.9	0.00013099	6.9	-0.00012630	6.9	0.00013505	6.9	-0.00000249
7.0	0.00012965	7.0	-0.00009298	7.0	0.00013635	7.0	0.00000789
7.1	0.00012739	7.1	-0.00006001	7.1	0.00013631	7.1	0.00001595
7.2	0.00012431	7.2	-0.00002782	7.2	0.00013507	7.2	0.00002202
7.3	0.00012052	7.3	0.00000317	7.3	0.00013273	7.3	0.00002650
7.4	0.00011608	7.4	0.00003249	7.4	0.00012942	7.4	0.00002958
7.5	0.00011107	7.5	0.00005973	7.5	0.00012521	7.5	0.00003155
7.6	0.00010556	7.6	0.00008443	7.6	0.00012022	7.6	0.00003256
7.7	0.00009961	7.7	0.00010620	7.7	0.00011450	7.7	0.00003276
7.8	0.00009325	7.8	0.00012465	7.8	0.00010812	7.8	0.00003227
7.9	0.00008656	7.9	0.00013947	7.9	0.00010117	7.9	0.00003122
8.0	0.00007957	8.0	0.00015032	8.0	0.00009369	8.0	0.00002967
8.1	0.00007232	8.1	0.00015694	8.1	0.00008574	8.1	0.00002771

8.2	0.00006484	8.2	0.00015911	8.2	0.00007737	8.2	0.00002540
8.3	0.00005717	8.3	0.00015664	8.3	0.00006864	8.3	0.00002281
8.4	0.00004933	8.4	0.00014933	8.4	0.00005956	8.4	0.00001997
8.5	0.00004133	8.5	0.00013709	8.5	0.00005019	8.5	0.00001691
8.6	0.00003324	8.6	0.00011982	8.6	0.00004057	8.6	0.00001373
8.7	0.00002504	8.7	0.00009746	8.7	0.00003071	8.7	0.00001043
8.8	0.00001675	8.8	0.00006999	8.8	0.00002063	8.8	0.00000701
8.9	0.00000841	8.9	0.00003748	8.9	0.00001040	8.9	0.00000353
9.0	0.00000000	9.0	0.00000000	9.0	0.00000000	9.0	0.00000000

Table 9 – Electronic energies (in Hartree) of the systems NO_2-GQD, NO_2-GQD@1B, NO_2-GQD@1N, and NO_2-GQD@1Al calculated at ωB97XD/6-31G(d,p) level.

NO_2-GQD		NO_2-GQD@1B		NO_2-GQD@1N		NO_2-GQD@1Al	
R(Å)	Energy (Ha)	R(Å)	Energy (Ha)	R(Å)	Energy (Ha)	R(Å)	Energy (Ha)
2.0	0.04473474	1.0	0.65809858	1.0	0.76492434	1.4	0.29372073
2.1	0.03090945	1.1	0.42411651	1.1	0.53508383	1.5	0.17101715
2.2	0.01997121	1.2	0.27045098	1.2	0.38361807	1.6	0.08576122
2.3	0.01165925	1.3	0.16551984	1.3	0.27732960	1.7	0.02677676
2.4	0.00546575	1.4	0.09164419	1.4	0.19869096	1.8	-0.01357214
2.5	0.00108317	1.5	0.03871239	1.5	0.13775086	1.9	-0.04055383
2.6	-0.00188070	1.6	0.00058160	1.6	0.08915472	2.0	-0.05808592
2.7	-0.00378714	1.7	-0.02643541	1.7	0.04998397	2.1	-0.06891742
2.8	-0.00491075	1.8	-0.04518363	1.8	0.01911263	2.2	-0.07484439
2.9	-0.00546660	1.9	-0.05757272	1.9	-0.00458729	2.3	-0.07753360
2.95	-0.00559687	2.0	-0.06527038	2.0	-0.02217678	2.35	-0.07797146
2.96	-0.00561328	2.1	-0.06950812	2.1	-0.03464157	2.36	-0.07798819
2.97	-0.00562665	2.15	-0.07057419	2.2	-0.04301085	2.37	-0.07798374
2.98	-0.00563707	2.16	-0.07071774	2.3	-0.04816326	2.38	-0.07795970
2.99	-0.00564459	2.17	-0.07084070	2.4	-0.05096322	2.39	-0.07791776
3.0	-0.00564928	2.18	-0.07094378	2.45	-0.05166249	2.4	-0.07785971
3.01	-0.00565118	2.19	-0.07102735	2.46	-0.05175217	2.41	-0.07778687
3.02	-0.00565037	2.2	-0.07109152	2.47	-0.05182614	2.42	-0.07770052
3.03	-0.00564703	2.21	-0.07113647	2.48	-0.05188510	2.43	-0.07760156
3.04	-0.00564141	2.22	-0.07116253	2.49	-0.05192987	2.44	-0.07749057
3.05	-0.00563384	2.23	-0.07117022	2.5	-0.05196123	2.45	-0.07736800
3.1	-0.00556768	2.24	-0.07116020	2.51	-0.05197976	2.5	-0.07658866
3.2	-0.00530638	2.25	-0.07113328	2.52	-0.05198585	2.6	-0.07428719
3.3	-0.00496432	2.3	-0.07077841	2.53	-0.05198000	2.7	-0.07130420
3.4	-0.00457672	2.4	-0.06925207	2.54	-0.05196310	2.8	-0.06791446
3.5	-0.00416070	2.5	-0.06680789	2.55	-0.05193621	2.9	-0.06435510
3.6	-0.00375177	2.6	-0.06382674	2.6	-0.05166391	3.0	-0.06069068
3.7	-0.00337765	2.7	-0.06052144	2.7	-0.05052909	3.1	-0.05708611
3.8	-0.00302849	2.8	-0.05708156	2.8	-0.04883909	3.2	-0.05359827
3.9	-0.00270573	2.9	-0.05366486	2.9	-0.04679783	3.3	-0.05024982
4.0	-0.00241534	3.0	-0.05030562	3.0	-0.04459410	3.4	-0.04706651
4.1	-0.00215412	3.1	-0.04704501	3.1	-0.04234801	3.5	-0.04409591
4.2	-0.00192121	3.2	-0.04396821	3.2	-0.04012557	3.6	-0.04131032

4.3	-0.00171215	3.3	-0.04105431	3.3	-0.03796052	3.7	-0.03870993
4.4	-0.00152211	3.4	-0.03831010	3.4	-0.03589685	3.8	-0.03629909
4.5	-0.00135124	3.5	-0.03575145	3.5	-0.03396491	3.9	-0.03406433
4.6	-0.00119849	3.6	-0.03336895	3.6	-0.03216795	4.0	-0.03200081
4.7	-0.00106542	3.7	-0.03117770	3.7	-0.03151926	4.1	-0.03007792
4.8	-0.00094849	3.8	-0.02914737	3.8	-0.03021103	4.2	-0.02829792
4.9	-0.00084492	3.9	-0.02726635	3.9	-0.02894913	4.3	-0.02665998
5.0	-0.00075295	4.0	-0.02553846	4.0	-0.02773041	4.4	-0.02514153
5.1	-0.00067165	4.1	-0.02395577	4.1	-0.02654867	4.5	-0.02372623
5.2	-0.00059971	4.2	-0.02251040	4.2	-0.02543289	4.6	-0.02241853
5.3	-0.00053560	4.3	-0.02118779	4.3	-0.02437705	4.7	-0.02120822
5.4	-0.00047806	4.4	-0.01996954	4.4	-0.02336564	4.8	-0.02008287
5.5	-0.00042631	4.5	-0.01884677	4.5	-0.02238695	4.9	-0.01903227
5.6	-0.00037956	4.6	-0.01781307	4.6	-0.02145902	5.0	-0.01805019
5.7	-0.00033724	4.7	-0.01685844	4.7	-0.02058584	5.1	-0.01713533
5.8	-0.00029890	4.8	-0.01597585	4.8	-0.01976116	5.2	-0.01628396
5.9	-0.00026414	4.9	-0.01516014	4.9	-0.01897702	5.3	-0.01548891
6.0	-0.00023260	5.0	-0.01440245	5.0	-0.01823197	5.4	-0.01474404
6.1	-0.00020400	5.1	-0.01369641	5.1	-0.01752157	5.5	-0.01404419
6.2	-0.00017807	5.2	-0.01303714	5.2	-0.01684502	5.6	-0.01338683
6.3	-0.00015457	5.3	-0.01242075	5.3	-0.01619980	5.7	-0.01276908
6.4	-0.00013330	5.4	-0.01184126	5.4	-0.01558218	5.8	-0.01218726
6.5	-0.00011408	5.5	-0.01129405	5.5	-0.01498974	5.9	-0.01163657
6.6	-0.00009674	5.6	-0.01077457	5.6	-0.01442057	6.0	-0.01111402
6.7	-0.00008115	5.7	-0.01028009	5.7	-0.01387291	6.1	-0.01061715
6.8	-0.00006718	5.8	-0.00980775	5.8	-0.01334489	6.2	-0.01014297
6.9	-0.00005467	5.9	-0.00935498	5.9	-0.01283534	6.3	-0.00968966
7.0	-0.00004353	6.0	-0.00891965	6.0	-0.01234273	6.4	-0.00925470
7.1	-0.00003368	6.1	-0.00849998	6.1	-0.01183569	6.5	-0.00883659
7.2	-0.00002502	6.2	-0.00809446	6.2	-0.01138182	6.6	-0.00843384
7.3	-0.00001746	6.3	-0.00770182	6.3	-0.01093970	6.7	-0.00804533
7.4	-0.00001093	6.4	-0.00732102	6.4	-0.01050893	6.8	-0.00766987
7.5	-0.00000534	6.5	-0.00695114	6.5	-0.01008914	6.9	-0.00730621
7.6	-0.00000064	6.6	-0.00659143	6.6	-0.00968001	7.0	-0.00695360
7.7	0.00000324	6.7	-0.00622504	6.7	-0.00928499	7.1	-0.00661131
7.8	0.00000632	6.8	-0.00589988	6.8	-0.00889471	7.2	-0.00627858
7.9	0.00000871	6.9	-0.00555853	6.9	-0.00851427	7.3	-0.00595494
8.0	0.00001042	7.0	-0.00524196	7.0	-0.00814328	7.4	-0.00563981
8.1	0.00001150	7.1	-0.00492457	7.1	-0.00778124	7.5	-0.00533274

8.2	0.00001203	7.2	-0.00461441	7.2	-0.00742779	7.6	-0.00503315
8.3	0.00001203	7.3	-0.00431113	7.3	-0.00708263	7.7	-0.00474074
8.4	0.00001151	7.4	-0.00401452	7.4	-0.00674535	7.8	-0.00445518
8.5	0.00001054	7.5	-0.00372425	7.5	-0.00641567	7.9	-0.00417599
8.6	0.00000914	7.6	-0.00344012	7.6	-0.00609327	8.0	-0.00390319
8.7	0.00000736	7.7	-0.00316187	7.7	-0.00577792	8.1	-0.00363621
8.8	0.00000521	7.8	-0.00288936	7.8	-0.00546936	8.2	-0.00337480
8.9	0.00000274	7.9	-0.00262229	7.9	-0.00516730	8.3	-0.00311897
9.0	0.00000000	8.0	-0.00236056	8.0	-0.00487156	8.4	-0.00286827
-	-	8.1	-0.00210395	8.1	-0.00458189	8.5	-0.00262255
-	-	8.2	-0.00185229	8.2	-0.00429806	8.6	-0.00238163
-	-	8.3	-0.00160544	8.3	-0.00401989	8.7	-0.00214531
-	-	8.4	-0.00136326	8.4	-0.00374721	8.8	-0.00191343
-	-	8.5	-0.00112558	8.5	-0.00347980	8.9	-0.00168581
-	-	8.6	-0.00089227	8.6	-0.00321756	9.0	-0.00146229
-	-	8.7	-0.00066317	8.7	-0.00296023	9.1	-0.00124275
-	-	8.8	-0.00043820	8.8	-0.00270772	9.2	-0.00102701
-	-	8.9	-0.00021718	8.9	-0.00245985	9.3	-0.00081492
-	-	9.0	0.00000000	9.0	-0.00221646	9.4	-0.00060637
-	-	-	-	9.1	-0.00197743	9.5	-0.00040119
-	-	-	-	9.2	-0.00174262	9.6	-0.00019931
-	-	-	-	9.3	-0.00151189	9.7	0.00000000
-	-	-	-	9.4	-0.00128511	-	-
-	-	-	-	9.5	-0.00106214	-	-
-	-	-	-	9.6	-0.00084289	-	-
-	-	-	-	9.7	-0.00062714	-	-
-	-	-	-	9.8	-0.00041481	-	-
-	-	-	-	9.9	-0.00020578	-	-
-	-	-	-	10.0	0.00000000	-	-

Table 10 – Electronic energies (in Hartree) of the systems SO_2-GQD, SO_2-GQD@2B, SO_2-GQD@2N, and SO_2-GQD@2Al calculated at ωB97XD/6-31G(d,p) level.

SO_2-GQD		SO_2-GQD@2B		SO_2-GQD@2N		SO_2GQD@2Al	
R(Å)	Energy (Ha)	R(Å)	Energy (Ha)	R(Å)	Energy (Ha)	R(Å)	Energy (Ha)
2.0	0.13106745	2.0	0.06760929	2.0	0.13511567	2.0	0.08509949
2.1	0.09912208	2.1	0.05381456	2.1	0.09726547	2.1	0.06014532
2.2	0.07307073	2.2	0.04133833	2.2	0.06824394	2.2	0.04203414
2.3	0.05240822	2.3	0.03035899	2.3	0.04630398	2.3	0.02852276
2.4	0.03631708	2.4	0.02101692	2.4	0.03007407	2.4	0.01856354
2.5	0.02397769	2.5	0.01345378	2.5	0.01818023	2.5	0.01095192
2.6	0.01478422	2.6	0.00737089	2.6	0.00966318	2.6	0.00536166
2.7	0.00797230	2.7	0.00271068	2.7	0.00370916	2.7	0.00120285
2.8	0.00302855	2.8	-0.00079464	2.8	-0.00040613	2.8	-0.00172198
2.9	-0.00037024	2.9	-0.00331833	2.9	-0.00312158	2.9	-0.00376041
3.0	-0.00270580	3.0	-0.00503373	3.0	-0.00481710	3.0	-0.00514840
3.1	-0.00423987	3.1	-0.00619976	3.1	-0.00581481	3.1	-0.00602786
3.2	-0.00513422	3.2	-0.00687195	3.2	-0.00632420	3.2	-0.00652227
3.3	-0.00558467	3.3	-0.00715236	3.25	-0.00644496	3.3	-0.00676576
3.35	-0.00568774	3.35	-0.00720015	3.26	-0.00645875	3.35	-0.00682312
3.36	-0.00570185	3.36	-0.00720318	3.27	-0.00646884	3.36	-0.00682880
3.37	-0.00571391	3.37	-0.00720389	3.28	-0.00647537	3.37	-0.00683252
3.38	-0.00572406	3.38	-0.00720232	3.29	-0.00647867	3.38	-0.00683461
3.39	-0.00573215	3.39	-0.00719867	3.3	-0.00647940	3.39	-0.00683535
3.4	-0.00573832	3.4	-0.00719314	3.31	-0.00647824	3.4	-0.00683475
3.41	-0.00574256	3.41	-0.00718591	3.32	-0.00647582	3.41	-0.00683252
3.42	-0.00574486	3.42	-0.00717709	3.33	-0.00647214	3.42	-0.00682828
3.43	-0.00574520	3.43	-0.00716672	3.34	-0.00646682	3.43	-0.00682184
3.44	-0.00574360	3.44	-0.00715484	3.35	-0.00645951	3.44	-0.00681344
3.45	-0.00573995	3.45	-0.00714151	3.4	-0.00639429	3.45	-0.00680358
3.5	-0.00569098	3.5	-0.00705452	3.5	-0.00616338	3.5	-0.00674068
3.6	-0.00549075	3.6	-0.00677426	3.6	-0.00586295	3.6	-0.00656275
3.7	-0.00520860	3.7	-0.00641118	3.7	-0.00551739	3.7	-0.00630606
3.8	-0.00488507	3.8	-0.00600832	3.8	-0.00515101	3.8	-0.00598978
3.9	-0.00453776	3.9	-0.00558365	3.9	-0.00478436	3.9	-0.00563337
4.0	-0.00418514	4.0	-0.00515287	4.0	-0.00442949	4.0	-0.00525979
4.1	-0.00384675	4.1	-0.00474327	4.1	-0.00409971	4.1	-0.00489111
4.2	-0.00351753	4.2	-0.00435905	4.2	-0.00378281	4.2	-0.00452100

4.3	-0.00321136	4.3	-0.00400676	4.3	-0.00349115	4.3	-0.00416467
4.4	-0.00292938	4.4	-0.00368759	4.4	-0.00323333	4.4	-0.00382501
4.5	-0.00267549	4.5	-0.00340172	4.5	-0.00299813	4.5	-0.00350434
4.6	-0.00243956	4.6	-0.00314097	4.6	-0.00277065	4.6	-0.00320394
4.7	-0.00221677	4.7	-0.00290228	4.7	-0.00255271	4.7	-0.00292124
4.8	-0.00200542	4.8	-0.00268668	4.8	-0.00235317	4.8	-0.00266165
4.9	-0.00181387	4.9	-0.00249629	4.9	-0.00217677	4.9	-0.00242474
5.0	-0.00164307	5.0	-0.00233092	5.0	-0.00202112	5.0	-0.00220706
5.1	-0.00149399	5.1	-0.00218717	5.1	-0.00188086	5.1	-0.00200599
5.2	-0.00136180	5.2	-0.00205861	5.2	-0.00175452	5.2	-0.00181814
5.3	-0.00124006	5.3	-0.00194030	5.3	-0.00164020	5.3	-0.00164627
5.4	-0.00112822	5.4	-0.00183299	5.4	-0.00153569	5.4	-0.00149200
5.5	-0.00102771	5.5	-0.00173840	5.5	-0.00144067	5.5	-0.00135281
5.6	-0.00093825	5.6	-0.00165493	5.6	-0.00135603	5.6	-0.00122599
5.7	-0.00085912	5.7	-0.00158008	5.7	-0.00127922	5.7	-0.00111066
5.8	-0.00078771	5.8	-0.00151136	5.8	-0.00120785	5.8	-0.00100620
5.9	-0.00072265	5.9	-0.00144763	5.9	-0.00114222	5.9	-0.00091206
6.0	-0.00066297	6.0	-0.00138807	6.0	-0.00108143	6.0	-0.00082767
6.1	-0.00060835	6.1	-0.00133117	6.1	-0.00102417	6.1	-0.00075240
6.2	-0.00055838	6.2	-0.00127795	6.2	-0.00097044	6.2	-0.00068505
6.3	-0.00051254	6.3	-0.00122744	6.3	-0.00091919	6.3	-0.00062455
6.4	-0.00047044	6.4	-0.00117880	6.4	-0.00087069	6.4	-0.00057074
6.5	-0.00043161	6.5	-0.00113165	6.5	-0.00082452	6.5	-0.00052351
6.6	-0.00039567	6.6	-0.00108574	6.6	-0.00078052	6.6	-0.00048213
6.7	-0.00036241	6.7	-0.00104085	6.7	-0.00073844	6.7	-0.00044597
6.8	-0.00033168	6.8	-0.00099679	6.8	-0.00069803	6.8	-0.00041493
6.9	-0.00030330	6.9	-0.00095332	6.9	-0.00065906	6.9	-0.00038827
7.0	-0.00027714	7.0	-0.00091023	7.0	-0.00062138	7.0	-0.00036591
7.1	-0.00025291	7.1	-0.00086729	7.1	-0.00058486	7.1	-0.00034776
7.2	-0.00023042	7.2	-0.00082440	7.2	-0.00054943	7.2	-0.00033335
7.3	-0.00020959	7.3	-0.00078152	7.3	-0.00051510	7.3	-0.00032239
7.4	-0.00019030	7.4	-0.00073858	7.4	-0.00048180	7.4	-0.00031451
7.5	-0.00017237	7.5	-0.00069557	7.5	-0.00044951	7.5	-0.00030938
7.6	-0.00015579	7.6	-0.00065246	7.6	-0.00041821	7.6	-0.00030657
7.7	-0.00014031	7.7	-0.00060918	7.7	-0.00038780	7.7	-0.00030569
7.8	-0.00012596	7.8	-0.00056577	7.8	-0.00035827	7.8	-0.00030626
7.9	-0.00011252	7.9	-0.00052222	7.9	-0.00032960	7.9	-0.00030770
8.0	-0.00009991	8.0	-0.00047862	8.0	-0.00030180	8.0	-0.00030936
8.1	-0.00008808	8.1	-0.00043513	8.1	-0.00027491	8.1	-0.00031067

8.2	-0.00007681	8.2	-0.00039177	8.2	-0.00024885	8.2	-0.00031082
8.3	-0.00006604	8.3	-0.00034874	8.3	-0.00022364	8.3	-0.00030908
8.4	-0.00005574	8.4	-0.00030631	8.4	-0.00019941	8.4	-0.00030469
8.5	-0.00004578	8.5	-0.00026468	8.5	-0.00017612	8.5	-0.00029690
8.6	-0.00003617	8.6	-0.00022410	8.6	-0.00015386	8.6	-0.00028487
8.7	-0.00002669	8.7	-0.00018472	8.7	-0.00013254	8.7	-0.00026774
8.8	-0.00001734	8.8	-0.00014683	8.8	-0.00011223	8.8	-0.00024485
8.9	-0.00000794	8.9	-0.00011054	8.9	-0.00009279	8.9	-0.00021557
9.0	0.00000197	9.0	-0.00007584	9.0	-0.00007393	9.0	-0.00017957
9.1	0.00001271	9.1	-0.00004293	9.1	-0.00005543	9.1	-0.00013716
9.2	0.00002471	9.2	-0.00001191	9.2	-0.00003700	9.2	-0.00008949
9.3	0.00003800	9.3	0.00001667	9.3	-0.00001859	9.3	-0.00003875
9.4	0.00005209	9.4	0.00004201	9.4	-0.00000034	9.4	0.00001163
9.5	0.00006503	9.5	0.00006218	9.5	0.00001649	9.5	0.00005679
9.6	0.00007373	9.6	0.00007453	9.6	0.00002991	9.6	0.00009055
9.7	0.00007432	9.7	0.00007597	9.7	0.00003714	9.7	0.00010619
9.8	0.00006339	9.8	0.00006419	9.8	0.00003566	9.8	0.00009749
9.9	0.00003860	9.9	0.00003820	9.9	0.00002342	9.9	0.00006114
10.0	0.00000000	10.0	0.00000000	10.0	0.00000000	10.0	0.00000000

APPENDIX B – Rovibrational Energies

Table 11 – Rovibrational energies $E_{v,j}$ (cm^{-1}) of the systems CO-GQD, CO-GQD@2B, CO-GQD@2N, andCO-GQD@2Al.

v	j	CO-GQD	CO-GQD@2B	CO-GQD@2N	CO-GQD@2Al
0	0	27.99	32.51	34.67	34.14
1	0	82.71	95.87	101.88	101.65
2	0	135.52	156.88	166.16	168.06
3	0	186.19	215.53	227.51	233.36
4	0	234.49	271.82	285.90	297.50
5	0	280.20	325.74	341.32	360.47
6	0	323.09	377.30	393.78	422.22
7	0	362.99	426.52	443.27	482.74
8	0	399.75	473.41	489.81	541.99
9	0	433.35	518.01	533.42	599.95
10	0	463.86	560.34	574.12	656.58
11	0	491.50	600.46	611.98	711.87
12	0	516.56	638.39	647.03	765.77
13	0	539.32	674.18	679.35	818.27
14	0	559.97	707.89	709.02	869.33
15	0	578.58	739.53	736.12	918.94
16	0	595.08	769.16	760.72	967.07
17	0	609.28	796.82	782.90	1013.70
18	0	620.88	822.55	802.74	1058.80
19	0	629.75	846.41	820.27	1102.38
20	0	636.45	868.48	835.53	1144.41
21	0	-	888.89	848.55	1184.88
22	0	-	907.81	859.31	1223.78
23	0	-	925.44	867.81	1261.13
24	0	-	942.00	874.06	1296.91
25	0	-	957.69	-	1331.12
26	0	-	972.68	-	1363.78
27	0	-	987.09	-	1394.90
28	0	-	1000.98	-	1424.46
29	0	-	1014.40	-	1452.48
30	0	-	1027.36	-	1478.96

31	0	-	1039.83	-	1503.86
32	0	-	1051.78	-	1527.18
33	0	-	1063.13	-	1548.85
34	0	-	1073.77	-	1568.82
35	0	-	-	-	1586.99
36	0	-	-	-	1603.22
37	0	-	-	-	1617.35
38	0	-	-	-	1629.26
39	0	-	-	-	1639.11
40	0	-	-	-	1647.51
41	0	-	-	-	1655.14
42	0	-	-	-	1662.43
43	0	-	-	-	1669.82
44	0	-	-	-	1677.84

0	1	28.10	32.62	34.79	34.27
1	1	82.82	95.98	102.00	101.78
2	1	135.62	156.99	166.28	168.19
3	1	186.29	215.64	227.62	233.48
4	1	234.59	271.92	286.01	297.63
5	1	280.29	325.84	341.43	360.59
6	1	323.19	377.40	393.89	422.34
7	1	363.08	426.62	443.38	482.86
8	1	399.84	473.51	489.91	542.11
9	1	433.43	518.10	533.51	600.07
10	1	463.94	560.44	574.22	656.70
11	1	491.57	600.55	612.07	711.98
12	1	516.63	638.48	647.12	765.88
13	1	539.39	674.27	679.44	818.38
14	1	560.04	707.97	709.10	869.44
15	1	578.65	739.61	736.19	919.04
16	1	595.14	769.24	760.79	967.17
17	1	609.33	796.90	782.97	1013.80
18	1	620.93	822.62	802.80	1058.91
19	1	629.79	846.48	820.33	1102.48
20	1	636.49	868.55	835.59	1144.50
21	1	-	888.96	848.60	1184.97
22	1	-	907.87	859.35	1223.88
23	1	-	925.50	867.85	1261.22

24	1	-	942.05	874.10	1296.99
25	1	-	957.74	-	1331.21
26	1	-	972.73	-	1363.87
27	1	-	987.14	-	1394.98
28	1	-	1001.03	-	1424.54
29	1	-	1014.45	-	1452.56
30	1	-	1027.40	-	1479.03
31	1	-	1039.87	-	1503.93
32	1	-	1051.82	-	1527.25
33	1	-	1063.18	-	1548.92
34	1	-	1073.82	-	1568.89
35	1	-	-	-	1587.05
36	1	-	-	-	1603.27
37	1	-	-	-	1617.40
38	1	-	-	-	1629.31
39	1	-	-	-	1639.15
40	1	-	-	-	1647.55
41	1	-	-	-	1655.18
42	1	-	-	-	1662.47
43	1	-	-	-	1669.85
44	1	-	-	-	1677.88

Table 12 – Rovibrational energies $E_{v,j}$ (cm^{-1}) of the systems NH_3-GQD, NH_3-GQD@2B, NH_3-GQD@2N, and NH_3-GQD@2Al.

v	j	NH_3-GQD	NH_3-GQD@2B	NH_3-GQD@2N	NH_3-GQD@2Al
0	0	49.48	52.88	58.89	80.48
1	0	145.38	156.53	173.34	239.12
2	0	237.02	257.02	283.29	394.63
3	0	324.30	354.27	388.71	546.95
4	0	407.13	448.24	489.57	696.03
5	0	485.38	538.87	585.85	841.81
6	0	558.96	626.16	677.55	984.23
7	0	627.73	710.07	764.66	1123.24
8	0	691.58	790.64	847.19	1258.79
9	0	750.37	867.89	925.14	1390.85
10	0	804.00	941.88	998.55	1519.38
11	0	852.37	1012.69	1067.42	1644.35
12	0	895.42	1080.43	1131.80	1765.73
13	0	933.17	1145.19	1191.71	1883.53
14	0	965.75	1207.07	1247.17	1997.73
15	0	993.34	1266.17	1298.22	2108.36
16	0	1016.21	1322.56	1344.83	2215.42
17	0	-	1376.28	1387.01	2318.97
18	0	-	1427.34	1424.68	2419.05
19	0	-	1475.72	1457.76	2515.73
20	0	-	1521.31	1486.12	2609.08
21	0	-	1563.98	1509.62	2699.20
22	0	-	1603.51	-	2786.18
23	0	-	1639.55	-	2870.13
24	0	-	1671.63	-	2951.16
25	0	-	1699.14	-	3029.39
26	0	-	1721.59	-	3104.90
27	0	-	1739.72	-	3177.82
28	0	-	1755.82	-	3248.22
29	0	-	1771.35	-	3316.19
30	0	-	1786.58	-	3381.80
31	0	-	1801.53	-	3445.10
32	0	-	1816.05	-	3506.13
33	0	-	-	-	3564.92
34	0	-	-	-	3621.47

35	0	-	-	-	3675.78
36	0	-	-	-	3727.81
37	0	-	-	-	3777.53
38	0	-	-	-	3824.87
39	0	-	-	-	3869.73
40	0	-	-	-	3912.01
41	0	-	-	-	3951.54
42	0	-	-	-	3988.13
43	0	-	-	-	4021.50
44	0	-	-	-	4051.29
45	0	-	-	-	4076.94
46	0	-	-	-	4097.51

0	1	49.68	53.14	59.11	80.78
1	1	145.58	156.78	173.56	239.41
2	1	237.21	257.26	283.50	394.92
3	1	324.49	354.51	388.91	547.24
4	1	407.31	448.48	489.77	696.31
5	1	485.56	539.11	586.05	842.09
6	1	559.13	626.39	677.74	984.50
7	1	627.90	710.30	764.85	1123.51
8	1	691.74	790.86	847.37	1259.06
9	1	750.53	868.10	925.32	1391.11
10	1	804.15	942.09	998.72	1519.64
11	1	852.51	1012.90	1067.59	1644.60
12	1	895.55	1080.63	1131.96	1765.98
13	1	933.30	1145.38	1191.86	1883.77
14	1	965.86	1207.26	1247.32	1997.97
15	1	993.45	1266.35	1298.36	2108.59
16	1	1016.31	1322.74	1344.97	2215.65
17	1	-	1376.45	1387.13	2319.20
18	1	-	1427.51	1424.80	2419.27
19	1	-	1475.88	1457.87	2515.94
20	1	-	1521.47	1486.23	2609.29
21	1	-	1564.13	1509.72	2699.40
22	1	-	1603.65	-	2786.38
23	1	-	1639.68	-	2870.33
24	1	-	1671.76	-	2951.36
25	1	-	1699.26	-	3029.58

26	1	-	1721.69	-	3105.09
27	1	-	1739.81	-	3178.00
28	1	-	1755.91	-	3248.40
29	1	-	1771.43	-	3316.36
30	1	-	1786.67	-	3381.97
31	1	-	1801.61	-	3445.27
32	1	-	1816.13	-	3506.29
33	1	-	-	-	3565.08
34	1	-	-	-	3621.63
35	1	-	-	-	3675.93
36	1	-	-	-	3727.96
37	1	-	-	-	3777.67
38	1	-	-	-	3825.00
39	1	-	-	-	3869.87
40	1	-	-	-	3912.14
41	1	-	-	-	3951.66
42	1	-	-	-	3988.24
43	1	-	-	-	4021.61
44	1	-	-	-	4051.39
45	1	-	-	-	4077.03
46	1	-	-	-	4097.59

Table 13 – Rovibrational energies $E_{v,j}$ (cm^{-1}) of the systems NO_2-GQD, NO_2-GQD@1B, NO_2-GQD@1N, and NO_2-GQD@1Al.

v	j	NO_2-GQD	NO_2-GQD@1B	NO_2-GQD@1N	NO_2-GQD@1Al
0	0	32.31	84.26	71.54	88.55
1	0	95.62	251.90	213.57	264.64
2	0	157.10	418.36	354.11	439.40
3	0	216.77	583.63	493.15	612.84
4	0	274.62	747.73	630.69	784.96
5	0	330.64	910.64	766.72	955.77
6	0	384.82	1072.38	901.25	1125.29
7	0	437.18	1232.95	1034.27	1293.51
8	0	487.70	1392.35	1165.78	1460.43
9	0	536.39	1550.59	1295.77	1626.08
10	0	583.26	1707.67	1424.26	1790.45
11	0	628.30	1863.59	1551.22	1953.55
12	0	671.53	2018.35	1676.67	2115.39
13	0	712.95	2171.96	1800.60	2275.98
14	0	752.58	2324.43	1923.01	2435.31
15	0	790.44	2475.75	2043.91	2593.41
16	0	826.53	2625.94	2163.29	2750.27
17	0	860.89	2774.98	2281.16	2905.90
18	0	893.52	2922.89	2397.52	3060.31
19	0	924.46	3069.68	2512.38	3213.50
20	0	953.73	3215.33	2625.72	3365.49
21	0	981.37	3359.87	2737.57	3516.27
22	0	1007.40	3503.28	2847.93	3665.86
23	0	1031.86	3645.58	2956.79	3814.26
24	0	1054.78	3786.77	3064.17	3961.48
25	0	1076.20	3926.85	3170.08	4107.53
26	0	1096.15	4065.82	3274.51	4252.41
27	0	1114.68	4203.70	3377.49	4396.12
28	0	1131.82	4340.47	3479.02	4538.68
29	0	1147.62	4476.15	3579.11	4680.09
30	0	1162.12	4610.74	3677.77	4820.36
31	0	1175.39	4744.24	3775.02	4959.49
32	0	1187.46	4876.66	3870.86	5097.49
33	0	1198.39	5007.99	3965.32	5234.37
34	0	1208.25	5138.25	4058.40	5370.12

35	0	1217.08	5267.43	4150.12	5504.77
36	0	1224.91	5395.54	4240.49	5638.30
37	0	1231.75	5522.58	4329.55	5770.74
38	0	1237.54	5648.56	4417.29	5902.07
39	0	-	5773.47	4503.74	6032.32
40	0	-	5897.33	4588.93	6161.49
41	0	-	6020.12	4672.86	6289.57
42	0	-	6141.87	4755.56	6416.58
43	0	-	6262.56	4837.06	6542.51
44	0	-	6382.20	4917.36	6667.39
45	0	-	6500.80	4996.50	6791.20
46	0	-	6618.35	5074.49	6913.96
47	0	-	6734.86	5151.37	7035.67
48	0	-	6850.34	5227.14	7156.33
49	0	-	6964.78	5301.83	7275.95
50	0	-	7078.18	5375.47	7394.53
51	0	-	7190.56	5448.08	7512.08
52	0	-	7301.91	5519.68	7628.60
53	0	-	7412.23	5590.30	7744.10
54	0	-	7521.52	5659.95	7858.57
55	0	-	7629.80	5728.65	7972.03
56	0	-	7737.05	5796.44	8084.47
57	0	-	7843.29	5863.33	8195.91
58	0	-	7948.51	5929.34	8306.34
59	0	-	8052.71	5994.50	8415.76
60	0	-	8155.91	6058.82	8524.19
61	0	-	8258.10	6122.32	8631.62
62	0	-	8359.27	6185.03	8738.06
63	0	-	8459.45	6246.96	8843.51
64	0	-	8558.61	6308.13	8947.98
65	0	-	8656.78	6368.56	9051.46
66	0	-	8753.95	6428.26	9153.97
67	0	-	8850.12	6487.25	9255.49
68	0	-	8945.29	6545.55	9356.05
69	0	-	9039.47	6603.18	9455.63
70	0	-	9132.65	6660.14	9554.25
71	0	-	9224.85	6716.46	9651.90
72	0	-	9316.06	6772.15	9748.59
73	0	-	9406.29	6827.21	9844.32

74	0	-	9495.53	6881.67	9939.10
75	0	-	9583.79	6935.54	10032.92
76	0	-	9671.07	6988.82	10125.80
77	0	-	9757.38	7041.53	10217.73
78	0	-	9842.71	7093.68	10308.72
79	0	-	9927.07	7145.29	10398.76
80	0	-	10010.47	7196.35	10487.87
81	0	-	10092.90	7246.89	10576.05
82	0	-	10174.37	7296.90	10663.30
83	0	-	10254.88	7346.41	10749.62
84	0	-	10334.44	7395.41	10835.02
85	0	-	10413.04	7443.92	10919.50
86	0	-	10490.70	7491.94	11003.06
87	0	-	10567.41	7539.48	11085.72
88	0	-	10643.19	7586.55	11167.46
89	0	-	10718.03	7633.16	11248.31
90	0	-	10791.94	7679.31	11328.25
91	0	-	10864.93	7725.00	11407.30
92	0	-	10937.00	7770.26	11485.46
93	0	-	11008.15	7815.07	11562.73
94	0	-	11078.39	7859.45	11639.13
95	0	-	11147.73	7903.40	11714.65
96	0	-	11216.18	7946.93	11789.30
97	0	-	11283.73	7990.04	11863.09
98	0	-	11350.40	8032.74	11936.02
99	0	-	11416.19	8075.03	12008.09
100	0	-	11481.11	8116.92	12079.33
101	0	-	11545.17	8158.40	12149.72
102	0	-	11608.38	8199.50	12219.27
103	0	-	11670.73	8240.20	12288.01
104	0	-	11732.25	8280.52	12355.92
105	0	-	11792.94	8320.45	12423.02
106	0	-	11852.81	8360.01	12489.31
107	0	-	11911.86	8399.19	12554.81
108	0	-	11970.12	8438.00	12619.51
109	0	-	12027.57	8476.44	12683.44
110	0	-	12084.24	8514.52	12746.59
111	0	-	12140.14	8552.24	12808.97
112	0	-	12195.27	8589.61	12870.59

113	0	-	12249.64	8626.62	12931.47
114	0	-	12303.27	8663.28	12991.60
115	0	-	12356.16	8699.59	13051.01
116	0	-	12408.32	8735.56	13109.68
117	0	-	12459.77	8771.19	13167.65
118	0	-	12510.51	8806.49	13224.90
119	0	-	12560.56	8841.45	13281.46
120	0	-	12609.92	8876.09	13337.33
121	0	-	12658.61	8910.40	13392.52
122	0	-	12706.63	8944.38	13447.03
123	0	-	12754.00	8978.05	13500.89
124	0	-	12800.72	9011.41	13554.09
125	0	-	12846.81	9044.45	13606.64
126	0	-	12892.27	9077.19	13658.56
127	0	-	12937.12	9109.63	13709.85
128	0	-	12981.37	9141.76	13760.52
129	0	-	13025.02	9173.60	13810.58
130	0	-	13068.09	9205.15	13860.03
131	0	-	13110.58	9236.41	13908.89
132	0	-	13152.50	9267.39	13957.16
133	0	-	13193.87	9298.09	14004.85
134	0	-	13234.69	9328.51	14051.97
135	0	-	13274.98	9358.66	14098.52
136	0	-	13314.73	9388.55	14144.52
137	0	-	13353.97	9418.18	14189.96
138	0	-	13392.70	9447.54	14234.86
139	0	-	13430.93	9476.66	14279.23
140	0	-	13468.67	9505.53	14323.06
141	0	-	13505.93	9534.15	14366.37
142	0	-	13542.72	9562.53	14409.17
143	0	-	13579.04	9590.68	14451.45
144	0	-	13614.91	9618.60	14493.23
145	0	-	13650.33	9646.30	14534.51
146	0	-	13685.32	9673.77	14575.29
147	0	-	13719.88	9701.03	14615.59
148	0	-	13754.03	9728.07	14655.41
149	0	-	13787.76	9754.91	14694.76
150	0	-	13821.10	9781.54	14733.63
151	0	-	13854.05	9807.98	14772.04

152	0	-	13886.62	9834.22	14809.99
153	0	-	13918.82	9860.27	14847.49
154	0	-	13950.65	9886.13	14884.54
155	0	-	13982.13	9911.81	14921.14
156	0	-	14013.27	9937.31	14957.32
157	0	-	14044.07	9962.64	14993.06
158	0	-	14074.54	9987.80	15028.37
159	0	-	14104.70	10012.79	15063.27
160	0	-	14134.55	10037.62	15097.76
161	0	-	14164.10	10062.28	15131.84
162	0	-	14193.35	10086.79	15165.51
163	0	-	14222.32	10111.15	15198.80
164	0	-	14251.02	10135.35	15231.69
165	0	-	14279.44	10159.40	15264.20
166	0	-	14307.61	10183.31	15296.34
167	0	-	14335.52	10207.08	15328.11
168	0	-	14363.18	10230.71	15359.51
169	0	-	14390.60	10254.20	15390.56
170	0	-	14417.79	10277.55	15421.27
171	0	-	14444.75	10300.77	15451.63
172	0	-	14471.49	10323.86	15481.66
173	0	-	14498.02	10346.81	15511.36
174	0	-	14524.33	10369.64	15540.75
175	0	-	14550.44	10392.34	15569.82
176	0	-	14576.35	10414.92	15598.59
177	0	-	14602.06	10437.38	15627.06
178	0	-	14627.59	10459.71	15655.24
179	0	-	14652.92	10481.93	15683.14
180	0	-	14678.07	10504.04	15710.77
181	0	-	14703.05	10526.07	15738.14
182	0	-	14727.84	10548.09	15765.27
183	0	-	14752.47	10570.21	15792.26
184	0	-	14776.92	10592.57	15819.24
185	0	-	14801.20	10615.31	15846.48
186	0	-	14825.32	10638.53	15874.25
187	0	-	14849.27	10662.28	15902.75
188	0	-	14873.07	10686.56	15932.09
189	0	-	14896.70	10711.35	15962.26
190	0	-	14920.17	10736.62	15993.21

191	0	-	14943.49	10762.36	16024.92
192	0	-	14966.65	10788.53	16057.31
193	0	-	14989.66	10815.11	16090.36
194	0	-	15012.51	10842.08	16124.03
195	0	-	15035.20	10869.43	16158.28
196	0	-	15057.74	10897.14	16193.09
197	0	-	15080.13	10925.20	16228.44
198	0	-	15102.36	10953.60	16264.31
199	0	-	15124.44	10982.33	16300.67
200	0	-	15146.36	11011.38	16337.53
201	0	-	15168.13	11040.74	16374.85
202	0	-	15189.74	11070.40	16412.64
203	0	-	15211.20	11100.36	16450.88
204	0	-	15232.50	11130.62	16489.55
205	0	-	15253.65	11161.16	16528.65
206	0	-	15274.69	11191.99	16568.18
207	0	-	15295.68	11223.09	16608.11
208	0	-	15316.74	11254.46	16648.45
209	0	-	15338.06	11286.11	16689.20
210	0	-	15359.79	11318.01	16730.33
211	0	-	15382.04	11350.18	16771.85
212	0	-	15404.85	11382.61	16813.76
213	0	-	15428.20	-	16856.04
214	0	-	15452.09	-	16898.69
215	0	-	15476.47	-	16941.70
216	0	-	15501.31	-	16985.08
217	0	-	15526.59	-	17028.82
218	0	-	15552.29	-	17072.91
219	0	-	15578.39	-	-
220	0	-	15604.87	-	-

0	1	32.40	84.42	71.67	88.62
1	1	95.70	252.06	213.70	264.70
2	1	157.19	418.52	354.23	439.46
3	1	216.86	583.79	493.27	612.90
4	1	274.70	747.88	630.81	785.03
5	1	330.72	910.79	766.84	955.84
6	1	384.90	1072.53	901.37	1125.35
7	1	437.25	1233.10	1034.39	1293.57

8	1	487.78	1392.50	1165.90	1460.50
9	1	536.47	1550.74	1295.89	1626.15
10	1	583.33	1707.82	1424.37	1790.52
11	1	628.37	1863.73	1551.33	1953.62
12	1	671.60	2018.50	1676.78	2115.46
13	1	713.02	2172.11	1800.71	2276.04
14	1	752.65	2324.58	1923.12	2435.38
15	1	790.50	2475.90	2044.02	2593.47
16	1	826.60	2626.08	2163.41	2750.33
17	1	860.95	2775.13	2281.27	2905.96
18	1	893.58	2923.04	2397.63	3060.37
19	1	924.52	3069.82	2512.48	3213.56
20	1	953.79	3215.47	2625.83	3365.55
21	1	981.43	3360.01	2737.68	3516.33
22	1	1007.46	3503.42	2848.03	3665.92
23	1	1031.91	3645.72	2956.89	3814.32
24	1	1054.83	3786.91	3064.27	3961.54
25	1	1076.25	3926.99	3170.18	4107.59
26	1	1096.20	4065.96	3274.62	4252.47
27	1	1114.72	4203.83	3377.59	4396.18
28	1	1131.86	4340.61	3479.12	4538.74
29	1	1147.66	4476.29	3579.21	4680.15
30	1	1162.16	4610.87	3677.87	4820.42
31	1	1175.42	4744.37	3775.12	4959.55
32	1	1187.49	4876.79	3870.96	5097.55
33	1	1198.43	5008.12	3965.41	5234.42
34	1	1208.28	5138.38	4058.49	5370.18
35	1	1217.11	5267.56	4150.21	5504.82
36	1	1224.94	5395.67	4240.59	5638.36
37	1	1231.78	5522.71	4329.64	5770.79
38	1	1237.56	5648.69	4417.38	5902.13
39	1	-	5773.60	4503.84	6032.38
40	1	-	5897.45	4589.02	6161.54
41	1	-	6020.25	4672.95	6289.62
42	1	-	6141.99	4755.65	6416.63
43	1	-	6262.68	4837.15	6542.57
44	1	-	6382.32	4917.45	6667.44
45	1	-	6500.92	4996.59	6791.26
46	1	-	6618.47	5074.58	6914.01

47	1	-	6734.99	5151.45	7035.72
48	1	-	6850.46	5227.22	7156.38
49	1	-	6964.90	5301.92	7276.00
50	1	-	7078.30	5375.56	7394.58
51	1	-	7190.68	5448.16	7512.13
52	1	-	7302.02	5519.76	7628.65
53	1	-	7412.34	5590.38	7744.15
54	1	-	7521.64	5660.03	7858.62
55	1	-	7629.91	5728.73	7972.08
56	1	-	7737.17	5796.52	8084.53
57	1	-	7843.40	5863.41	8195.96
58	1	-	7948.62	5929.42	8306.39
59	1	-	8052.83	5994.58	8415.82
60	1	-	8156.02	6058.90	8524.24
61	1	-	8258.21	6122.40	8631.67
62	1	-	8359.38	6185.11	8738.11
63	1	-	8459.56	6247.03	8843.56
64	1	-	8558.72	6308.20	8948.03
65	1	-	8656.89	6368.63	9051.51
66	1	-	8754.05	6428.33	9154.02
67	1	-	8850.22	6487.32	9255.54
68	1	-	8945.39	6545.62	9356.10
69	1	-	9039.57	6603.25	9455.68
70	1	-	9132.76	6660.21	9554.29
71	1	-	9224.96	6716.53	9651.95
72	1	-	9316.16	6772.22	9748.64
73	1	-	9406.39	6827.28	9844.37
74	1	-	9495.63	6881.74	9939.15
75	1	-	9583.89	6935.60	10032.97
76	1	-	9671.17	6988.89	10125.85
77	1	-	9757.48	7041.60	10217.77
78	1	-	9842.81	7093.75	10308.76
79	1	-	9927.17	7145.35	10398.81
80	1	-	10010.56	7196.42	10487.92
81	1	-	10092.99	7246.95	10576.10
82	1	-	10174.46	7296.97	10663.34
83	1	-	10254.97	7346.47	10749.67
84	1	-	10334.53	7395.47	10835.06
85	1	-	10413.13	7443.98	10919.54

86	1	-	10490.79	7492.00	11003.11
87	1	-	10567.50	7539.54	11085.76
88	1	-	10643.28	7586.61	11167.51
89	1	-	10718.12	7633.22	11248.35
90	1	-	10792.03	7679.37	11328.29
91	1	-	10865.02	7725.06	11407.34
92	1	-	10937.08	7770.31	11485.50
93	1	-	11008.24	7815.13	11562.78
94	1	-	11078.48	7859.51	11639.17
95	1	-	11147.82	7903.46	11714.69
96	1	-	11216.26	7946.99	11789.34
97	1	-	11283.81	7990.10	11863.13
98	1	-	11350.48	8032.79	11936.06
99	1	-	11416.27	8075.08	12008.13
100	1	-	11481.19	8116.97	12079.37
101	1	-	11545.25	8158.46	12149.76
102	1	-	11608.46	8199.55	12219.31
103	1	-	11670.81	8240.25	12288.04
104	1	-	11732.33	8280.57	12355.96
105	1	-	11793.02	8320.51	12423.06
106	1	-	11852.89	8360.06	12489.35
107	1	-	11911.94	8399.24	12554.85
108	1	-	11970.19	8438.05	12619.55
109	1	-	12027.64	8476.49	12683.47
110	1	-	12084.31	8514.57	12746.62
111	1	-	12140.21	8552.29	12809.01
112	1	-	12195.34	8589.66	12870.63
113	1	-	12249.71	8626.66	12931.51
114	1	-	12303.34	8663.32	12991.64
115	1	-	12356.23	8699.64	13051.04
116	1	-	12408.39	8735.61	13109.72
117	1	-	12459.84	8771.24	13167.68
118	1	-	12510.58	8806.54	13224.94
119	1	-	12560.63	8841.50	13281.49
120	1	-	12609.99	8876.13	13337.36
121	1	-	12658.67	8910.44	13392.55
122	1	-	12706.70	8944.43	13447.07
123	1	-	12754.06	8978.10	13500.92
124	1	-	12800.78	9011.46	13554.12

125	1	-	12846.87	9044.50	13606.68
126	1	-	12892.34	9077.24	13658.59
127	1	-	12937.19	9109.67	13709.88
128	1	-	12981.43	9141.81	13760.55
129	1	-	13025.08	9173.64	13810.61
130	1	-	13068.15	9205.19	13860.06
131	1	-	13110.64	9236.45	13908.92
132	1	-	13152.56	9267.43	13957.19
133	1	-	13193.93	9298.13	14004.88
134	1	-	13234.75	9328.55	14052.00
135	1	-	13275.03	9358.70	14098.55
136	1	-	13314.79	9388.59	14144.55
137	1	-	13354.03	9418.22	14189.99
138	1	-	13392.76	9447.58	14234.90
139	1	-	13430.99	9476.70	14279.26
140	1	-	13468.73	9505.57	14323.09
141	1	-	13505.98	9534.19	14366.40
142	1	-	13542.77	9562.57	14409.20
143	1	-	13579.09	9590.72	14451.48
144	1	-	13614.96	9618.64	14493.26
145	1	-	13650.38	9646.33	14534.54
146	1	-	13685.37	9673.81	14575.32
147	1	-	13719.93	9701.06	14615.62
148	1	-	13754.08	9728.11	14655.44
149	1	-	13787.81	9754.94	14694.78
150	1	-	13821.15	9781.58	14733.66
151	1	-	13854.10	9808.01	14772.06
152	1	-	13886.67	9834.25	14810.02
153	1	-	13918.86	9860.30	14847.51
154	1	-	13950.70	9886.17	14884.56
155	1	-	13982.18	9911.85	14921.17
156	1	-	14013.31	9937.35	14957.34
157	1	-	14044.12	9962.68	14993.08
158	1	-	14074.59	9987.83	15028.40
159	1	-	14104.75	10012.82	15063.30
160	1	-	14134.60	10037.65	15097.78
161	1	-	14164.14	10062.32	15131.86
162	1	-	14193.40	10086.83	15165.54
163	1	-	14222.37	10111.18	15198.82

164	1	-	14251.06	10135.38	15231.72
165	1	-	14279.48	10159.44	15264.23
166	1	-	14307.65	10183.35	15296.36
167	1	-	14335.56	10207.12	15328.13
168	1	-	14363.22	10230.74	15359.54
169	1	-	14390.64	10254.23	15390.59
170	1	-	14417.83	10277.58	15421.29
171	1	-	14444.79	10300.80	15451.65
172	1	-	14471.53	10323.89	15481.68
173	1	-	14498.06	10346.85	15511.39
174	1	-	14524.37	10369.67	15540.77
175	1	-	14550.48	10392.38	15569.84
176	1	-	14576.39	10414.95	15598.61
177	1	-	14602.10	10437.41	15627.08
178	1	-	14627.63	10459.74	15655.26
179	1	-	14652.96	10481.96	15683.16
180	1	-	14678.11	10504.07	15710.79
181	1	-	14703.09	10526.10	15738.16
182	1	-	14727.88	10548.12	15765.30
183	1	-	14752.50	10570.24	15792.28
184	1	-	14776.96	10592.60	15819.26
185	1	-	14801.24	10615.34	15846.50
186	1	-	14825.36	10638.56	15874.27
187	1	-	14849.31	10662.31	15902.78
188	1	-	14873.10	10686.59	15932.11
189	1	-	14896.74	10711.38	15962.28
190	1	-	14920.21	10736.66	15993.24
191	1	-	14943.53	10762.39	16024.94
192	1	-	14966.69	10788.56	16057.33
193	1	-	14989.69	10815.14	16090.38
194	1	-	15012.54	10842.12	16124.05
195	1	-	15035.24	10869.47	16158.30
196	1	-	15057.78	10897.18	16193.11
197	1	-	15080.16	10925.24	16228.46
198	1	-	15102.40	10953.64	16264.33
199	1	-	15124.47	10982.37	16300.70
200	1	-	15146.40	11011.41	16337.55
201	1	-	15168.16	11040.77	16374.88
202	1	-	15189.78	11070.44	16412.67

203	1	-	15211.23	11100.40	16450.90
204	1	-	15232.53	11130.66	16489.57
205	1	-	15253.68	11161.20	16528.68
206	1	-	15274.72	11192.02	16568.20
207	1	-	15295.71	11223.13	16608.14
208	1	-	15316.78	11254.50	16648.48
209	1	-	15338.09	11286.14	16689.22
210	1	-	15359.83	11318.05	16730.36
211	1	-	15382.08	11350.22	16771.88
212	1	-	15404.88	11382.65	16813.78
213	1	-	15428.24	-	16856.06
214	1	-	15452.12	-	16898.71
215	1	-	15476.50	-	16941.73
216	1	-	15501.35	-	16985.11
217	1	-	15526.63	-	17028.85
218	1	-	15552.33	-	17072.94
219	1	-	15578.43	-	-
220	1	-	15604.90	-	-

Table 14 – Rovibrational energies $E_{v,j}$ (cm^{-1}) of the systems SO_2-GQD, SO_2-GQD@2B, SO_2-GQD@2N, and SO_2-GQD@2Al.

v	j	SO_2-GQD	SO_2-GQD@2B	SO_2-GQD@2N	SO_2-GQD@2Al
0	0	24.14	25.59	26.46	21.41
1	0	71.70	76.18	78.36	63.84
2	0	118.29	125.92	128.89	105.80
3	0	163.91	174.81	178.04	147.28
4	0	208.55	222.83	225.82	188.27
5	0	252.22	269.96	272.25	228.77
6	0	294.90	316.21	317.32	268.76
7	0	336.60	361.54	361.05	308.24
8	0	377.31	405.95	403.46	347.19
9	0	417.03	449.43	444.57	385.61
10	0	455.76	491.95	484.40	423.48
11	0	493.48	533.51	522.98	460.79
12	0	530.19	574.09	560.33	497.54
13	0	565.90	613.68	596.49	533.71
14	0	600.59	652.25	631.47	569.28
15	0	634.27	689.81	665.33	604.26
16	0	666.92	726.33	698.09	638.61
17	0	698.55	761.80	729.78	672.34
18	0	729.15	796.21	760.43	705.43
19	0	758.72	829.55	790.09	737.87
20	0	787.26	861.81	818.77	769.65
21	0	814.78	892.99	846.52	800.75
22	0	841.26	923.07	873.34	831.17
23	0	866.73	952.05	899.26	860.89
24	0	891.19	979.95	924.32	889.91
25	0	914.64	1006.74	948.51	918.22
26	0	937.10	1032.46	971.85	945.81
27	0	958.59	1057.09	994.36	972.68
28	0	979.13	1080.67	1016.03	998.82
29	0	998.73	1103.21	1036.89	1024.23
30	0	1017.43	1124.72	1056.92	1048.91
31	0	1035.24	1145.24	1076.12	1072.87
32	0	1052.20	1164.78	1094.50	1096.11
33	0	1068.34	1183.39	1112.06	1118.63
34	0	1083.69	1201.09	1128.79	1140.44

35	0	1098.27	1217.91	1144.69	1161.57
36	0	1112.11	1233.88	1159.77	1182.01
37	0	1125.24	1249.04	1174.05	1201.78
38	0	1137.67	1263.42	1187.54	1220.89
39	0	1149.43	1277.06	1200.28	1239.36
40	0	1160.53	1290.00	1212.31	1257.20
41	0	1170.98	1302.30	1223.70	1274.42
42	0	1180.79	1314.00	1234.52	1291.02
43	0	1189.98	1325.17	1244.85	1307.00
44	0	1198.54	1335.86	1254.74	1322.37
45	0	1206.51	1346.15	1264.28	1337.11
46	0	1213.90	1356.10	1273.50	1351.20
47	0	1220.74	1365.75	1282.46	1364.63
48	0	1227.08	1375.17	1291.19	1377.34
49	0	1232.97	1384.39	1299.70	1389.28
50	0	1238.47	1393.44	1308.03	1400.36
51	0	1243.72	1402.35	1316.17	1410.44
52	0	1248.99	1411.14	1324.14	1419.26
53	0	1254.62	1419.81	1331.94	1426.21
54	0	1260.73	1428.39	1339.57	1429.95
55	0	-	1436.87	1347.02	1433.14
56	0	-	1445.26	1354.30	1437.12
57	0	-	1453.56	1361.41	1441.66
58	0	-	1461.77	1368.34	1446.74
59	0	-	1469.90	1375.19	1452.33
60	0	-	1477.93	1382.12	1458.39
61	0	-	1485.88	1389.34	1464.88
62	0	-	1493.74	1396.95	1471.78
63	0	-	1501.55	1404.97	1479.05
64	0	-	1509.39	1413.37	1486.67
65	0	-	1517.39	-	1494.62
66	0	-	1525.68	-	-
67	0	-	1534.33	-	-
68	0	-	1543.34	-	-
69	0	-	1552.71	-	-
70	0	-	1562.41	-	-
71	0	-	1572.42	-	-
0	1	24.19	25.64	26.51	21.46

1	1	71.75	76.23	78.42	63.89
2	1	118.34	125.97	128.94	105.85
3	1	163.96	174.86	178.09	147.33
4	1	208.60	222.87	225.87	188.32
5	1	252.26	270.01	272.29	228.81
6	1	294.95	316.25	317.36	268.81
7	1	336.65	361.59	361.10	308.28
8	1	377.36	406.00	403.51	347.24
9	1	417.08	449.47	444.62	385.65
10	1	455.80	492.00	484.45	423.52
11	1	493.52	533.56	523.03	460.84
12	1	530.24	574.14	560.38	497.59
13	1	565.94	613.72	596.53	533.75
14	1	600.63	652.30	631.52	569.33
15	1	634.31	689.85	665.37	604.30
16	1	666.96	726.37	698.13	638.66
17	1	698.59	761.84	729.82	672.38
18	1	729.19	796.25	760.47	705.47
19	1	758.76	829.59	790.13	737.91
20	1	787.30	861.85	818.81	769.69
21	1	814.81	893.03	846.55	800.79
22	1	841.30	923.11	873.38	831.21
23	1	866.77	952.09	899.30	860.93
24	1	891.22	979.98	924.35	889.95
25	1	914.67	1006.78	948.54	918.26
26	1	937.14	1032.49	971.88	945.85
27	1	958.63	1057.13	994.39	972.72
28	1	979.16	1080.71	1016.07	998.86
29	1	998.76	1103.24	1036.92	1024.27
30	1	1017.46	1124.75	1056.95	1048.95
31	1	1035.27	1145.27	1076.15	1072.91
32	1	1052.23	1164.82	1094.53	1096.14
33	1	1068.37	1183.42	1112.09	1118.66
34	1	1083.72	1201.12	1128.82	1140.48
35	1	1098.30	1217.93	1144.72	1161.60
36	1	1112.14	1233.91	1159.80	1182.04
37	1	1125.26	1249.06	1174.08	1201.81
38	1	1137.70	1263.44	1187.56	1220.92
39	1	1149.46	1277.08	1200.30	1239.39

40	1	1160.55	1290.03	1212.34	1257.23
41	1	1171.00	1302.32	1223.73	1274.45
42	1	1180.81	1314.02	1234.55	1291.05
43	1	1190.00	1325.19	1244.87	1307.03
44	1	1198.56	1335.88	1254.76	1322.40
45	1	1206.53	1346.17	1264.30	1337.13
46	1	1213.92	1356.12	1273.52	1351.23
47	1	1220.76	1365.78	1282.48	1364.65
48	1	1227.10	1375.19	1291.21	1377.36
49	1	1232.99	1384.41	1299.72	1389.30
50	1	1238.49	1393.47	1308.05	1400.38
51	1	1243.73	1402.37	1316.19	1410.46
52	1	1249.01	1411.16	1324.16	1419.28
53	1	1254.63	1419.83	1331.96	1426.23
54	1	1260.74	1428.41	1339.58	1429.96
55	1	-	1436.89	1347.04	1433.15
56	1	-	1445.27	1354.32	1437.14
57	1	-	1453.58	1361.42	1441.67
58	1	-	1461.79	1368.36	1446.76
59	1	-	1469.92	1375.21	1452.35
60	1	-	1477.95	1382.14	1458.41
61	1	-	1485.90	1389.35	1464.90
62	1	-	1493.76	1396.96	1471.79
63	1	-	1501.57	1404.98	1479.06
64	1	-	1509.40	1413.39	1486.68
65	1	-	1517.40	-	1494.64
66	1	-	1525.70	-	-
67	1	-	1534.35	-	-
68	1	-	1543.36	-	-
69	1	-	1552.73	-	-
70	1	-	1562.43	-	-
71	1	-	1572.44	-	-